

NASA Contractor Report 3541

Advanced Space Shuttle Simulation Model

Frank B. Tatom and S. Ray Smith

CONTRACT NAS8-33818
APRIL 1982



NASA Contractor Report 3541

Advanced Space Shuttle Simulation Model

Frank B. Tatom and S. Ray Smith

*Engineering Analysis, Inc.
Huntsville, Alabama*

**Prepared for
Marshall Space Flight Center
under Contract NAS8-33818**



**Scientific and Technical
Information Branch**

1982

TABLE OF CONTENTS

<u>Section</u>		<u>Page</u>
1	INTRODUCTION	1-1
2	TURBULENCE GENERATION PROCEDURE	2-1
2.1	Background.	2-1
2.2	Selection of Atmospheric Bands	2-2
2.3	Development of von Karman Spectra with Finite Upper Limits	2-2
2.3.1	Upper Limits of Integration	2-4
2.3.2	One-Dimensional Spectra	2-6
2.3.3	Dimensionless Energy Content	2-7
2.4	Digital Filter Simulation	2-8
2.5	Effects of Digitization	2-11
3	SIMULATED TURBULENCE TAPES	3-1
3.1	Validation of Simulated Turbulence	3-1
3.2	Conversion to Dimensional Values	3-2
4	CONCLUSIONS AND RECOMMENDATIONS	4-1
5	REFERENCES CITED	5-1
APPENDIX A	Dimensionless von Karman Spectra with Finite Upper Limits	A-1
APPENDIX B	Establishment of Lower Frequency Limits	B-1
APPENDIX C	Spectral Analysis of Simulated Turbulence	C-1
APPENDIX D	Statistical Analysis of Simulated Turbulence	D-1

LIST OF TABLES

<u>Table</u>		<u>Page</u>
2-1	Variation of Standard Deviation and Length Scale with Altitude	2-3
2-2	Summary of Turbulence Parameters in Discrete Altitude Bands	2-5
2-3	Characteristic Dimensions of the Space Shuttle	2-6
2-4	Types of Simulated Turbulence	2-7
2-5	Dimensionless Energy Content for Gusts and Gust Gradients	2-7
3-1	Index of Shuttle Simulated Turbulence Tapes (SSTT)	3-1
3-2	Variation of Shuttle Speed with Altitude	3-5
A-1	Dimensionless Spectrum for Altitude Band #1	A-2
A-2	Dimensionless Spectrum for Altitude Band #2	A-3
A-3	Dimensionless Spectrum for Altitude Band #3	A-5
A-4	Dimensionless Spectrum for Altitude Band #4	A-7
A-5	Dimensionless Spectrum for Altitude Band #5	A-9
A-6	Dimensionless Spectrum for Altitude Band #6	A-11
B-1	Dimensional and Dimensionless Minimum Frequency Limits	B-4
C-1	Matrix of Spectral Analysis Figures	C-1
D-1	Mean Value of Gust and Gust Gradients	D-1
D-2	Standard Deviation of Gust and Gust Gradients	D-2
D-3	Ratio of the Theoretical Energy Content to the Square of the Observed Standard Deviation	D-2
D-4	Matrix of Statistical Analysis Figures	D-3

LIST OF ILLUSTRATIONS

<u>Figure</u>		<u>Page</u>
2-1	Discrete White Noise Series	2-11
2-2	White Noise Spectra	2-12
2-3	Effects of Aliasing on White Noise Spectrum.	2-16
3-1	Relationship Between t_{iM} , $t_{iM'}$, and $t_{iM'+1}$	3-4
B-1	Spectrum of $\Phi_{33/11}$ for Impulse Response Function with $t_{\max} = 42.10573$	B-2
B-2	Spectrum of $\Phi_{33/11}$ for Impulse Response Function with $t_{\max} = 85.895689$	B-3
C-1	u_1 - Gust Spectrum. Altitude Band #1	C-2
c-2	u_1 - Gust Spectrum. Altitude Band #2	C-2
c-3	u_1 - Gust Spectrum. Altitude Band #3	C-3
c-4	u_1 - Gust Spectrum. Altitude Band #4	C-3
c-5	u_1 - Gust Spectrum. Altitude Band #5	C-4
C-6	u_1 - Gust Spectrum. Altitude Band #6	C-4
c-7	u_2 - Gust Spectrum. Altitude Band #1	C-5
C-8	u_2 - Gust Spectrum. Altitude Band #2	C-5
c-9	u_2 - Gust Spectrum. Altitude Band #3	C-6
C-10	u_2 - Gust Spectrum. Altitude Band #4	C-6
C-11	u_2 - Gust Spectrum. Altitude Band #5	C-7
C-12	u_2 - Gust Spectrum. Altitude Band #6	C-7
C-13	u_3 - Gust Spectrum. Altitude Band #1	C-8
C-14	u_3 - Gust Spectrum. Altitude Band #2	C-8
C-15	u_3 - Gust Spectrum. Altitude Band #3	C-9
C-16	u_3 - Gust Spectrum. Altitude Band #4	C-9
C-17	u_3 - Gust Spectrum. Altitude Band #5	C-10
C-18	u_3 - Gust Spectrum. Altitude Band #6	C-10
c-19	$\partial u_2 / \partial x_1$ - Gust Gradient Spectrum. Altitude Band #1	C-11
c-20	$\partial u_2 / \partial x_1$ - Gust Gradient Spectrum. Altitude Band #2	C-11
C-21	$\partial u_2 / \partial x_1$ - Gust Gradient Spectrum. Altitude Band #3	C-12

LIST OF ILLUSTRATIONS
(Continued)

<u>Figure</u>		<u>Page</u>
c-22	$\partial u_2 / \partial x_1$ - Gust Gradient Spectrum, Altitude Band #4	C-12
C-23	$\partial u_2 / \partial x_1$ - Gust Gradient Spectrum, Altitude Band #5	C-13
C-24	$\partial u_2 / \partial x_1$ - Gust Gradient Spectrum, Altitude Band #6	C-13
C-25	$\partial u_3 / \partial x_1$ - Gust Gradient Spectrum, Altitude Band #1	C-14
C-26	$\partial u_3 / \partial x_1$ - Gust Gradient Spectrum, Altitude Band #2	C-14
C-27	$\partial u_3 / \partial x_1$ - Gust Gradient Spectrum, Altitude Band #3	C-15
C-28	$\partial u_3 / \partial x_1$ - Gust Gradient Spectrum, Altitude Band #4	6-15
c-29	$\partial u_3 / \partial x_1$ - Gust Gradient Spectrum, Altitude Band #5	C-16
C-30	$\partial u_3 / \partial x_1$ - Gust Gradient Spectrum, Altitude Band #6	C-16
C-31	$\partial u_3 / \partial x_2$ - Gust Gradient Spectrum, Altitude Band #1	C-17
C-32	$\partial u_3 / \partial x_2$ - Gust Gradient Spectrum, Altitude Band #2	C-17
c-33	$\partial u_3 / \partial x_2$ - Gust Gradient Spectrum, Altitude Band #3	C-18
c-34	$\partial u_3 / \partial x_2$ - Gust Gradient Spectrum, Altitude Band #4	C-18
c-35	$\partial u_3 / \partial x_2$ - Gust Gradient Spectrum, Altitude Band #5	C-19
C-36	$\partial u_3 / \partial x_2$ - Gust Gradient Spectrum, Altitude Band #6	C-19
D-1	u_1 - Gust Probability Density Distribution, Altitude Band #1 . . .	D-4
D-2	u_1 - Gust Probability Density Distribution, Altitude Band #2 . . .	D-5
D-3	u_1 - Gust Probability Density Distribution, Altitude Band #3 . . .	D-6
D-4	u_1 - Gust Probability Density Distribution, Altitude Band #4 . . .	D-7
D-5	u_1 - Gust Probability Density Distribution, Altitude Band #5 . . .	D-8
D-6	u_1 - Gust Probability Density Distribution, Altitude Band #6 . . .	D-9
D-7	u_2 - Gust Probability Density Distribution, Altitude Band #1 . . .	D-10
D-8	u_2 - Gust Probability Density Distribution, Altitude Band #2 . . .	D-11
D-9	u_2 - Gust Probability Density Distribution, Altitude Band #3 . . .	D-12
D-10	u_2 - Gust Probability Density Distribution, Altitude Band #4 . . .	D-13
D-11	u_2 - Gust Probability Density Distribution, Altitude Band #5 . . .	D-14
D-12	u_2 - Gust Probability Density Distribution, Altitude Band #6 . . .	D-15
D-13	u_3 - Gust Probability Density Distribution, Altitude Band #1 . . .	D-16
D-14	u_3 - Gust Probability Density Distribution, Altitude Band #2 . . .	D-17
D-15	u_3 - Gust Probability Density Distribution, Altitude Band #3 . . .	D-18

LIST OF ILLUSTRATIONS

(Continued)

<u>Figure</u>		<u>Page</u>
D-16	u_3 - Gust Probability Density Distribution, Altitude Band #4 . . .	D-19
D-17	u_3 - Gust Probability Density Distribution, Altitude Band #5 . . .	D-20
D-18	u_3 - Gust Probability Density Distribution, Altitude Band #6 . . .	D-21
D-19	$\partial u_2 / \partial x_1$ - Gust Gradient Probability Density Distribution, Altitude Band #1	D-22
D-20	$\partial u_2 / \partial x_1$ - Gust Gradient Probability Density Distribution, Altitude Band #2	D-23
D-21	$\partial u_2 / \partial x_1$ - Gust Gradient Probability Density Distribution, Altitude Band #3	D-24
D-22	$\partial u_2 / \partial x_1$ - Gust Gradient Probability Density Distribution, Altitude Band #4	D-25
D-23	$\partial u_2 / \partial x_1$ - Gust Gradient Probability Density Distribution, Altitude Band #5	D-26
D-24	$\partial u_2 / \partial x_1$ - Gust Gradient Probability Density Distribution, Altitude Band #6	D-27
D-25	$\partial u_3 / \partial x_1$ - Gust Gradient Probability Density Distribution, Altitude Band #1	D-28
D-26	$\partial u_3 / \partial x_1$ - Gust Gradient Probability Density Distribution, Altitude Band #2	D-29
D-27	$\partial u_3 / \partial x_1$ - Gust Gradient Probability Density Distribution, Altitude Band #3	D-30
D-28	$\partial u_3 / \partial x_1$ - Gust Gradient Probability Density Distribution, Altitude Band #4	D-31
D-29	$\partial u_3 / \partial x_1$ - Gust Gradient Probability Density Distribution, Altitude Band #5	D-32
D-30	$\partial u_3 / \partial x_1$ - Gust Gradient Probability Density Distribution, Altitude Band #6	D-33
D-31	$\partial u_3 / \partial x_2$ - Gust Gradient Probability Density Distribution, Altitude Band #1	D-34
D-32	$\partial u_3 / \partial x_2$ - Gust Gradient Probability Density Distribution, Altitude Band #2	D-35
D-33	$\partial u_3 / \partial x_2$ - Gust Gradient Probability Density Distribution, Altitude Band #3	D-36
D-34	$\partial u_3 / \partial x_2$ - Gust Gradient Probability Density Distribution, Altitude Band #4	D-37

LIST OF ILLUSTRATIONS
(Concluded)

<u>Figure</u>		<u>Page</u>
D-35	$\partial u_3 / \partial x_2$ - Gust Gradient Probability Density Distribution, Altitude Band #5	D-38
D-36	$\partial u_3 / \partial x_2$ - Gust Gradient Probability Density Distribution, Altitude Band #6	D-39

1. INTRODUCTION

The effects of atmospheric turbulence in both horizontal and near-horizontal flight, during the return of the Space Shuttle, are important for **determining** design, control, and "pilot-in-the-loop" effects. A non-recursive model (based on von Karman spectra) for atmospheric turbulence along the flight path of the Shuttle Orbiter has been developed which provides for simulation of instantaneous vertical and horizontal gusts at the vehicle center-of-gravity, and also for simulation of instantaneous gust gradients. Based on **this** model the time series for both gusts and gust gradients have been generated and stored on a series of magnetic tapes which are entitled Shuttle Stimulation Turbulence Tapes (SSTT). The time series are designed to represent atmospheric turbulence from ground level to an altitude of 120,000 meters,

A **description** of the turbulence generation procedure is provided in Section 2. The results of validating the simulated turbulence are described in Section 3. Conclusions and **recommendations** are presented in Section 4 with Section 5 containing references cited. Appendix A contains the tabulated one-dimensional von Karman spectra while Appendix B provides a discussion of the minimum frequency stimulated. Appendices C and D present the results of spectral and statistical analyses of the SSTT. A more detailed description of the proper use of the tapes is provided elsewhere [1].

2. TURBULENCE GENERATION PROCEDURE

The non-recursive turbulence model used to generate the SSTT is based on von Karman spectra with finite upper limits corresponding to the dimensions of the Space Shuttle, relative to the scale of turbulence in the atmosphere. Because the scale of turbulence increases with altitude while the dimensions of the Space Shuttle are fixed, the finite upper limits of the von Karman spectra increase with altitude. In order to take into account the resulting spectral changes, the atmosphere, extending from ground level to 120,000 meters, was divided into six altitude bands. The subsections which follow provide a description of the development and application of the turbulence generation procedures.

2.1 BACKGROUND

The current turbulence model represents the results of the development and evaluation of several different turbulence simulation techniques. Two of the earlier techniques, which were given serious consideration, warrant further discussion.

Initial efforts involved refinement and evaluation of a turbulence model, TBMOD [2], which had been developed elsewhere [3]. This model was based on discretization of the Fourier integral representation of turbulence and was designed for use with von Karman spectra. Several problems were encountered with TBMOD, both theoretical and practical. First, from a theoretical standpoint, the assumptions used in the development of the shear (gust gradient) simulation were difficult to justify. Second, from a practical standpoint, the output of TBMOD, representing turbulent gusts, when subjected to Fast Fourier Transform (FFT) spectral analysis, did not possess the proper von Karman spectral shape. Because of such problems, further development of the model was halted.

The second simulation technique was based on digital filter theory coupled with a combined von Karman - Saffman spectral model [4]. Meromorphic functions were used to approximate the various spectra. Based on **z-transform** theory, recursive difference equations were derived from such approximations. Such difference equations were then used to generate

the appropriate turbulence gusts and gust gradients. Unfortunately the recursive difference equations, in addition to being somewhat complex, proved numerically unstable and could not be used in their original recursive form [5].

A non-recursive version of the same difference equations was subsequently developed in an effort to overcome the stability problem [5]. These difference equations were also quite complex but resembled in form the output of digital filters, characterized by some impulse response function, with a white noise input. The present model, as described in subsections 2.2 through 2.4, was an outgrowth of this resemblance.

2.2 SELECTION OF ATMOSPHERIC BANDS

The standard deviations ($\sigma_1, \sigma_2, \sigma_3$) and the integral scale lengths (L_1, L_2, L_3) of atmospheric turbulence are functions of altitude, as shown in Table 2-1. Notice should be taken that the values for σ_i and L_i presented in this table are consistent with those presented in JSC 7700 [6]. Based on the variation of σ_i and L_i presented in Table 2-1, the atmosphere was divided into six altitude bands as presented in Table 2-2. Within each band, as also indicated in Table 2-2, characteristic integral scales of turbulence were selected for use in calculating the finite upper limit of the turbulence spectral model discussed in subsection 2.3.

2.3 DEVELOPMENT OF VON KARMAN SPECTRA WITH FINITE UPPER LIMITS

As developed previously [5] the basic three-dimensional von Karman relation to be integrated for the dimensionless gust spectra is,

$$\phi_{11}(\Omega_1, \Omega_2, \Omega_3) = \frac{55}{36\pi^2} \frac{\Omega^2 - \Omega_1^2}{(1+\Omega^2)^{17/6}} \quad (2-1)$$

The corresponding von Karman relation for dimensionless gust gradient spectra is

$$\phi_{11/jj}(\Omega_1, \Omega_2, \Omega_3) = \frac{55}{36\pi^2 a_3} \frac{\Omega^2 - \Omega_1^2}{(1+\Omega^2)^{17/6}} \quad (2-2)$$

These three-dimensional spectral relations must be integrated over certain ranges of values of Ω_2 and Ω_3 to obtain one-dimensional spectral models $\Phi_{11}(\Omega_1)$ and $\Phi_{11/jj}(\Omega_1)$.

TABLE 2-1. VARIATION OF STANDARD DEVIATION
AND LENGTH SCALE WITH ALTITUDE*

ALTITUDE (m)	STANDARD DEVIATION OF TURBULENCE			INTEGRAL SCALES OF TURBULENCE		
	σ_1 (m/sec)	σ_2 (m/sec)	σ_3 (m/sec)	L_1 (m)	L_2 (m)	L_3 (m)
10	2.31	1.67	1.15	21	11	5
20	2.58	1.98	1.46	33	19	11
30	2.75	2.20	1.71	43	28	17
40	2.88	2.36	1.89	52	35	23
50	2.98	2.49	2.05	61	42	29
60	3.07	2.61	2.19	68	49	35
70	3.15	2.71	2.32	75	56	41
80	3.22	2.81	2.43	82	63	47
90	3.28	2.89	2.54	89	69	53
100	3.33	2.97	2.64	95	75	59
200	3.72	3.53	3.38	149	134	123
304.8	31.95/4.37	3.95/4.37	3.95/4.37	1961300	190/300	1921300
400	4.39	4.39	4.39	300	300	300
500	4.39	4.39	4.39	300	300	300
600	4.39	4.39	4.39	300	300	300
700	4.39	4.39	4.39	300	300	300
762	4.39/5.70	4.39/5.70	4.39/5.70	300/533	300/533	300/533
800	5.70	5.70	5.70	533	533	533
900	5.70	5.70	5.70	533	533	533
1524	5.70/5.79	5.70/5.79	5.70/5.79	533	533	533
2000	5.79	5.79	5.79	533	533	533
3048	51.79/5.52	5.79/5.52	51.79/5.52	533	533	533
4000	5.52	5.52	5.52	533	533	533
5000	5.52	5.52	5.52	533	533	533
6096	51.52/5.27	5.52/5.27	5.52/5.27	533	533	533
7000	5.27	5.27	5.27	533	533	533
8000	5.27	5.27	5.27	533	533	533
9144	5.27/4.22	5.27/4.22	5.27/4.22	533	533	533
10000	4.22	4.22	4.22	533	533	533
20000	6.01	6.01	4.22	6691	6691	955

Double entries for a tabulated altitude indicate a step change in standard deviation or integral scale at that altitude.

TABLE 2-1. VARIATION OF STANDARD DEVIATION
AND LENGTH SCALE WITH ALTITUDE (Continued)

ALTITUDE (m)	STANDARD DEVIATION OF TURBULENCE			INTEGRAL SCALES OF TURBULENCE		
	σ_1 (m/sec)	σ_2 (m/sec)	σ_3 (m/sec)	L_1 (m)	L_2 (m)	L_3 (m)
27000	7.00	7.00	4.22	20000	20000	1230
30000	8.23	8.23	4.66	23533	23533	1443
40000	12.82	12.82	6.09	36693	36693	2231
50000	18.08	18.08	7.51	51786	51786	3128
60000	23.94	23.94	8.90	68623	68623	4124
70000	30.36	30.36	10.28	87063	87063	5208
80000	37.29	37.29	11.65	106998	106998	6376
90000	44.70	44.70	13.01	128338	128338	7622
100000	52.58	52.58	14.35	151010	151010	8941
110000	60.89	60.89	15.69	174950	174950	10330
120000	69.62	69.62	17.02	200000	200000	11800

2.3.1 Upper Limits of Integration

The upper limits of integration for $j = 2$ and 3 are calculated according to the relation [7]

$$\Omega_{ijmax} = aL_i/\lambda_j \quad (j = 2, 3) \quad (2-3)$$

where

$$a = 1,339$$

L_i = integral scale of turbulence associated with the $\Phi_{ii}(\Omega_1)$ spectrum

λ_j = characteristic length of Space Shuttle in the j th direction

Values of L_i for the six bands are given in Table 2-2 while the characteristic lengths, λ_j s are presented in Table 2-3.

TABLE 2-2. SUMMARY OF TURBULENCE PARAMETERS
IN DISCRETE ALTITUDE BANDS

BAND #	LOWER LIMIT (m)	UPPER LIMIT (m)	TURBULENCE LENGTH L _i (m)			TIME INTERVAL T _i (dimensionless)	MAXIMUM FREQUENCY Ω _{i1max} (dimensionless)		
			i = 1	i = 2	i = 3		i = 1	i = 2	i = 3
1	0	30	43.4	27.7	16.8	.6520	1.022	1.684	4.818
2	30	304.8	196	190	192	.1444	.1489	.1474	21.76
3	304.8	762	300	300	300	.09432	.09432	.09432	33.310
4	762	10,000	533	533	533	.05309	.05309	.05309	59.180
5	10,000	27,000	20,000	20,000	1,230	.004266	.004266	.06785	736.5
6	27,000	120,000	200,000	200,000	11,800	.003511	.003511	.05950	894.9
									52.80

NOTE: i = 1 applies to u₁-gust
 i = 2 applies to u₂-gust and $\partial u_2 / \partial x_i$ gust gradients
 i = 3 applies to u₃-gust and $\partial u_3 / \partial x_1$ gust gradients

TABLE 2-3. CHARACTERISTIC DIMENSIONS
OF THE SPACE SHUTTLE [8]

Characteristic Length	Magnitude (ft) (m)		Explanation
ℓ_1	39.56	12.06	mean aerodynamic chord
	39.05	11.9	1/2 wingspan
ℓ_3	10.95	3.34	1/2 fuselage thickness

In the case of $\Omega_{i1\max}$ special consideration must be given to the dimensional frequencies corresponding to the dimensionless limits. The dimensional frequency limit satisfies the relation

$$f_{1\max} = \Omega_{i1\max} V / (2\pi a L_i) \quad (2-4)$$

where

V = vehicle velocity

The maximum dimensional frequency which the Space Shuttle simulators are capable of handling is 4 hertz. Thus any higher frequencies should be excluded from the simulation. For this reason the dimensionless frequency limit $\Omega_{i1\max}$ must satisfy the relation

$$\Omega_{i1\max} = \min(a L_i / \ell_1, 2\pi a L_i f_{1\max} / V) \quad (2-5)$$

where

$$f_{1\max} = 4 \text{ hertz}$$

Values of $\Omega_{i1\max}$ based on Eq (2-5) are included in Table 2-2.

2.3.2 One-Dimensional Spectra

There are six spectra of primary interest for turbulence simulation, as indicated in Table 2-4. Based on second-order numerical integration, the six corresponding three-dimensional gust and gust gradient spectral relations, as given by Eqs (2-1) and (2-2), were integrated over Ω_3 and Ω_2 (with the appropriate upper limits). The resulting one-dimensional spectra for all altitude bands are presented in Appendix A. These spectra were used in establishing the impulse response functions associated with digital filter simulation processes described in subsection 2.4.

TABLE 2-4. TYPES OF SIMULATED TURBULENCE

Type	Corresponding Spectrum	Comments
u_1	Φ_{11}	longitudinal gust
u_2	Φ_{22}	transverse gust
u_3	Φ_{33}	vertical gust
$\partial u_2 / \partial x_1$	$\Phi_{22/11}$	yaw
$\partial u_3 / \partial x_1$	$\Phi_{33/11}$	pitch
$\partial u_3 / \partial x_2$	$\Phi_{33/22}$	roll

2.3.3 Dimensionless Energy Content

The total dimensionless energy content of each one-dimensional spectra in each altitude band was established by integrating the corresponding spectra over the appropriate finite limits, indicated in Table 2-2. The resulting energy content is presented in Table 2-5. As might be expected

TABLE 2-5. DIMENSIONLESS ENERGY CONTENT FOR GUSTS AND GUST GRADIENTS

ALTITUDE BAND	SPECTRUM					
	Φ_{11}	Φ_{22}	Φ_{33}	$\Phi_{22/11}$	$\Phi_{33/11}$	$\Phi_{33/22}$
1	.6225	.5010	.2752	.5877	.1525	.1557
2	.8595	.8560	.8383	13.147	12.171	12.308
3	.8956	.8952	.8809	24.767	22.643	22.890
4	.9298	.9296	.9197	54.123	49.527	50.060
5	.9977	.9953	.9251	1740.	41.71	95.62
6	1.000	.9973	.9363	2309.	52.08	391.6

the total dimensionless energy content of each of the turbulent gust series is less than unity. The dimensionless energy content for each gust gradient, however, is not limited in such a manner and range as high as 391.6. For both gusts and gust gradients the total energy content increases with altitude because of similar increases in the limits of integration,

2.4 DIGITAL FILTER SIMULATION

As suggested in subsection 2.1, simulated turbulence, $\gamma(t)$, can be interpreted as the response or output of a control system [9] with double-sided response functions, $h(t)$, subject to an input consisting of Gaussian white noise $I(t)$. This response can be represented by the convolution integral

$$\gamma(t) = \int_{-\infty}^{\infty} h(\tau) I(t-\tau) d\tau \quad (2-6)$$

Based on filter theory the double-sided spectrum, $\Phi_{DY}(\Omega)$, of the simulated turbulence satisfies the relation

$$\Phi_{DY}(\Omega_1) = H(\Omega_1)H^*(\Omega_1)\Phi_{DI}(\Omega_1) \quad (2-7)$$

where $H(\Omega_1) = F[h(t)]$

$\Phi_{DI}(\Omega_1)$ = double-sided power spectrum for white noise

Generally the standard deviation of any white noise signal has a value of unity. Furthermore in most practical situations the white noise is defined to occur over some interval extending from $-\Omega_{1max}$ to $+\Omega_{1max}$. For this case ,

$$\begin{aligned} \Phi_{DI}(\Omega_1) &= \frac{1}{2\Omega_{1max}} \\ &= \frac{T}{2\pi} \end{aligned} \quad (2-8)$$

* Actually the term "energy" is not precise when dealing with gust gradients.

** The subscript, i , normally applied to the variables Ω_{1max} and T , has been suppressed in Eqs (2-8) through (2-13) for simplicity.

where

$T = \text{time interval associated with generation process } (= \pi/\Omega_{\max})$

By substitution,

$$\Phi_{DY}(\Omega_1) = H(\Omega_1)H^*(\Omega_1) \frac{T}{2\pi} \quad (2-9)$$

If $H(\Omega_1)$ is limited to real values,

$$\Phi_{DY}(\Omega_1) = H^2(\Omega_1) \frac{T}{2\pi} \quad (2-10)$$

Rearrangement of Eq (2-10) yields

$$H(\Omega_1) = \sqrt{\frac{2\pi}{T} \Phi_{DY}(\Omega_1)} \quad (2-11)$$

Then based on the definition of the inverse Fourier transform, the double-sided impulse response function $h(t)$ can be expressed as

$$\begin{aligned} h(t) &= F^{-1}[H(\Omega_1)] \\ &= \int_{-\infty}^{\infty} \sqrt{\frac{2\pi}{T} \Phi_{DY}(\Omega_1)} \cos(\Omega_1 t) d\Omega_1 \\ &= 2 \int_0^{\infty} \sqrt{\frac{2\pi}{T} \Phi_{DY}(\Omega_1)} \cos(\Omega_1 t) d\Omega_1 \\ &= 2 \int_0^{\infty} \sqrt{\frac{2\pi}{T} \frac{\Phi_Y(\Omega_1)}{2}} \cos(\Omega_1 t) d\Omega_1 \\ &= 2 \sqrt{\frac{\pi}{T}} \int_0^{\infty} \sqrt{\Phi_Y(\Omega_1)} \cos(\Omega_1 t) d\Omega_1 \end{aligned} \quad (2-12)$$

where

$\Phi_Y(\Omega_1) = \text{single-sided spectrum of } Y(t)$

The single-sided spectra tabulated in Appendix A correspond to $\Phi_Y(\Omega_1)$

The discrete version of the convolution integral given in Eq (2-6) yields

$$Y(k) = \sum_{j=-N}^{+N} h(j) I(k-j) T \quad (2-13)$$

where

$Y(k)$ = discrete sampled turbulence output

$h(j)$ = discrete double-sided impulse response function $h(jT)$

$I(k)$ = discrete sampled white noise input

Eq (2-13) represents the basic, non-recursive relation for the generation of simulated turbulence. The impulse response functions $h(t)$ were evaluated by means of second-order numerical integration of Eq (2-12) using the six spectra from Appendix A. In carrying out this evaluation some maximum value of t must be established, corresponding to the value of N for Eq (2-13), and replacing the infinite limit of Eq (2-6). As discussed in Appendix B this maximum time limit determines the minimum frequency, $\Omega_{i1\max}$, for which the corresponding spectrum is accurately simulated.

The values of dimensionless time increment, T_i , used for the six altitude bands are included in Table 2-2 and are based on the values of Ω_{imax} shown in the same table. Thus the Nyquist generation frequencies Ω_{ING} for the simulated turbulence correspond to the upper frequency limits for Ω_{i1} as computed by Eq (2-5) for each altitude band,

*

In certain references 19,111 to correct for the "effect of digitizing" the series represented by Eq (2-13) has been divided by \sqrt{T} . This process can be seen to be dimensionally incorrect and actually results from the use of a white noise spectrum with unit strength instead of a strength of $T/2\pi$.

2.5 EFFECTS OF DIGITIZATION

The effects of digitization in turbulence simulation have been considered by a number of investigators [9-12]. As a result of these studies two basic digitization effects have been generally identified.

The first effect results from the assumption of a white noise spectrum **with unit strength** instead of **unit power**, noted in subsection 2.4. To correct for such an "effect" the proposed procedure is to divide the series approximation of the convolution integral by \sqrt{T} . This "effect" disappears when the white noise spectrum has unit power.

The second effect involves the *tapering* of the spectrum of simulated white noise, Φ_1^t , in the vicinity of the Nyquist generation frequency, Ω_{NG} . Some investigators [10,12] have considered it necessary, because of the tapering effect, to generate the simulated turbulence time series at a rate from four to ten times the rate at which the series will be sampled.

The second effect arises from the discrete processes associated with both the generation and sampling of the simulated turbulence. In the case of discrete white noise with unit variance, the time series involved is basically a train of step functions as shown in Figure 2-1. The autocorrelation function of the train of step functions depicted in Figure 2-1 can

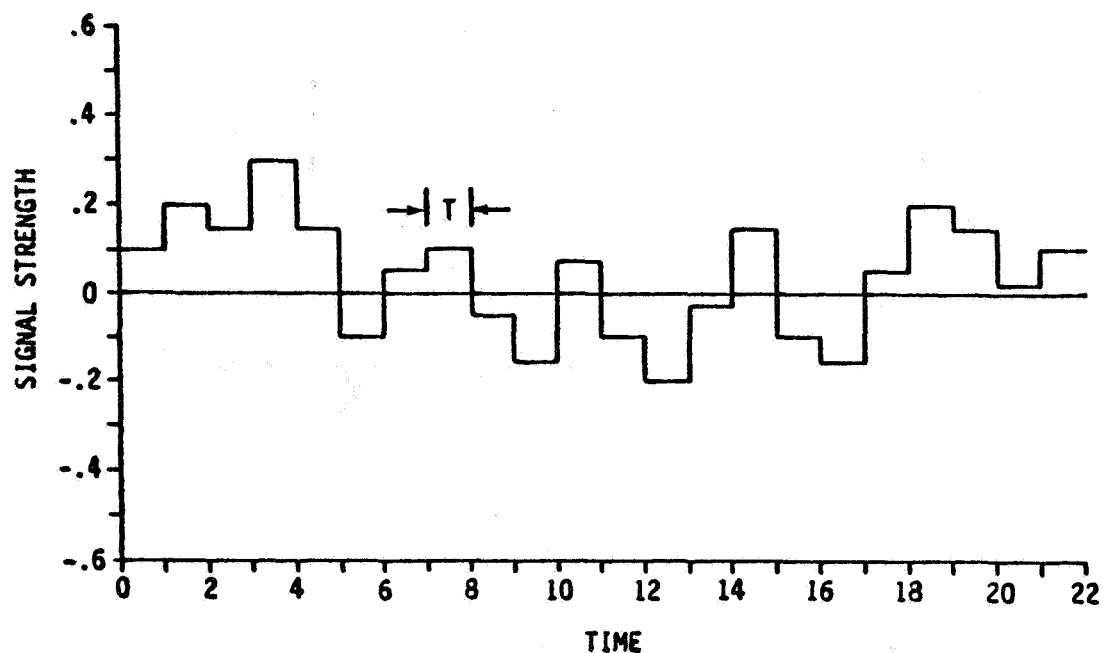


Figure 2-1. Discrete White Noise Series

be shown to be

$$R_{DI}(\tau) = \begin{cases} 1 - \frac{|\tau|}{T_G} & (|\tau| \leq T_G) \\ 0 & (|\tau| > T_G) \end{cases} \quad (2-14)$$

The corresponding double-sided power spectrum by definition is

$$\begin{aligned} \Phi_{DI}^*(\Omega) &\equiv E[R_{DI}(\tau)] \\ &= \frac{T_G}{2\pi} \frac{\sin^2(\Omega T_G/2)}{(\Omega T_G/2)^2} \\ &= \frac{1}{2\Omega_{NG}} \frac{\sin^2(\Omega\pi/2\Omega_{NG})}{(\Omega\pi/2\Omega_{NG})^2} \end{aligned} \quad (2-15)$$

The single-sided version of this power spectrum is shown in Figure 2-2.

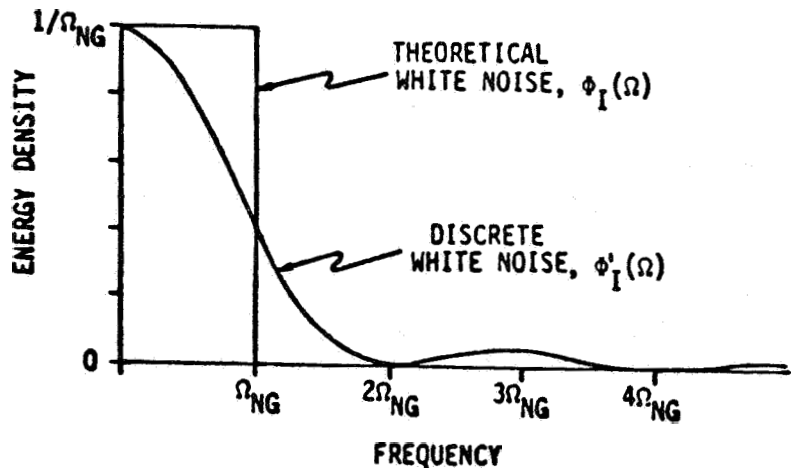


Figure 2-2. White Noise Spectra

Theoretical white noise, by definition, is characterized by a uniform power spectral distribution. In order to avoid infinite power, such a spectral distribution is normally restricted to the frequency band ($-\Omega_{NG} \leq \omega \leq \Omega_{NG}$) for a double-sided spectrum. For a signal with unit power the spectral density function for such white noise is

$$\Phi_{DI}(\Omega) = \begin{cases} \frac{1}{2\Omega_{NG}} & (-\Omega_{NG} \leq \Omega \leq \Omega_{NG}) \\ 0 & (\Omega_{NG} < |\Omega|) \end{cases} \quad (2-16)$$

Such a theoretical distribution in single-sided form is also shown in Figure 2-2.

It is important to note that the two power spectra shown in Figure 2-2 are both normalized and thus

$$\int_{-\infty}^{\infty} \Phi_{DI}(\Omega) d\Omega = \int_{-\infty}^{\infty} \Phi'_{DI}(\Omega) d\Omega = 1 \quad (2-17)$$

The theoretical spectrum is basically a rectangular pulse function while the discrete spectrum is characterized by tapering. The difference between these two spectra is generally considered the basis for the second digitization effect,

The preceding descriptions of the two spectra $\Phi_I(\Omega)$ and $\Phi_{DI}(\Omega)$ are based purely on mathematical theory. To observe such spectra in reality the corresponding time series would have to be sampled with an infinitesimal sampling interval. Actually, finite sampling intervals, T_s , must be used but this finite (or discrete) sampling process results in *aliasing*. The aliased spectrum, $\Phi^+(\Omega)$, based on the finite sampling process, is related to the original spectrum according to the relation [13]

$$\Phi^+(\Omega) = \sum_{k=-\infty}^{\infty} \Phi(\Omega + 2k\Omega_{NS}) \quad (2-18)$$

where

$$\Omega = \text{Nyquist sampling frequency } (\pi/T_S)$$

For the case of the discrete white noise

$$\begin{aligned} \Phi'^+_{DI}(\Omega) &= \sum_{k=-\infty}^{\infty} \Phi'_{DI}(\Omega + 2k\Omega_{NS}) \\ &= \frac{1}{2\Omega_{NG}} \sum_{k=-\infty}^{\infty} \frac{\sin^2[(\Omega + 2k\Omega_{NS})\pi/2\Omega_{NG}]}{[(\Omega + 2k\Omega_{NS})\pi/2\Omega_{NG}]^2} \end{aligned} \quad (2-19)$$

Numerical evaluation of this series has been carried out for $\Omega_{NG} = 100$ with various ratios of Ω_{NS}/Ω_{NG} , including .5, 1, 2, and 4. The resulting aliased spectra are presented in Figure 2-3. It is important to note that the figure indicates that

$$\Phi'^+_{DI}(\Omega) = \begin{cases} \frac{1}{2\Omega_{NG}} & (-\Omega_{NG} \leq \Omega \leq \Omega_{NG}) \\ 0 & (\Omega_{NG} < |\Omega|) \end{cases} \quad (\Omega_{NG} = \Omega_{NS}) \quad (2-20)$$

In this case, by comparison with $\Phi_{DI}(\Omega)$,

$$\Phi'^+_{DI}(\Omega) = \Phi_{DI}(\Omega) \quad (\Omega_{NG} = \Omega_{NS}) \quad (2-21)$$

Thus for white noise *the aliasing due to discrete sampling exactly offsets the tapering due to discrete generation when the sampling frequency equals the generation frequency.* Based on this fundamental point, it is clear that in the simulation of white noise no tapering of the spectrum occurs as long as the sampling rate equals the generation rate. Under most conditions this equality is automatically satisfied,

The process of convolving the white noise with the appropriate impulse response function is also carried out in a discrete manner. The process involves selecting (or sampling) values of the white noise signal and the impulse response function at equal intervals in time and then approximating the convolution integral by a summation of products. It is important to note that the discrete sampling of both the white noise and the impulse response function normally occurs at the same rate as the generation rate for the white noise. Thus the resulting spectra for the sampled discrete white noise, as previously shown, will be uniform. According to the convolution theorem, the spectrum of the output signal equals the spectrum of the input white noise multiplied by the product of the Fourier transform of the impulse response function and its complex conjugate. Thus, as previously noted in subsection 2.4, for a continuous signal,

$$\Phi_{DY}(\Omega) = \Phi_{DI}(\Omega)H(\Omega)H^*(\Omega) \quad (2-22)$$

The Fourier transform $H(\Omega)$ for the *continuous* impulse function, $h(t)$, is

$$\begin{aligned} H(\Omega) &= F[h(t)] \\ &= \sqrt{\frac{2\pi}{T}} \Phi_{DY}(\Omega) \end{aligned} \quad (2-23)$$

The corresponding output spectrum for a discrete signal would be

$$\Phi'_{DY}(\Omega) = \Phi'_{DI}(\Omega)H'(\Omega)H'^*(\Omega) \quad (2-24)$$

The Fourier transform $H'(\Omega)$ of the *discrete* impulse response function, $h'(t)$, is

$$H'(\Omega) = F[h'(t)] \quad (2-25)$$

Based on the preceding development, for cases in which the sampling frequency equals the generation frequency, any difference between the discrete turbulence spectrum and the continuous spectrum apparently originates because of some difference between $H(\Omega)$ and $H'(\Omega)$.

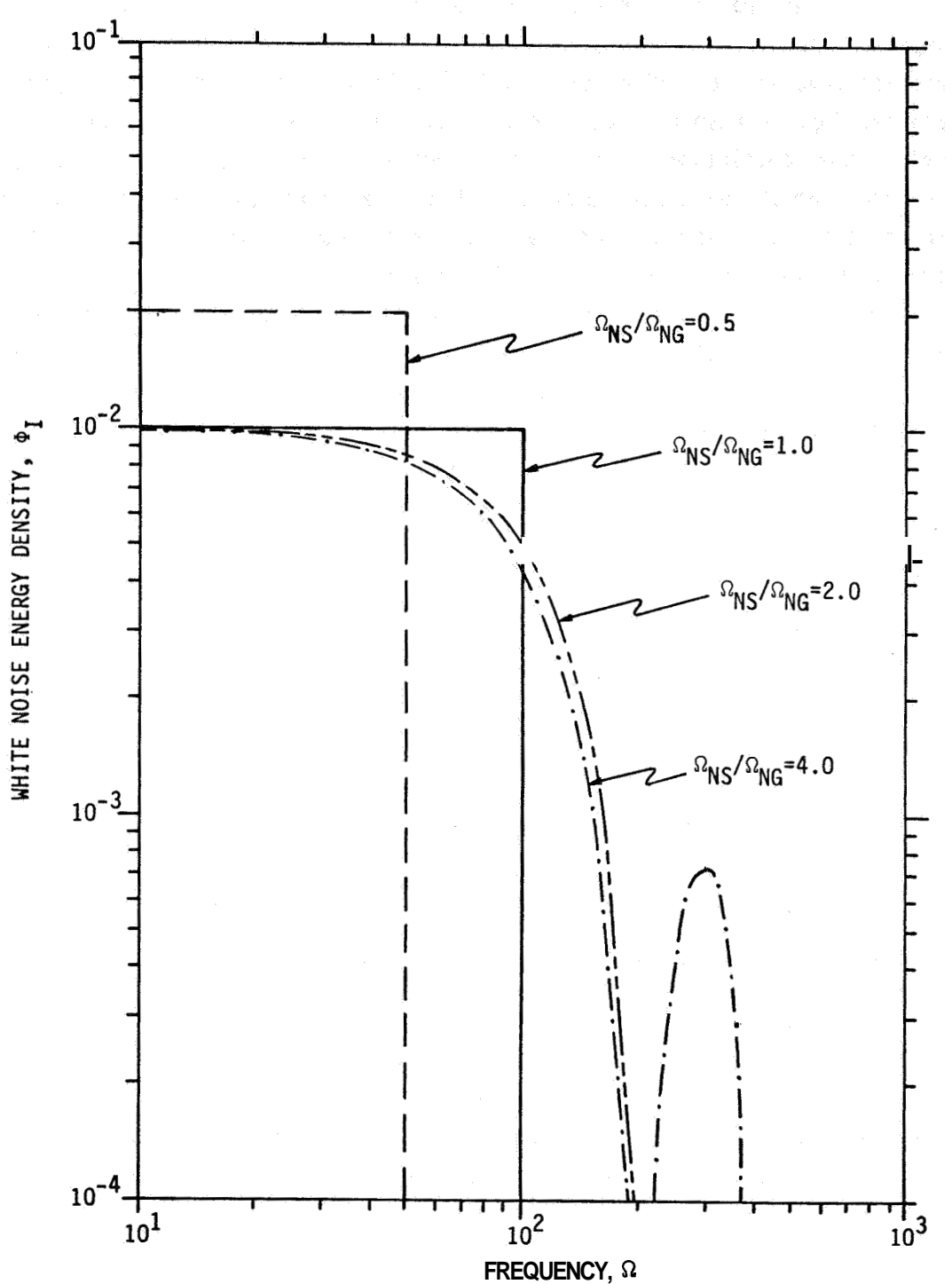


Figure 2-3. Effects of Aliasing on White Noise Spectrum

3. SIMULATED TURBULENCE TAPES

The turbulence generation procedure described in Section 2 has been used to generate six dimensionless simulated turbulence time series which are stored on magnetic tapes as summarized in Table 3-1. The appropriate procedures for using the tapes are described elsewhere [1]. Subsection 3.1 provides a description of the results of validating the tapes while subsection 3.2 presents an explanation of the process for converting from dimensionless to dimensional values.

TABLE 3-1. INDEX OF SHUTTLE SIMULATED
TURBULENCE TAPES (SSTT)

Tape	Time Series	Comments
SSTT-1	u_1 - gust	longitudinal gust
SSTT-2	u_2 - gust	transverse gust
SSTT-3	u_3 - gust	vertical gust
SSTT-4	$\partial u_2 / \partial x_1$ - gust gradient	yaw
SSTT-5	$\partial u_3 / \partial x_1$ - gust gradient	pitch
SSTT-6	$\partial u_3 / \partial x_2$ - gust gradient	roll

3.1 VALDIATION OF SIMULATED TURBULENCE

A spectral analysis of each of the dimensionless time series has been carried out by means of a Fast Fourier Transform FFT4 [14]. The results, which are presented in Appendix C, demonstrate that the simulated turbulence possesses the proper von Karman spectral characteristics.

All of the dimensionless time series have also been analyzed statistically to determine the gust and gust gradient probability density functions. As shown in Appendix D the results of these analyses indicate that both the simulated gusts and gust gradients are normally distributed, with near-zero means and standard deviations consistent with the energy content presented in Table 2-5.

3.2 CONVERSION TO DIMENSIONAL VALUES

The dimensionless time series on each tape must be converted to dimensional form before actual use in a simulation exercise. The conversion process generally involves multiplication and/or division by the appropriate turbulence parameters. For dimensionless gusts, u_i^* , the corresponding standard deviation, σ_i , should be used. Thus

$$u_i^* = \sigma_i u_i \quad (3-1)$$

where

$$u_i^* = \text{dimensional gust}$$

For dimensionless gust gradient, $\frac{\partial u_i^*}{\partial x_j}$, the parameters σ_i and L_i are used. Thus

$$\frac{\partial u_i^*}{\partial x_j} = \frac{\sigma_i}{L_i} \frac{\partial u_i}{\partial x_j} \quad (3-2)$$

where

$$\frac{\partial u_i^*}{\partial x_j} = \text{dimensional gust gradient}$$

In the case of dimensionless time it is necessary to develop the procedures for converting both from dimensionless to dimensional form and also to dimensionless from dimensional. In proceeding from dimensionless to dimensional time the dimensionless time step, T_i^* , represents the basic unit to be converted. The conversion involves the vehicle velocity, V , and the turbulence scale, L_i . Thus

$$T_i^* = a L_i T_i / V \quad (3-3)$$

where

$$T_i^* = \text{dimensional time step}$$

It is important to note that because both L_i and V vary with altitude, the resulting dimensional time step Δt_i^* is not a constant. To obtain dimensional time, t_i , a summation process is involved as follows:

$$\begin{aligned} t_{iN}^* &= \sum_{n=1}^N \Delta t_{in}^* \\ &= a T_i \sum_{n=1}^N L_{in} / V_n \end{aligned} \quad (3-4)$$

where

$$\begin{aligned} L_{in} &= L_i(z_n) \\ V_n &= V(z_n) \\ z_n &= \text{altitude at } n\text{th step} \end{aligned}$$

In converting to dimensionless from dimensional time the basic unit, the dimensional time step, δt , will normally be a constant. The corresponding dimensionless time interval, T_{im}^* , will be

$$T_{im}^* = \frac{V_m \delta t}{a L_{im}} \quad (3-5)$$

The total dimensionless time, t_{iM}^* , will be

$$\begin{aligned} t_{iM}^* &= \sum_{m=1}^M T_{im}^* \\ &= \sum_{m=1}^M \frac{V_m \delta t^*}{a L_{im}} \\ &= \frac{\delta t^*}{a} \sum_{m=1}^M V_m / L_{im} \end{aligned} \quad (3-6)$$

The dimensionless time, t_{iM} , corresponds to some M' dimensionless time intervals, T_i , plus some fractional interval, T' , as follows:

$$t_{iM} = M'T_i + T' \quad (3-7)$$

where

$$0 \leq T' \leq T_i$$

Thus the number of dimensionless time intervals, M' , can be computed as

$$\begin{aligned} M' &= \text{Int}(t_{iM}/T_i) \\ &= \text{Int}\left(\frac{\delta t^*}{aT_i} \sum_{m=1}^{M'} V_m/L_{im}\right) \end{aligned} \quad (3-8)$$

where

$$\text{Int}() = \text{integer value of } ()$$

The fractional interval, T' , can be computed by the relation

$$T' = t_{iM} - M'T_i \quad (3-9)$$

The interpolation process will involve interpolating between $t_{iM'}$ and $t_{iM'+1}$ at the point t_{iM} as shown in Figure 3-1.

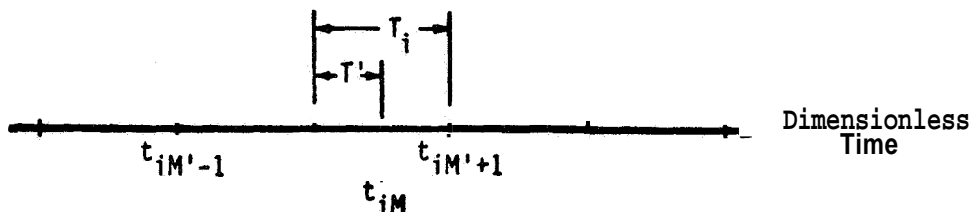


Figure 3-1. Relationship Between t_{iM} , $t_{iM'}$, and $t_{iM'+1}$

In the conversion to or from dimensional values three parameters are required: standard deviation, integral scale of turbulence, and vehicle

speed. The variation of the turbulence standard deviation, σ_i , with altitude was presented in Table 2-1. The same table contains the turbulence scale, L_i , as a function of altitude. The vehicle speed, V , is a function of altitude but also may vary from one trajectory to another. Table 3-2 provides *representative* values of V as a function of altitude.

TABLE 3-2. VARIATION OF SHUTTLE SPEED
WITH ALTITUDE [12]

ALTITUDE (m)	V (m/sec)
100	152
300	156
500	158
2000	170
4000	188
6000	200
8000	240
10000	300
20000	500
40000	1928
60000	4695
80000	7468
100000	7521
120000	7510

4. CONCLUSIONS AND RECOMMENDATIONS

By means of a non-recursive discrete generation process, based on a von Karman spectral model with finite upper limits, dimensionless simulated turbulence **time** series have been developed and stored on six magnetic tapes. Longitudinal, transverse, and vertical gusts are simulated as well as the gust gradients associated with yaw, **pitch**, and roll. For each gust or gust gradient six separate time series (corresponding to the six altitude bands extending from ground level to 120,000 meters) have been stored on each tape.

The results of spectral analyses of each tape reveals that the simulated turbulence possesses the appropriate von Karman spectral characteristics. Statistical analyses of the tapes indicate that both the simulated gust and gust gradients are normally distributed with near-zero means. Furthermore the standard deviation **of** each series is constant with the theoretical energy content.

The Shuttle Simulated Turbulence Tapes (SSTT) are now ready for actual use for simulating turbulence at altitudes up to 120,000 meters,

5. REFERENCES CITED

1. Tatom, Frank B., and Smith, S. Ray, "Space Shuttle Simulation Model", *EAI-TR-80-003A*, Final Report, Engineering Analysis, Inc., Huntsville, AL, November 17, 1980.
2. Tatom, Frank B., and King, Richard L., "Turbulence Simulation Mechanization for Space Shuttle Orbiter Dynamics and Control Studies", *SAI-78-766-HU*, Summary Report, Science Applications, Inc., Huntsville, AL, December 1977.
3. Scharf, L. L., Wells, M. K., and Winn, C. B., "The Simulation of Atmospheric Turbulence for Space Shuttle Response Studies", Colorado State University, Fort Collins, Colorado,
4. Tatom, Frank B., and Smith, S. Ray, "Shuttle Orbiter Turbulence Simulation Model Development", *EAI-TR-79-001*, Summary Report, Engineering Analysis, Inc., Huntsville, AL, March 27, 1979.
5. Tatom, Frank B., and Smith, S. Ray, "Atmospheric Turbulence Simulation for Shuttle Orbiter", *EAI-TR-79-004*, Engineering Analysis, Inc., Huntsville, AL, August 31, 1979.
6. Space Shuttle Program: Natural Environment Design Requirements. Appendix 10.10, Space Shuttle Flight and Ground Specification, Level II Program Definition and Requirements, *JSC 07700*, Vol. X, Revision B. NASA-Lyndon B. Johnson Space Center, Houston, TX, August 18, 1975.
7. Etkin, B., *Dynamics of Atmospheric Flight*, John Wiley & Sons, Inc., New York, 1972.
8. Rockwell International Corporation, "Aerodynamic Design Substantiation Report", *SD74-SH-0206*, 1974.
9. Fichtl, George H., Perlmutter, Morris, and Frost, Walter, "Monte Carlo Turbulence Simulation", *Handbook of Turbulence*, Vol. 1, Chapter 14, Plenum Publishing Corporation, 1977.
10. Neuman, Frank, and Foster, John D., "Investigation of a Digital Automatic Aircraft Landing System in Turbulence", *NASA TN D-66066*, National Aeronautics and Space Administration, Washington, D.C., October 1970.
11. Perlmutter, Morris, "Stochastic Simulation of Ocean Waves for SRB Simulation", *NASA TR-230-1446*, George C. Marshall Space Flight Center, Marshall Space Flight Center, Alabama, May 1975.
12. Fichtl, George H., "A Technique for Simulating Turbulence for Aerospace Vehicle Flight Simulation Studies", *NASA TM 78242*, George C. Marshall Space Flight Center, Marshall Space Flight Center, Alabama, November 1977.
13. Bloomfield, Peter, *Fourier Analysis of Time Series: An Introduction*, John Wiley & Sons, Inc., 1976,

14. Maynard, Harry W., "An Evaluation of Ten Fast Fourier Transform (FFT) Programs", *Research and Development Technical Report ECOM-5476*, U.S. Army Electronics Command, Fort Monmouth, NJ, March 1973.

APPENDIX A

DIMENSIONLESS VON KARMAN SPECTRA WITH FINITE UPPER LIMITS

For each altitude band, the three-dimensional spectral model for gusts, as given by Eq (2-1), and the three-dimensional model for gust gradients, as given by Eq (2-2), have been integrated with respect to Ω_2 and Ω_3 over the finite limits calculated according to Eq (2-3). The six resulting one-dimensional spectra are presented in Tables A-1 through A-6, corresponding to Altitude Bands #1 through 6 respectively. These spectra were used in the numerical evaluation of the impulse response functions described in subsection 2.4.

TABLE A-1. DIMENSIONLESS SPECTRUM FOR ALTITUDE BAND # 1

Ω_1	Φ_{11}	$i=1$		$i=2$		$i=3$		
		DIMENSION-LESS WAVE NUMBER	Ω_1	Φ_{22}	$\Phi_{22/11}$	Ω_1	Φ_{33}	$\Phi_{33/11}$
0.00000	44171	0.00000	21638	0.00000	0.00000	14709	0.00000	10454
.01000	44167	.01000	21640	.12070E-04	.01000	14711	.82051E-05	10454
.02000	44156	.02000	21646	.48293E-04	.02000	14717	.32834E-04	10454
.03000	44136	.03000	21656	.10371E-03	.03000	14728	.73930E-04	10453
.04000	44109	.04000	21670	.19339E-03	.04000	14742	.13156E-03	10452
.05000	44072	.05000	21688	.30242E-03	.05000	14761	.20582E-03	10451
.06000	44029	.06000	21710	.43591E-03	.06000	14783	.29684E-03	10450
.07000	43978	.07000	21735	.59402E-03	.07000	14810	.40475E-03	10449
.08000	43919	.08000	21765	.77691E-03	.08000	14840	.52974E-03	10447
.09000	43852	.09000	21797	.98475E-03	.09000	14875	.67200E-03	10445
.10000	43779	.10000	21834	.12178E-02	.10000	14912	.83173E-03	10443
.19000	42785	.19000	22295	.448390E-02	.19000	15395	.30997E-02	10413
.28000	41270	.28000	22910	.10013E-01	.28000	16046	.70165E-02	10355
.37000	39343	.37000	23541	.17975E-01	.37000	16726	.12771E-01	10262
.46000	37147	.46000	24056	.28391E-01	.46000	17305	.20423E-01	10127
.55000	34736	.55000	24364	.41107E-01	.55000	17692	.29950E-01	99460E-01
.64000	32369	.64000	24419	.55787E-01	.64000	17841	.40757E-01	97177E-01
.73000	29973	.73000	24217	.71973E-01	.73000	17745	.52742E-01	94454E-01
.82000	27671	.82000	23780	.39131E-01	.82000	17423	.65360E-01	91349E-01
.91000	25485	.91000	23148	.10692	.91000	16928	.78137E-01	87935E-01
1.00000	23441	1.00000	22368	.12476	1.00000	16290	.90959E-01	84293E-01
1.38186	16426	1.20755	.20235	.16457	1.08653	.15596	.10263	80650E-01
1.76373	11685	1.41510	.17955	.20054	1.17305	.14827	.11379	.76934E-01
2.14559	34380E-01	1.62264	.15772	.23161	1.25958	.14039	.12423	.73201E-01
2.52745	.63167E-01	1.83019	.13792	.25766	1.34611	.13246	.13387	.69498E-01
2.90931	47895E-01	2.03774	.12048	.27903	1.43264	.12463	.14267	.65865E-01
3.29117	36960E-01	2.24529	.10535	.29623	1.51916	.11702	.15063	.62331E-01
3.67304	28969E-01	2.45284	.92322E-01	.30990	1.60569	.10971	.15776	.58919E-01
4.05490	23021E-01	2.66039	.91130E-01	.32026	1.69222	.10274	.16410	.55643E-01
4.43676	18521E-01	2.86793	.71517E-01	.32803	1.77875	.96161E-01	.16969	.52514E-01
4.81862	.15066E-01	3.07548	.63248E-01	.33356	1.86527	.89967E-01	.17453	.49538E-01

TABLE A-2. DIMENSIONLESS SPECTRUM FOR ALTITUDE BAND # 2

Ω_1	Φ_{11}	$i=1$		$i=2$		$i=3$		
		DIMENSION-LESS WAVE NUMBER	Ω_1	Φ_{22}	$\Phi_{22/11}$	Ω_1	Φ_{33}	$\Phi_{33/11}$
0.00000	47130	0.00000	23623	0.00000	0.00000	23492	0.00000	1.4485
.01000	47126	.01000	23625	.3177E-04	.01000	23494	.13104E-04	1.4484
.02000	47114	.02000	23632	.58722E-04	.02000	23500	.52429E-04	1.4484
.03000	47094	.03000	23642	.118E85-03	.03000	23510	.11802E-03	1.4484
.04000	47066	.04000	23656	.2110E-03	.04000	23524	.20993E-03	1.4483
.05000	47030	.05000	23674	.33010E-03	.05000	23543	.32827E-03	1.4483
.06000	46936	.06000	23696	.47579E-03	.06000	23565	.47315E-03	1.4492
.07000	46934	.07000	23722	.64831E-03	.07000	23590	.64472E-03	1.4481
.08000	46875	.08000	23751	.84783E-03	.08000	23620	.84314E-03	1.4480
.09000	46908	.09000	23785	.107<5E-02	.09000	23653	.10696E-02	1.4479
.10000	46733	.10000	23821	.13236E-02	.10000	23690	.13213E-02	1.4478
.19000	45731	.19000	24289	.43305E-02	.19000	24158	.48641E-02	1.4461
.28000	44205	.28000	24914	.10894E-01	.28000	24783	.10837E-01	1.4433
.37000	42269	.37000	25555	.19512E-01	.37000	25423	.19412E-01	1.4393
.46000	40053	.46000	26079	.30778E-01	.46000	25948	.30624E-01	1.4341
.55000	37673	.55000	26395	.44533E-01	.55000	26264	.44312E-01	1.4276
.64000	35250	.64000	26455	.60037E-01	.64000	26324	.60138E-01	1.4198
.73000	32849	.73000	26254	.730T3E-01	.73000	26123	.77645E-01	1.4110
.82000	30531	.82000	25617	.96823E-01	.82000	25687	.96333E-01	1.4010
.91000	29336	.91000	25185	.11632	.91000	25055	.11572	1.3902
1.00000	26282	1.00000	24404	.13611	1.00000	24274	.13539	1.3795
1.19000	13051	1.19000	15244	.30693	1.19000	.15117	.30438	.42978
2.30000	74892E-01	2.30000	.95050E-01	.41E53	2.30000	.93329E-01	.41028	.39314
3.70000	48151E-01	3.70000	.63922E-01	.48309	3.70000	.62751E-01	.47914	.34244
4.60000	33430E-01	4.60000	.45937E-01	.50097	4.60000	.44713E-01	.52776	.30634
5.50000	24468E-01	5.50000	.34499E-01	.58207	5.50000	.33429E-01	.56401	.27562
6.40000	13602E-01	6.40000	.26931E-01	.61E20	6.40000	.25906E-01	.59182	.24317
7.30000	14550E-01	7.30000	.21622E-01	.64267	7.30000	.20637E-01	.61339	.22400
8.20000	11636E-01	8.20000	.17747E-01	.66553	8.20000	.16301E-01	.63009	.20265
9.10000	94722E-02	9.10000	.14323E-01	.68486	9.10000	.13919E-01	.64286	.18376
10.00000	.78233E-02	10.00000	.12570E-01	.70107	10.00000	.11697E-01	.65240	.16700

TABLE A-2. DIMENSIONLESS SPECTRUM FOR ALTITUDE BAND # 2 (continued)

Ω_1	Φ_{11}	1=1		1=2		1=3	
		Ω_1	DIMENSION-LESS WAVE NUMBER	Φ_{22}	DIMENSION-LESS SPECTRUM	Ω_1	DIMENSION-LESS WAVE NUMBER
11.17616	62035E-02	11.10954	.10423E-01	.71748	11.13174	.95590E-02	.66066
12.35231	50019E-02	12.21907	.87718E-02	.73047	12.26348	.79344E-02	.66555
13.52945	208915E-02	13.32361	.74735E-02	.74052	13.39522	.66722E-02	.66774
14.70461	33820E-02	14.43814	.64331E-02	.74796	14.52696	.56732E-02	.66776
15.88077	22252E-02	15.54769	.55859E-02	.75312	15.65870	.48701E-02	.66602
17.05692	23807E-02	16.65722	.43867E-02	.75624	15.79045	.42156E-02	.66287
18.23307	2021E-02	17.76675	.43030E-02	.75757	17.92219	.36760E-02	.65957
19.40922	17287E-02	18.87629	.39107E-02	.75731	19.05393	.32265E-02	.65334
20.58537	14875E-02	19.98532	.33919E-02	.75566	20.18567	.28486E-02	.64737
21.76152	12872E-02	21.09536	.30329E-02	.75279	21.31741	.25283E-02	.64081
							.48338

TABLE A-3. DIMENSIONLESS SPECTRUM FOR ALTITUDE BAND # 3

Ω_1	Φ_{11}	i=1		i=2		i=3		DIMENSIONLESS SPECTRUM	
		Ω_1	Φ_{22}	$\Phi_{22}/11$	Ω_1	Φ_{33}	$\Phi_{33}/11$	Ω_1	$\Phi_{33}/22$
0.00000	.47307	0.00000	.23698	0.00000	0.00000	.23610	0.00000	1.8735	
.01000	.47303	.01000	.23700	.13213E-04	.01000	.23612	.13169E-04	1.8735	
.02000	.47291	.02000	.23706	.52987E-04	.02000	.23618	.52691E-04	1.8735	
.03000	.47271	.03000	.23716	.11905E-03	.03000	.23628	.11861E-03	1.8735	
.04000	.47243	.04000	.23730	.21177E-03	.04000	.23642	.21098E-03	1.8734	
.05000	.47207	.05000	.23748	.33114E-03	.05000	.23660	.32991E-03	1.8734	
.06000	.47164	.06000	.23770	.47723E-03	.06000	.23682	.47551E-03	1.8733	
.07000	.47112	.07000	.23796	.65034E-03	.07000	.23708	.64793E-03	1.8732	
.08000	.47052	.08000	.23826	.95047E-03	.08000	.23737	.84733E-03	1.8731	
.09000	.46985	.09000	.23859	.10779E-02	.09000	.23771	.10739E-02	1.8730	
.10000	.46910	.10000	.23896	.13328E-02	.10000	.23807	.13279E-02	1.8729	
.19000	.45909	.19000	.24363	.49055E-02	.19000	.24275	.48878E-02	1.8712	
.28000	.44382	.28000	.24938	.10927E-01	.28000	.24900	.10888E-01	1.8683	
.37000	.42447	.37000	.25629	.19569E-01	.37000	.25541	.19502E-01	1.8643	
.46000	.40230	.46000	.26153	.30966E-01	.46000	.26065	.30762E-01	1.8589	
.55000	.37855	.55000	.26469	.44658E-01	.55000	.26381	.44510E-01	1.8524	
.64000	.35426	.64000	.26529	.60606E-01	.64000	.26441	.60406E-01	1.8446	
.73000	.33025	.73000	.26328	.78253E-01	.73000	.26241	.77995E-01	1.8356	
.82000	.30707	.82000	.25391	.97099E-01	.82000	.25804	.96774E-01	1.8255	
.91000	.28512	.91000	.25259	.11665	.91000	.25172	.11626	1.8146	
1.00000	.26458	1.00000	.24477	.13652	1.00000	.24391	.13604	1.8023	
1.90000	.13222	1.90000	.15316	.30833	1.90000	.15235	.30675	1.6640	
2.80000	.76534E-01	2.80000	.95746E-01	.11867	2.80000	.94999E-01	.41541	1.5254	
3.79000	.49712E-01	3.79000	.64531E-01	.49319	3.70000	.63915E-01	.48803	1.4019	
4.60000	.34905E-01	4.60000	.46476E-01	.54851	4.60000	.45366E-01	.54131	1.2930	
5.50000	.25960E-01	5.50000	.35110E-01	.53237	5.50000	.34555E-01	.53301	1.1965	
6.40000	.19915E-01	6.40000	.27517E-01	.62354	6.40000	.27002E-01	.61688	1.1101	
7.30000	.15792E-01	7.30000	.22137E-01	.65945	7.30000	.21699E-01	.64496	1.0323	
8.20000	.12812E-01	8.20000	.18295E-01	.68612	8.20000	.17825E-01	.66848	9.6174	
9.10000	.10588E-01	9.10000	.15363E-01	.70955	9.10000	.14902E-01	.68927	.89746	
10.00000	.88940E-02	10.00000	.13095E-01	.73035	10.00000	.12639E-01	.70496	.83368	

TABLE A-3. DIMENSIONLESS SPECTRUM FOR ALTITUDE BAND # 3 (continued)

Ω_1	Φ_{11}	$i=1$		$i=2$		$i=3$	
		DIMENSION-LESS WAVE NUMBER	Ω_1	DIMENSION-LESS SPECTRUM	Φ_{22}	Φ_{22}/Φ_{11}	Ω_1
12.33085	.59522E-02	12.33085	.91368E-02	.77485	12.33085	.86903E-02	.73698
14.66170	.42188E-02	14.66170	.67485E-02	.80912	14.66170	.63163E-02	.75731
16.99254	.31087E-02	16.99254	.51879E-02	.83551	16.99254	.47784E-02	.76956
19.32339	.23566E-02	19.32339	.41069E-02	.85530	19.32339	.37255E-02	.77588
21.65423	.18260E-02	21.65423	.33244E-02	.86943	21.65423	.29733E-02	.77762
23.98508	.14401E-02	23.98508	.27383E-02	.87863	23.98508	.24177E-02	.77575
26.31592	.11523E-02	26.31592	.22875E-02	.88358	26.31592	.19961E-02	.77102
28.64677	.93463E-03	28.64677	.19333E-02	.88438	28.64677	.16693E-02	.76404
30.97761	.76627E-03	30.97761	.16499E-02	.88309	30.97761	.14113E-02	.75533
33.30846	.63450E-03	33.30846	.14201E-02	.87863	33.30846	.12045E-02	.74533
							.19419

TABLE A-4. DIMENSIONLESS SPECTRUM FOR ALTITUDE BAND # 4

Ω_1	Φ_{11}	$i=1$		$i=2$		$i=3$	
		Ω_1	Φ_{22}	$\Phi_{22}/11$	Ω_1	Φ_{33}	$\Phi_{33}/11$
0.00000	47403	0.00000	23725	0.00000	0.00000	23678	0.00000
.01000	47399	.01000	23727	.13234E-04	.01000	23680	.13207E-04
.02000	47397	.02000	23733	.52949E-04	.02000	23686	.52843E-04
.03000	47367	.03000	23744	.11919E-03	.03000	23696	.11895E-03
.04000	47339	.04000	23759	.21201E-03	.04000	23710	.21159E-03
.05000	47303	.05000	23776	.33152E-03	.05000	23729	.33086E-03
.06000	47259	.06000	23798	.47784E-03	.06000	23750	.47689E-03
.07000	47203	.07000	23824	.65109E-03	.07000	23776	.64979E-03
.09000	47148	.09000	23853	.85146E-03	.09000	23805	.84976E-03
.09000	47081	.09000	23886	.10791E-02	.09000	23839	.10770E-02
.10000	47006	.10000	23923	.13343E-02	.10000	23875	.13317E-02
.19000	46005	.19000	24391	.49111E-02	.19000	24343	.49014E-02
.28000	44478	.28000	25016	.10939E-01	.28000	24968	.10918E-01
.37000	42542	.37000	25656	.19590E-01	.37000	25609	.19554E-01
.46000	40326	.46000	26181	.30899E-01	.46000	26133	.30843E-01
.55000	37951	.55000	26496	.44704E-01	.55000	26449	.44625E-01
.64000	35522	.64000	26556	.60669E-01	.64000	26509	.60561E-01
.73000	33120	.73000	26356	.78336E-01	.73000	26309	.78196E-01
.82000	30803	.82000	26181	.97204E-01	.82000	.25972	.97028E-01
.91000	28607	.91000	25287	.11679	.91000	.25240	.11658
1.00000	26553	1.00000	24505	.13663	1.00000	.24459	.13642
1.90000	13316	1.90000	15344	.30895	1.90000	.15301	.30809
2.80000	77440E-01	2.80000	96030E-01	.41992	2.80000	.95655E-01	.41828
3.70000	.50590E-01	3.70000	.64876E-01	.49537	3.70000	.64556E-01	.49292
4.60000	.35757E-01	4.60000	.46762E-01	.55188	4.60000	.46492E-01	.54870
5.50000	.26637E-01	5.50000	.35394E-01	.59716	5.50000	.35166E-01	.59331
6.40000	.20721E-01	6.40000	.27797E-01	.63503	6.40000	.27599E-01	.63052
7.30000	.16579E-01	7.30000	.22463E-01	.66765	7.30000	.22284E-01	.66234
8.20000	.13584E-01	8.20000	.18567E-01	.69632	8.20000	.18398E-01	.68999
9.10000	.11346E-01	9.10000	.15631E-01	.72195	9.10000	.15465E-01	.71430
10.00000	.96272E-02	10.00000	.13361E-01	.74519	10.00000	.13194E-01	.73587

TABLE A-4. DIMENSIONLESS SPECTRUM FOR ALTITUDE BAND # 4 (continued)

Ω_1	Φ_{11}	$i=1$		$i=2$		$i=3$		$\Phi_{33}/22$
		DIMENSION-LESS WAVE NUMBER	Ω_1	DIMENSION-LESS SPECTRUM	$\Phi_{22}/11$	DIMENSION-LESS WAVE NUMBER	Ω_1	DIMENSIONLESS SPECTRUM
14.91780	.47319E-02	14.91780	.68101E-02	.84529	14.91780	.66213E-02	.82185	1.1506
19.83561	.27884E-02	19.83561	.41933E-02	.91302	19.83561	.39942E-02	.87653	.93474
24.75341	.18076E-02	24.75341	.28455E-02	.97244	24.75341	.26687E-02	.91204	.76806
29.67122	.12440E-02	29.67122	.20620E-02	1.0125	29.67122	.19004E-02	.93314	.63641
34.58902	.89257E-03	34.58902	.15598E-02	1.0408	34.58902	.14135E-02	.94319	.53107
39.50682	.66065E-03	39.50682	.12170E-02	1.0594	39.50682	.10854E-02	.94489	.44603
44.42462	.50109E-03	44.42462	.97201E-03	1.0699	44.42462	.85433E-03	.94040	.37691
49.34242	.38773E-03	49.34242	.79069E-03	1.0737	49.34242	.69586E-03	.93136	.32040
54.26022	.30509E-03	54.26022	.65279E-03	1.0719	54.26022	.55968E-03	.91905	.27394
59.17802	.24355E-03	59.17802	.54558E-03	1.0657	59.17802	.46304E-03	.90444	.23553

TABLE A-5. DIMENSIONLESS SPECTRUM FOR ALTITUDE BAND # 5

Ω_1	1=1		1=2		1=3						
	DIMENSION-LESS WAVE SPECTRUM	Φ_{11}	DIMENSION-LESS WAVE NUMBER	Ω_1	DIMENSION-LESS SPECTRUM	$\Phi_{22}/11$	DIMENSION-LESS WAVE NUMBER	Ω_1	DIMENSIONLESS SPECTRUM	$\Phi_{33}/11$	DIMENSIONLESS SPECTRUM
0.00000	.47517	0.00000	.23758	0.00000	0.00000	.23748	0.00000	.23750	0.00000	.13246E-04	3.7129
.01000	.47513	.01000	.23760	.13252E-04	.01000	.23750	.53023E-04	.23756	.52999E-04	3.7129	
.02000	.47501	.02000	.23766	.11935E-04	.02000	.23756	.21231E-03	.23766	.11930E-03	3.7128	
.03000	.47481	.03000	.23777	.21231E-03	.03000	.23766	.04000	.23780	.21221E-03	3.7128	
.04000	.47453	.04000	.23791	.33198E-03	.04000	.23780	.05000	.23798	.B3183E-03	3.7127	
.05000	.47417	.05000	.23809	.47950E-03	.05000	.23798	.06000	.23820	.47828E-03	3.7127	
.06000	.47373	.06000	.23831	.65200E-03	.06000	.23820	.07000	.23946	.65170E-03	3.7126	
.07000	.47321	.07000	.23857	.85264E-03	.07000	.23946	.08000	.23876	.85226E-03	3.7125	
.08000	.47262	.08000	.23886	.10806E-02	.08000	.23876	.09000	.23909	.10801E-02	3.7124	
.09000	.47195	.09000	.23919	.13362E-02	.09000	.23909	.10000	.23946	.13356E-02	3.7122	
.10000	.47120	.10000	.23956	.19000	.10000	.23946	.19000	.24413	.49156E-02	3.7105	
.19000	.46118	.19000	.24424	.49177E-02	.19000	.24424	.28000	.25038	.10949E-01	3.7076	
.28000	.44591	.28000	.25049	.10953E-01	.28000	.25038	.19615E-01	.25679	.19607E-01	3.7035	
.37000	.42656	.37000	.25699	.30938E-01	.37000	.25679	.30938E-01	.46080	.30925E-01	3.6981	
.46000	.40439	.46000	.26214	.44760E-01	.46000	.26203	.44760E-01	.55000	.44742E-01	3.6915	
.55000	.38064	.55000	.26530	.97328E-01	.55000	.26519	.97328E-01	.64000	.26579	.97205E-01	3.6835
.64000	.35635	.64000	.26590	.60745E-01	.64000	.26579	.60745E-01	.73000	.26373	.78470E-01	3.6744
.73000	.33232	.73000	.26389	.78434E-01	.73000	.26373	.78434E-01	.92000	.25941	.972H6E-01	3.6643
.82000	.30915	.82000	.25952	.91000	.82000	.25941	.91000	.25309	.11090	.3.6531	
.91000	.28719	.91000	.25320	.11695	.91000	.25309	.11695	.1.00000	.24528	.13680	.3.6411
1.00000	.26664	1.00000	.24539	.13686	1.00000	.24528	.13686	.1.00000	.24528	.13680	.3.6411
1.19000	.13421	1.19000	.15378	.30964	1.19000	.15368	.30964	.1.90000	.15368	.30942	.3.4999
2.80000	.78413E-01	2.80000	.96333E-01	.42146	2.80000	.96276E-01	.42146	.80000	.96276E-01	.42099	.3.3575
3.70000	.51470E-01	3.70000	.65236E-01	.49812	3.70000	.65129E-01	.49812	.70000	.65129E-01	.49730	.3.2290
4.60000	.36545E-01	4.60000	.47121E-01	.55612	4.60000	.47014E-01	.55612	.50000	.35639E-01	.55486	.3.143
5.50000	.27395E-01	5.50000	.35746E-01	.60310	5.50000	.35639E-01	.60310	.40000	.28028E-01	.60129	.3.0113
6.40000	.21364E-01	6.40000	.28134E-01	.64274	6.40000	.28028E-01	.64274	.40000	.64030	.2.9178	
7.30000	.17173E-01	7.30000	.22791E-01	.67709	7.30000	.22674E-01	.67709	.30000	.67392	.2.8323	
8.20000	.14143E-01	8.20000	.18863E-01	.70741	8.20000	.18756E-01	.70741	.20000	.J0360	.2.7534	
9.10000	.11882E-01	9.10000	.15904E-01	.73457	9.10000	.15797E-01	.73457	.10000	.75328	.2.6801	
10.00000	.10150E-01	10.00000	.13612E-01	.75923	10.00000	.13506E-01	.75923	.00000	.75328	.2.6116	

TABLE A-5. DIMENSIONLESS SPECTRUM FOR ALTITUDE BAND # 5 (continued)

Ω_1	Φ_{11}	1=2		1=3		$\Phi_{33}/11$	$\Phi_{33}/22$
		DIMENSION-LESS WAVE NUMBER	Ω_1	Φ_{22}	$\Phi_{22}/11$		
19.00000	.35256E-02	19.00000	.46754E-02	.94138	19.00000	.45700E-02	.92017
28.00001	.1820E-02	28.00001	.24617E-02	1.0765	28.00001	.23585E-02	1.0313
37.00001	.11733E-02	37.00001	.15535E-02	1.1862	37.00001	.10531E-02	1.1095
46.00001	.8125E-03	46.00001	.10839E-02	1.2793	46.00001	.98684E-03	1.1647
55.00001	.60468E-03	55.00001	.80633E-03	1.3604	55.00001	.71299E-03	1.2030
64.00002	.46794E-03	64.00002	.62699E-03	1.4324	64.00002	.53764E-03	1.2283
73.00002	.37409E-03	73.00002	.50358E-03	1.4968	73.00002	.41833E-03	1.2434
82.00002	.30690E-03	82.00002	.41460E-03	1.5549	82.00002	.33340E-03	1.2504
91.00002	.25687E-03	91.00002	.34810E-03	1.6073	91.00002	.27084E-03	1.2509
100.00002	.21879E-03	100.00002	.29698E-03	1.6564	100.00002	.22347E-03	1.2464
110.00003	.17443E-04	190.00003	.10056E-03	2.0249	103.65648	.20548E-03	1.2434
120.00006	.38592E-04	280.00006	.52567E-04	2.2986	107.31294	.193E-03	1.2398
130.00006	.23822E-04	370.00006	.32946E-04	2.5156	110.96941	.17991E-03	1.2357
140.00005	.16216E-04	460.00006	.22822E-04	2.6935	114.62587	.16798E-03	1.2310
150.00012	.11742E-04	550.00012	.16851E-04	2.8430	118.28233	.15711E-03	1.2260
160.00012	.88702E-05	640.00012	.13003E-04	2.9705	121.93880	.14718E-03	1.2206
170.00012	.69113E-05	730.00012	.10363E-04	3.0300	125.59526	.13808E-03	1.2148
180.00012	.55136E-05	820.00012	.84644E-05	3.1744	129.25174	.12972E-03	1.2088
190.00012	.44814E-05	910.00012	.70491E-05	3.2553	132.90820	.12205E-03	1.2025
200.00010	.36930E-05	1000.00010	.59628E-05	3.3257	136.56467	.11497E-03	1.1959
210.00010	.36930E-05	1000.00020	.59628E-05	3.3257			
220.00010	.29062E-05	1122.05660	.1122.05660	.48484E-05	3.4046		
230.00010	.23262E-05	1244.11300	.1244.11300	.40164E-05	3.4673		
240.00010	.18901E-05	1366.16940	.1366.16940	.33773E-05	3.5158		
250.00010	.15551E-05	1488.22500	.1488.22500	.28750E-05	3.5515		
260.00010	.12931E-05	1610.28220	.1610.28220	.24726E-05	3.5760		
270.00010	.10852E-05	1732.33860	.1732.33860	.21450E-05	3.5903		
280.00010	.91821E-06	1850.39500	.1850.39500	.18748E-05	3.5957		
290.00010	.78255E-06	1976.45140	.1976.45140	.16492E-05	3.5932		
300.00010	.67131E-06	2098.50780	.2098.50780	.14591E-05	3.5838		
310.00010	.57933E-06	2220.56400	.2220.56400	.12974E-05	3.5682		

TABLE A-6. DIMENSIONLESS SPECTRUM FOR ALTITUDE BAND # 6

i=1		i=2		DIMENSIONLESS SPECTRUM		DIMENSIONLESS WAVE NUMBER Ω_1		DIMENSIONLESS SPECTRUM		DIMENSIONLESS WAVE NUMBER Ω_1		DIMENSIONLESS SPECTRUM	
DIMENSION-LESS WAVE NUMBER Ω_1	DIMENSIONLESS SPECTRUM Φ_{11}	DIMENSION-LESS WAVE NUMBER Ω_1	DIMENSIONLESS SPECTRUM Φ_{22}	DIMENSION-LESS WAVE NUMBER Ω_1	DIMENSIONLESS SPECTRUM $\Phi_{22/11}$	DIMENSION-LESS WAVE NUMBER Ω_1	DIMENSIONLESS SPECTRUM $\Phi_{22/11}$	DIMENSION-LESS WAVE NUMBER Ω_1	DIMENSIONLESS SPECTRUM Φ_{33}	DIMENSION-LESS WAVE NUMBER Ω_1	DIMENSIONLESS SPECTRUM $\Phi_{33/11}$	DIMENSIONLESS SPECTRUM $\Phi_{33/22}$	
0.00000	47517	0.00000	23750	0.00000	0.00000	23758	0.00000	0.00000	23758	0.00000	0.00000	9.2415	
0.01000	47513	.01000	23760	.13252E-04	.01000	.23760	.13252E-04	.01000	.23760	.13252E-04	.01000	9.2415	
0.02000	47501	.02000	23767	.53023E-04	.02000	.23766	.53022E-04	.02000	.23766	.53022E-04	.02000	9.2415	
0.03000	47481	.03000	23777	.11935E-03	.03000	.23776	.11935E-03	.03000	.23776	.11935E-03	.03000	9.2414	
0.04000	47453	.04000	23791	.21231E-03	.04000	.23791	.21231E-03	.04000	.23791	.21231E-03	.04000	9.2414	
0.05000	47417	.05000	23809	.33198E-03	.05000	.23809	.33198E-03	.05000	.23809	.33198E-03	.05000	9.2413	
0.06000	47373	.06000	23831	.47950E-03	.06000	.23831	.47949E-03	.06000	.23831	.47949E-03	.06000	9.2413	
0.07000	47322	.07000	23857	.65200E-03	.07000	.23856	.65199E-03	.07000	.23856	.65199E-03	.07000	9.2412	
0.08000	47262	.08000	23886	.85264E-03	.08000	.23896	.85264E-03	.08000	.23896	.85264E-03	.08000	9.2411	
0.09000	47195	.09000	23920	.10806E-02	.09000	.23919	.10806E-02	.09000	.23919	.10806E-02	.09000	9.2410	
0.10000	47120	.10000	23956	.13362E-02	.10000	.23956	.13362E-02	.10000	.23956	.13362E-02	.10000	9.2408	
0.19000	46118	.19000	24424	.49177E-02	.19000	.24424	.49177E-02	.19000	.24424	.49177E-02	.19000	9.2391	
0.28000	44592	.28000	25049	.10953E-01	.28000	.25049	.10953E-01	.28000	.25049	.10953E-01	.28000	9.2362	
0.37000	42656	.37000	25689	.19615E-01	.37000	.25689	.19615E-01	.37000	.25689	.19615E-01	.37000	9.2321	
0.46000	40439	.46000	26214	.30938E-01	.46000	.26214	.30938E-01	.46000	.26214	.30938E-01	.46000	9.2267	
0.55000	38064	.55000	26530	.44760E-01	.55000	.26529	.44760E-01	.55000	.26529	.44760E-01	.55000	9.2200	
0.64000	35635	.64000	26590	.60745E-01	.64000	.26589	.60745E-01	.64000	.26589	.60745E-01	.64000	9.2121	
0.73000	33233	.73000	26389	.78435E-01	.73000	.26389	.78435E-01	.73000	.26389	.78435E-01	.73000	9.2030	
0.82000	30915	.82000	25952	.97329E-01	.82000	.25952	.97329E-01	.82000	.25952	.97329E-01	.82000	9.1928	
0.91000	28719	.91000	25320	.11695	.91000	.25320	.11695	.91000	.25320	.11695	.91000	9.1816	
1.00000	26665	1.00000	24H39	.13686	1.00000	.24538	.13686	1.00000	.24538	.13686	1.00000	9.1697	
1.13400	13421	1.13400	15379	.30964	1.13400	.15378	.30964	1.13400	.15378	.30964	1.13400	9.0282	
2.30000	73414E-01	2.30000	96384E-01	.42146	2.30000	.96382E-01	.42146	2.30000	.96382E-01	.42146	2.30000	8.8855	
3.70000	51471E-01	3.70000	65237E-01	.49812	3.70000	.65234E-01	.49812	3.70000	.65234E-01	.49812	3.70000	8.7566	
4.60000	36547E-01	4.60000	47125E-01	.55613	4.60000	.47113E-01	.55613	4.60000	.47113E-01	.55613	4.60000	8.6413	
5.50000	27396E-01	5.50000	35746E-01	.60311	5.50000	.35744E-01	.60311	5.50000	.35744E-01	.60307	5.50000	8.5376	
6.40000	21365E-01	6.40000	23135E-01	.64276	6.40000	.28133E-01	.64276	6.40000	.28133E-01	.64270	6.40000	8.4433	
7.30000	17175E-01	7.30000	22781E-01	.67711	7.30000	.22779E-01	.67711	7.30000	.22779E-01	.67704	7.30000	8.3568	
8.20000	14145E-01	8.20000	18632E-01	.70743	8.20000	.18861E-01	.70743	8.20000	.18861E-01	.70737	8.20000	8.2769	
9.10000	11324E-01	9.10000	15905E-01	.73459	9.10000	.15902E-01	.73459	9.10000	.15902E-01	.73448	9.10000	8.2024	
10.00000	10152E-01	10.00000	136ME-01	.75926	10.00000	.13611E-01	.75926	10.00000	.13611E-01	.75913	10.00000	8.1326	

TABLE A-6. DIMENSIONLESS SPECTRUM FOR ALTITUDE BAND # 6 (continued)

Ω_1	Φ_{11}	1=1		1=2		1=3	
		DIMENSION-LESS WAVE SPECTRUM	Ω_1	DIMENSION-LESS WAVE SPECTRUM	Φ_{22}	DIMENSION-LESS WAVE SPECTRUM	Ω_1
19.00000	.35273E-02	19.	0.0000	.46761E-02	.94149	19.	0.0000
28.0001	.18637E-02	28.	0.0001	.24623E-02	1.0767	28.	0.0001
37.0001	.11750E-02	37.	0.0001	.15541E-02	1.1866	37.	0.0001
46.0001	.81798E-03	46.	0.0001	.10845E-02	1.2799	46.	0.0001
55.0001	.60640E-03	55.	0.0001	.80690E-03	1.3614	55.	0.0001
64.0002	.46966E-03	64.	0.0002	.62756E-03	1.4337	64.	0.0002
73.0002	.37581E-03	73.	0.0002	.50415E-03	1.4985	73.	0.0002
82.0002	.30851E-03	82.	0.0002	.41517E-03	1.5570	82.	0.0002
91.0002	.25858E-03	91.	0.0002	.34386E-03	1.6104	91.	0.0002
100.0002	.22050E-03	100.	0.0002	.29755E-03	1.6596	100.	0.0002
119.0003	.76128E-04	190.	0.0003	.10113E-03	2.0362	190.	0.0003
128.0006	.40158E-04	280.	0.0006	.53133E-04	2.3234	280.	0.0006
137.0006	.25293E-04	370.	0.0006	.33505E-04	2.5583	370.	0.0006
146.0.0006	.17593E-04	460.	0.0006	.23369E-04	2.7580	460.	0.0006
155.0.0012	.13031E-04	550.	0.0012	.17380E-04	2.9324	550.	0.0012
164.0.0012	.10083E-04	640.	0.0012	.13513E-04	3.0870	640.	0.0012
173.0.0012	.80609E-05	730.	0.0012	.10852E-04	3.2255	730.	0.0012
182.0.0012	.66106E-05	820.	0.0012	.89342E-05	3.3506	820.	0.0012
191.0.0012	.55347E-05	910.	0.0012	.75009E-05	3.4645	910.	0.0012
200.0.0010	.47141E-05	1000.	0.0010	.63991E-05	3.5691	1000.	0.0010
2100.0.0020	.47141E-05	1000.	0.0020	.63991E-05	3.5691	1000.	0.0020
2190.0.0050	.16047E-05	1900.	0.0050	.24666E-05	4.3624	1031.	0.1340
2280.0.0100	.93145E-06	2800.	0.0100	.11325E-05	4.9523	1062.	0.2660
2370.0.0150	.51323E-06	3700.	0.0150	.70998E-06	5.4198	1093.	0.3980
2460.0.0200	.34936E-06	4600.	0.0200	.49170E-06	5.8030	1124.	0.5300
2550.0.0200	.25297E-06	5500.	0.0200	.36304E-06	6.1252	1155.	0.6620
2640.0.0200	.19110E-06	6400.	0.0200	.28014E-06	6.3938	1186.	0.7930
2730.0.0200	.14890E-06	7300.	0.0200	.22326E-06	6.6358	1217.	0.9250
2820.0.0200	.11879E-06	8200.	0.0200	.18236E-06	6.8391	1248.	1.0570
2910.0.0200	.96550E-07	9100.	0.0200	.15187E-06	7.0144	1279.	1.1890
3000.0.0200	.79671E-07	10000.	0.0200	.12846E-06	7.1651	1310.	1.3210

TABLE A-6. DIMENSIONLESS SPECTRUM FOR ALTITUDE BAND # 6 (concluded)

Ω_1	Φ_{11}	$i=2$		$i=3$	
		Ω_1	Φ_{22}	$\Phi_{22/11}$	Ω_1
11220.566	.62612E-07	11220.566	.10446E-06	7.3351	
12441.131	.50118E-07	12441.131	.86531E-07	7.4701	
13661.695	.40722E-07	13661.695	.722762E-07	7.5745	
14882.260	.33503E-07	14882.260	.61940E-07	7.6515	
16102.824	.27859E-07	16102.824	.532270E-07	7.7042	
17323.387	.23381E-07	17323.387	.46213E-07	7.7351	
18543.949	.19782E-07	18543.949	.40390E-07	7.7468	
19764.512	.16960E-07	19764.512	.35531E-07	7.7414	
20985.074	.14463E-07	20985.074	.31435E-07	7.7210	
22205.637	.12481E-07	22205.637	.27952E-07	7.6875	

APPENDIX B

ESTABLISHMENT OF LOWER FREQUENCY LIMITS

The maximum time limit, t_{\max} , for which the impulse response function is computed, determines the minimum frequency, Ω_{i1min} , for which the corresponding spectrum is accurately simulated according to the relation

$$\Omega_{i1min} = \pi/t_{\max} \quad (B-1)$$

The simulated turbulence may contain lower frequencies, depending on the total length of the time series, but the shape of the actual spectrum for any frequencies less than Ω_{i1min} will not in general match the theoretical spectral shape. To verify this point for the $\Phi_{33/11}$ spectrum two impulse response functions were generated, the first extending out to a t_{\max} of 42.10573 and the second extending out to a t_{\max} of 85.895689. Two separate turbulence time series were then generated, one for each impulse function. The results of spectral analysis of these two time series is presented in Figures B-1 and B-2. As indicated in each figure, the observed spectrum tends to drift away from the theoretical spectrum for frequencies below π/t_{\max} . The impulse response function with the larger t_{\max} produces a time series whose spectral shape matches the theoretical spectrum to the lower frequency.

Based on various characteristics of the Space Shuttle simulators, a minimum frequency, f_{1min} , of .04 hertz was established for generating simulated turbulence. The dimensional frequency, f_{1min} , is related to the dimensionless frequency, Ω_{i1min} , according to the relation

$$\Omega_{i1min} = 2\pi a L_i f_{1min}/V \quad (B-2)$$

By substitution and rearrangement,

$$t_{\max} = V/(2aL_i f_{1min}) \quad (B-3)$$

To satisfy the requirement for a minimum simulation frequency of .04 hertz, values of each impulse response function were computed for 100 dimensionless time intervals. As shown in Table B-1, by using a constant number of time

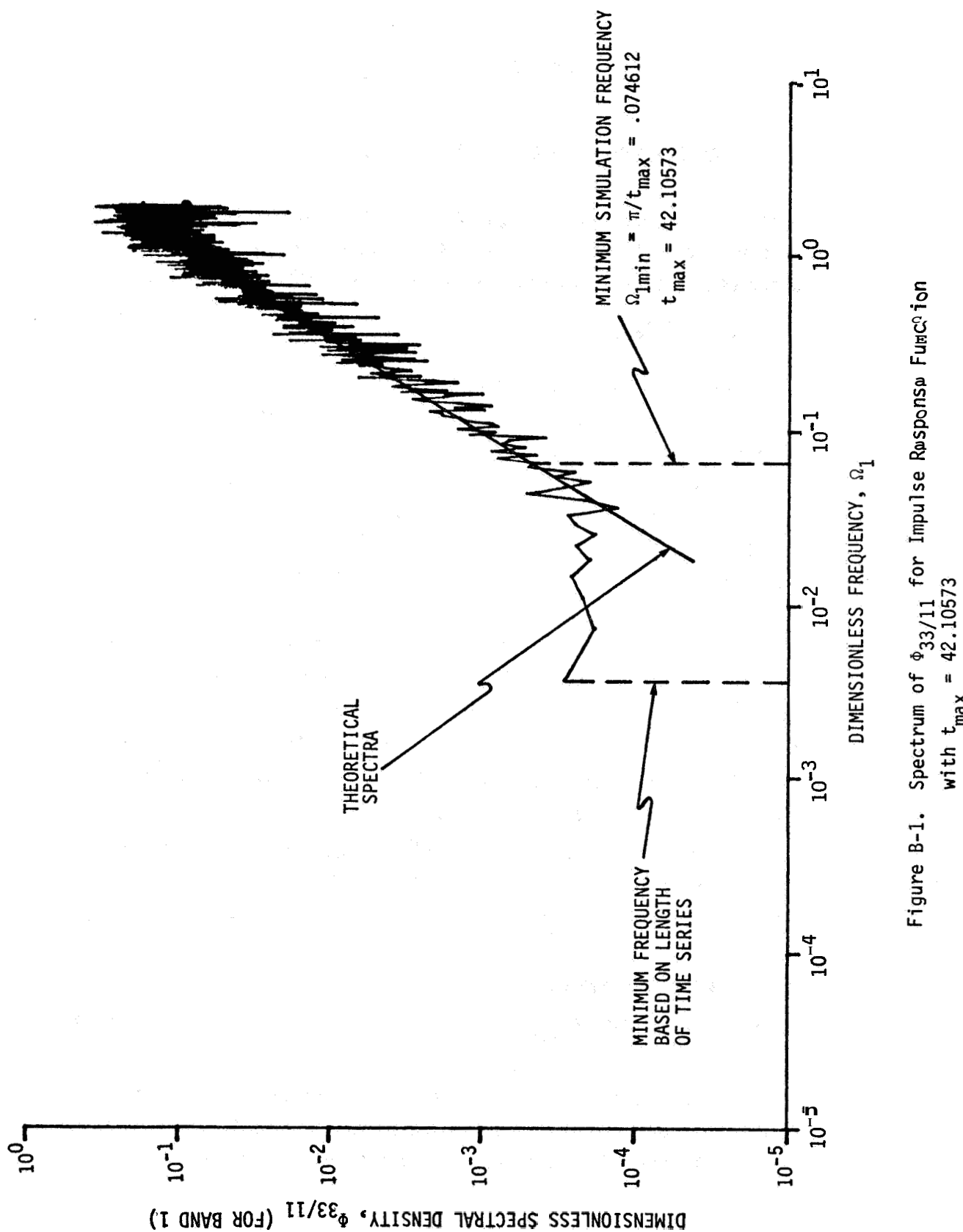


Figure B-1. Spectrum of $\phi_{33/11}$ for Impulse Response Function with $t_{\max} = 42.10573$

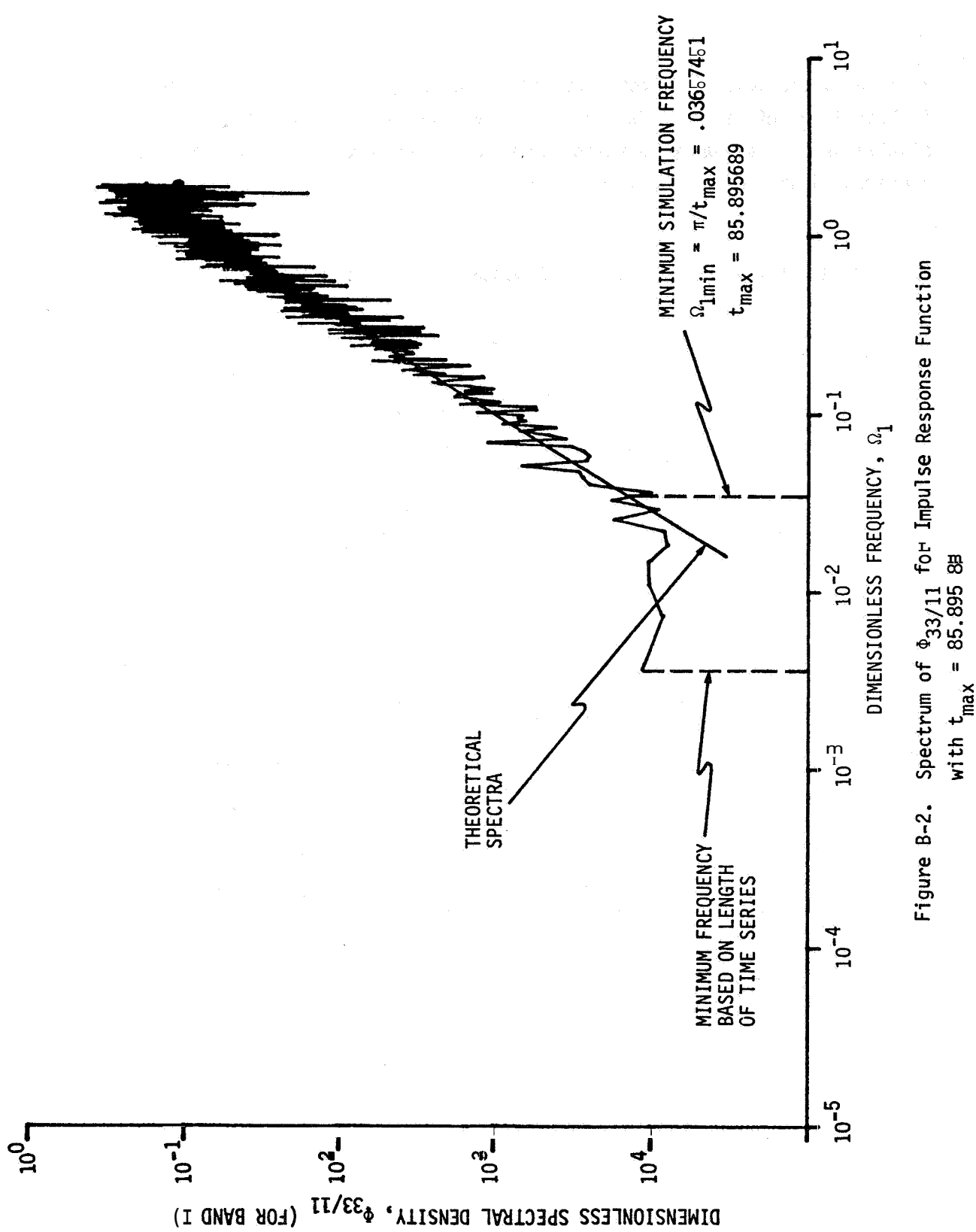


Figure B-2. Spectrum of $\phi_{33/11}$ for Impulse Response Function
 with $t_{\max} = 85.895$ 8

intervals, the actual minimum simulation frequency varies from .0174 hertz in Band 1 to .04 hertz in Band 6. Thus, at the lower altitudes the turbulence simulation will actually be valid for frequencies somewhat lower than the required minimum as given by Eq (B-2).

TABLE B-1. DIMENSIONAL AND DIMENSIONLESS MINIMUM FREQUENCY LIMITS

i	SPECTRA	BAND	MINIMUM SIMULATION FREQUENCY LIMITS	
			DIMENSIONAL	DIMENSIONLESS
1	Φ_{11}	1	.0174	.04818
		2	.0212	.2176
		3	.0211	.3331
		4	.0396	.5918
		5	.04	7.365
		6	.04	8.949
2	$\Phi_{22}, \Phi_{22/11}$	1	.0174	.03075
		2	.0206	.2110
		3	.0211	.3331
		4	.0396	.5918
		5	.04	7.365
		6	.04	8.949
3	$\Phi_{33}, \Phi_{33/11}$ $, \Phi_{33/22}$	1	.0174	.01865
		2	.0208	.2132
		3	.0211	.3331
		4	.0396	.5918
		5	.04	.4630
		6	.04	.5280

APPENDIX C

SPECTRAL ANALYSIS OF SIMULATED TURBULENCE

By means of a Fast Fourier Transform [14] spectral analyses of all simulated turbulence have been performed. The results are presented in dimensionless form in Figures C-1 through C-36. Table C-1 provides a summary of these figures. Also included in each figure is the theoretical von Karman spectra. The agreement between the theoretical spectra and the computed spectra is quite satisfactory.

TABLE C-1. MATRIX OF SPECTRAL ANALYSIS FIGURES

SERIES TYPE	ALTITUDE BAND					
	1	2	3	4	5	6
u_1	C-1	C-2	C-3	C-4	C-5	C-6
u_2	C-7	C-8	C-9	C-10	C-11	C-12
u_3	C-13	C-14	C-15	C-16	C-17	C-18
$\partial u_2 / \partial x_1$	C-19	C-20	C-21	C-22	C-23	C-24
$\partial u_3 / \partial x_1$	C-25	C-26	C-27	C-28	C-29	C-30
$\partial u_3 / \partial x_2$	C-31	C-32	C-33	C-34	C-35	C-36

*The spectral analysis involved the first 4096 terms of each time series except for bands 5 and 6 for the u_1 and u_2 gusts. For these cases 8192 terms were used.

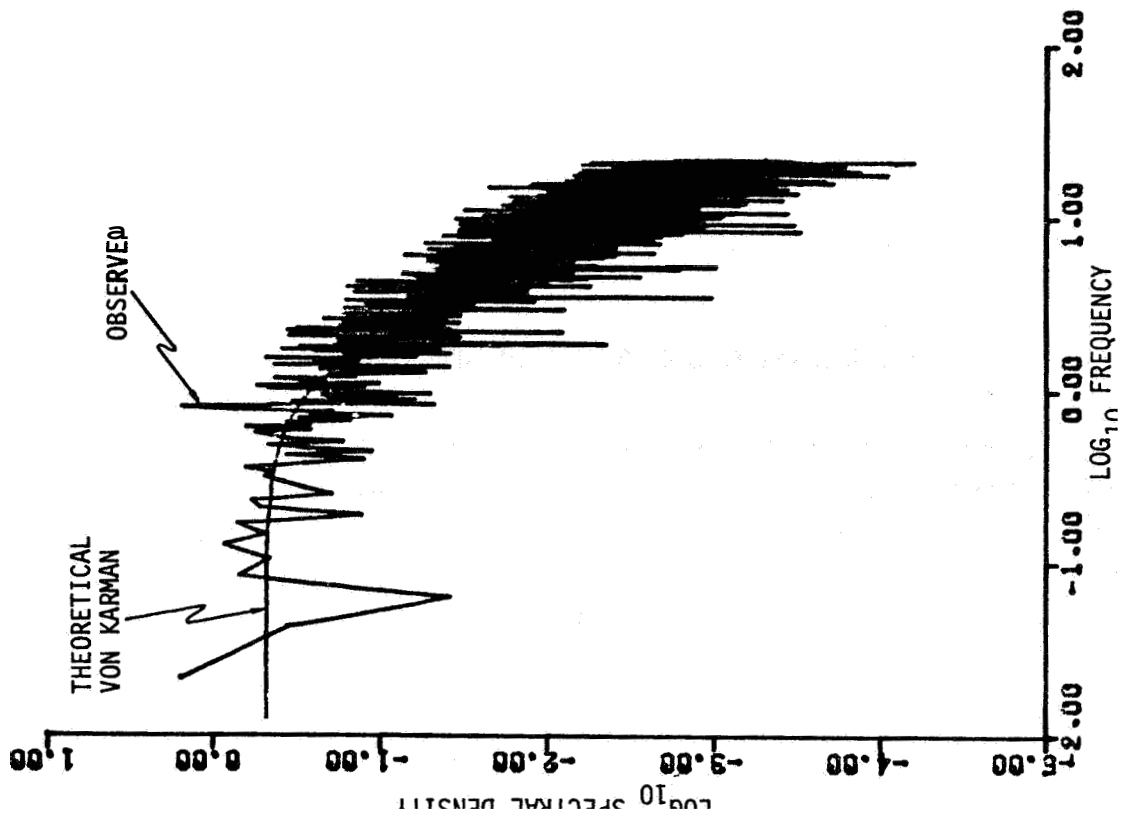
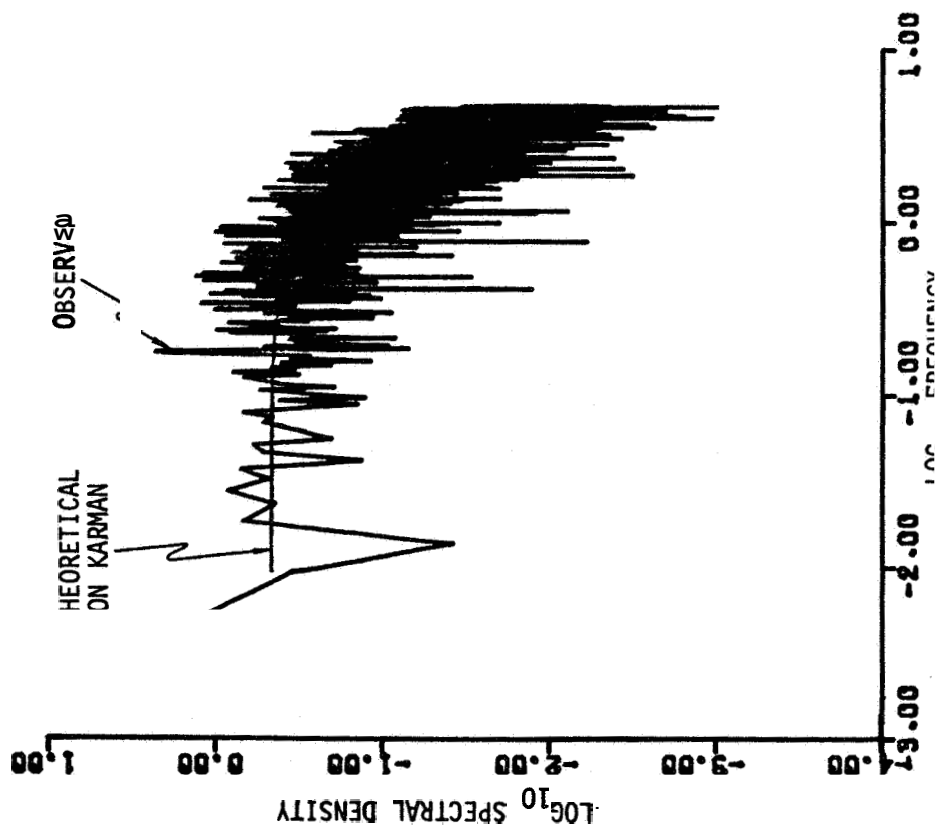
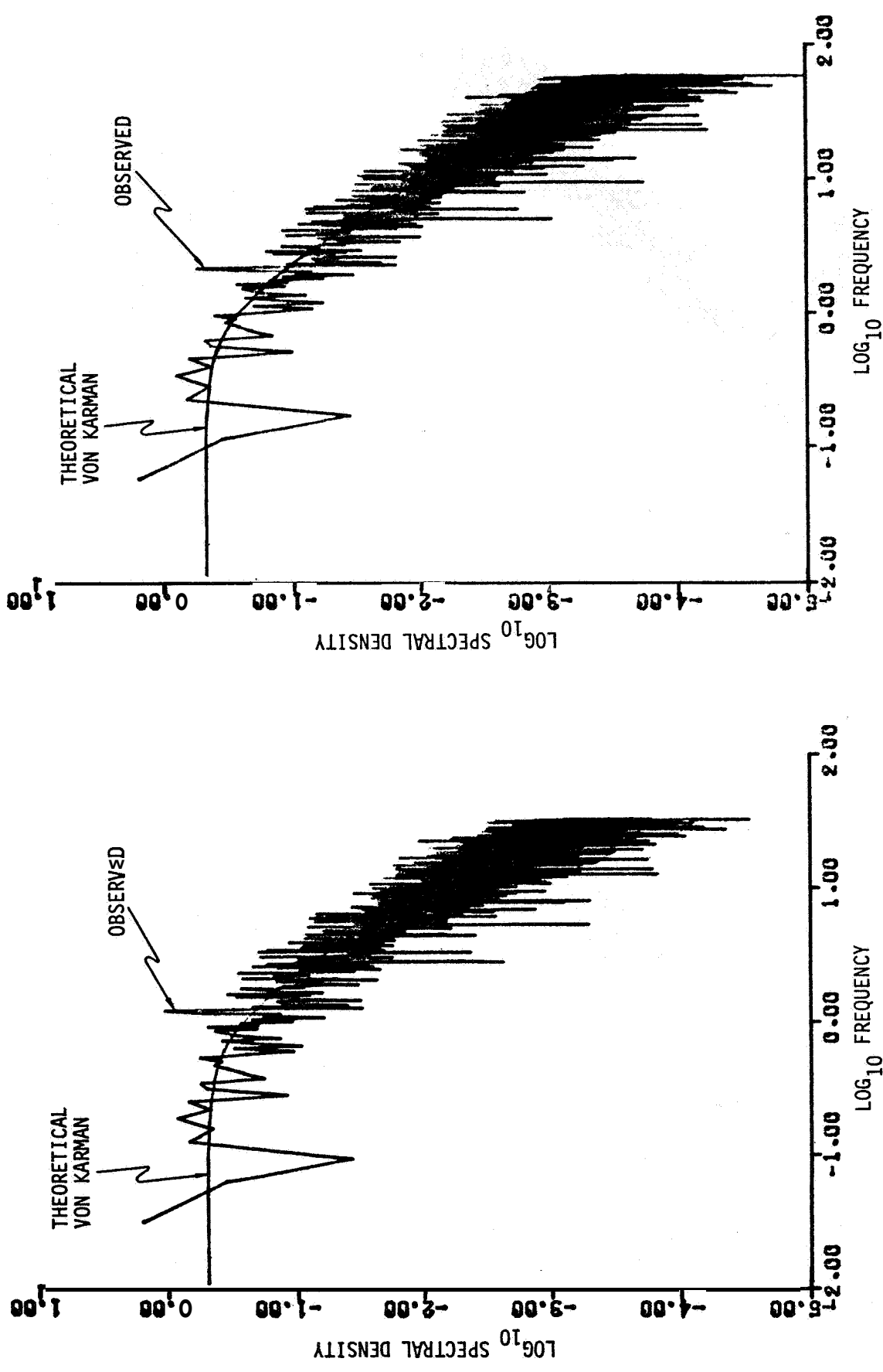


Figure C-1. u_1 - Gust Spectrum, Altitude Band #1
Figure C-2. u_1 - Gust Spectrum, Altitude Band #2

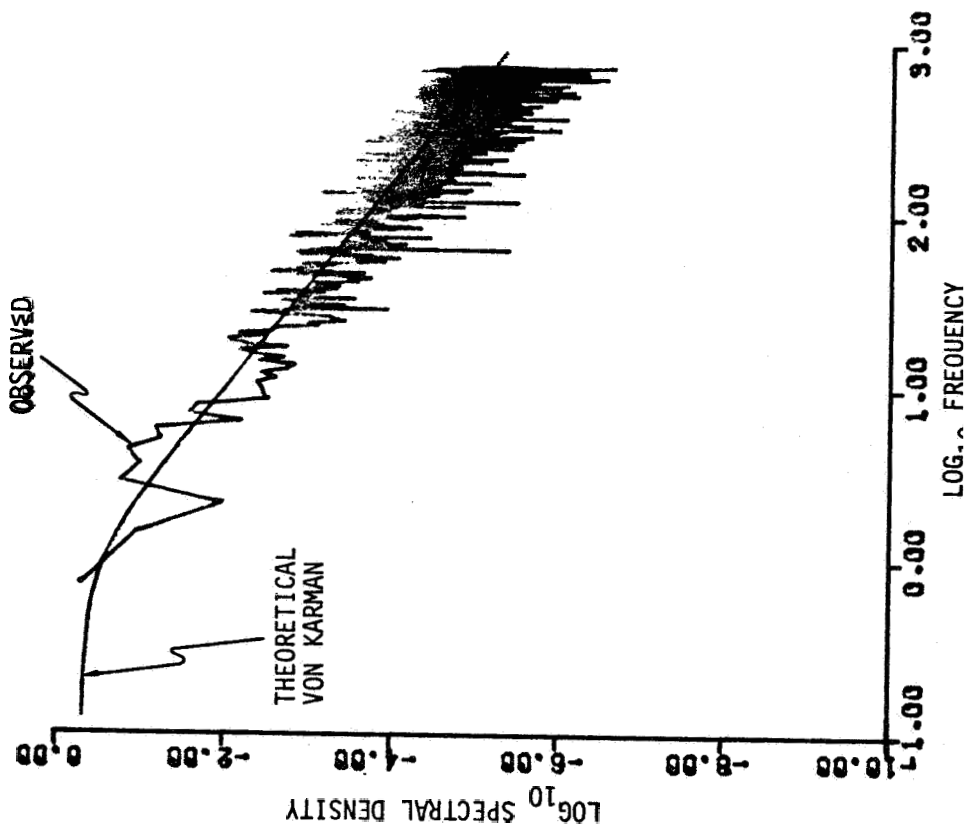
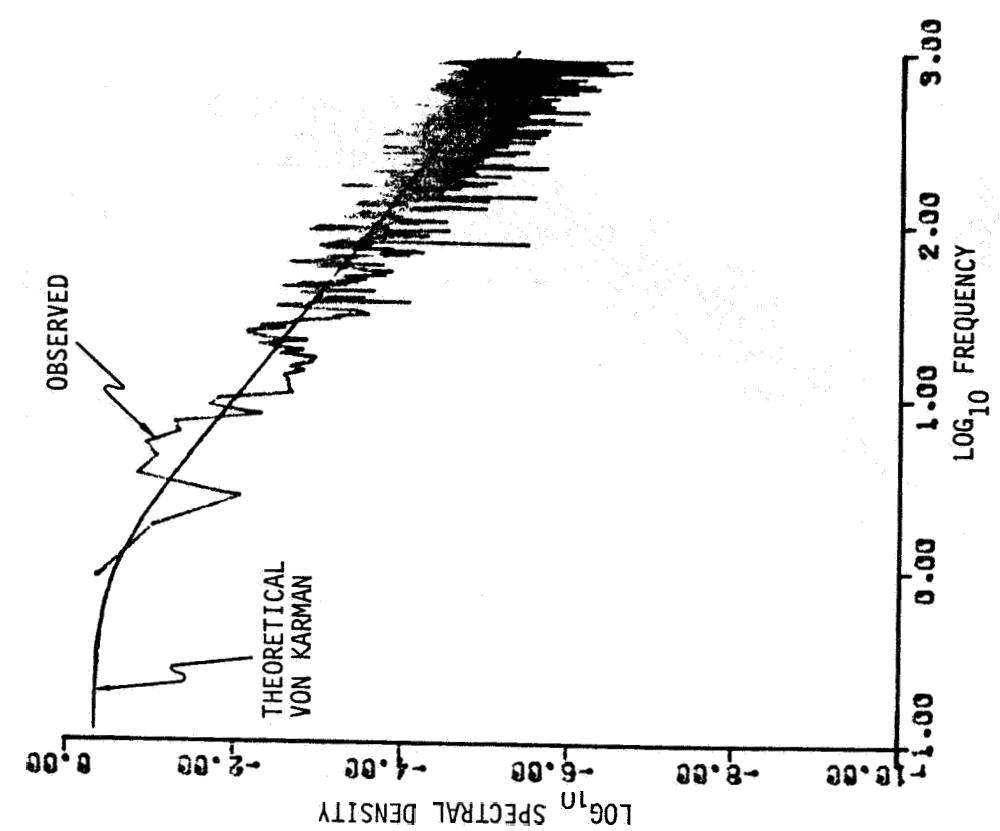




C-3

Figure C-3. u_1 - Gust Spectrum, Altitude Band #3

Figure C-4. u_1 - Gust Spectrum, Altitude Band #4



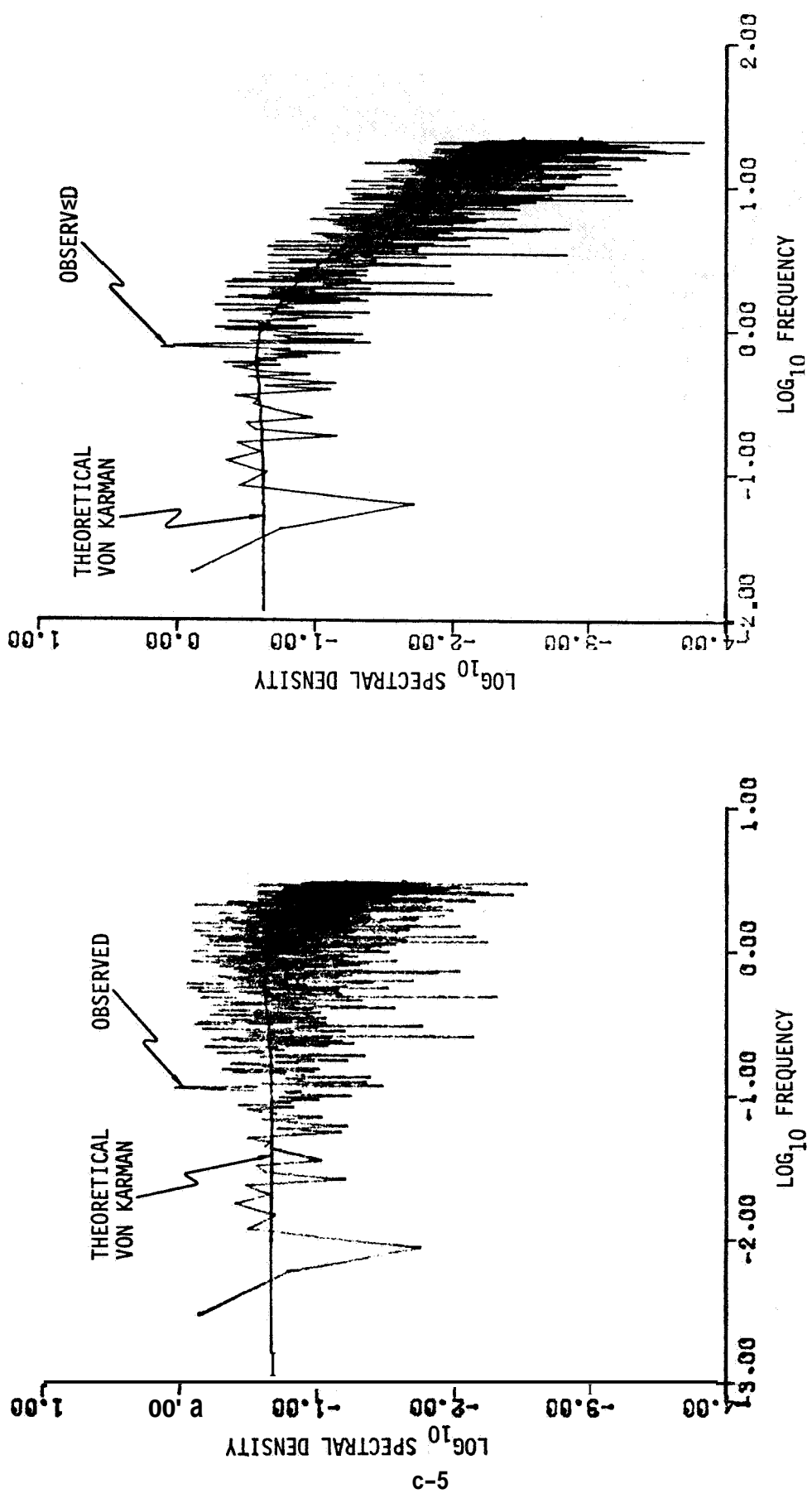
C-4

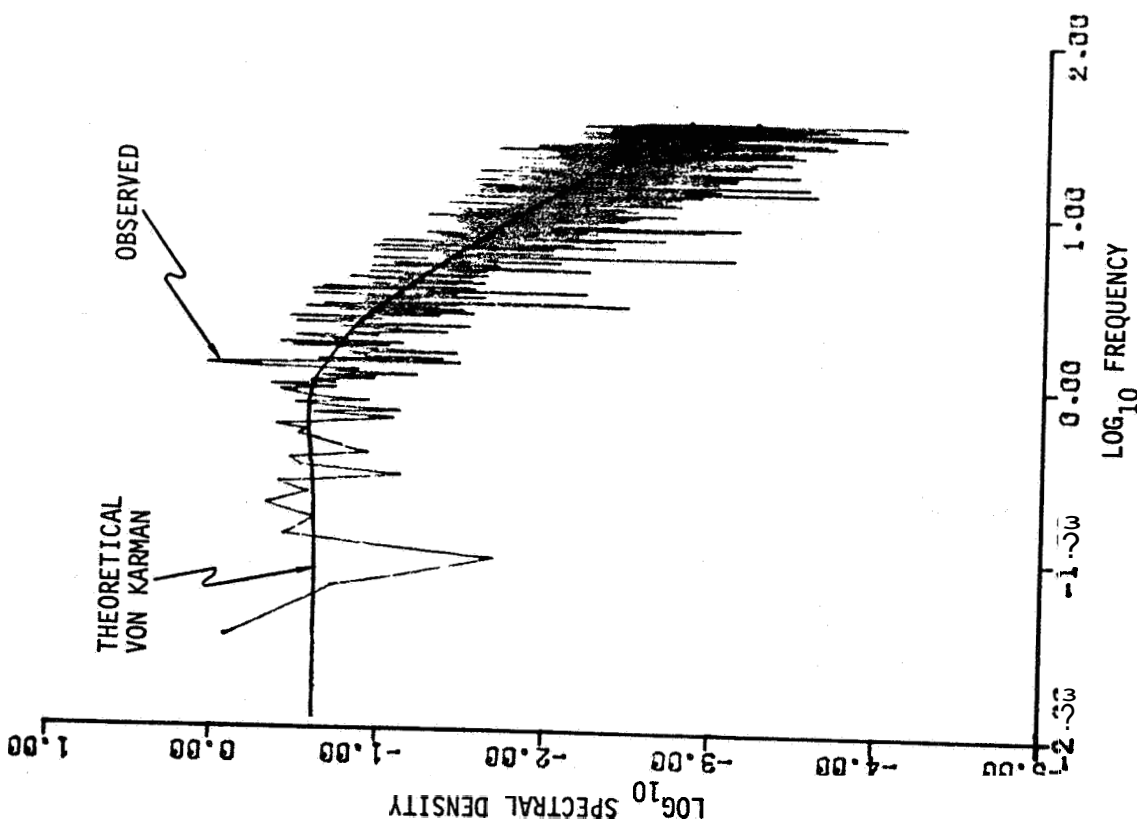
Figure C-5. u_1 - Gust Spectrum, Altitude Band #5

Figure C-6. u_1 - Gust Spectrum, Altitude Band #6

Figure C-8. u_2 - Gust Spectrum, Altitude Band #2

Figure C-7. u_2 - Gust Spectrum, Altitude Band #1





C-9

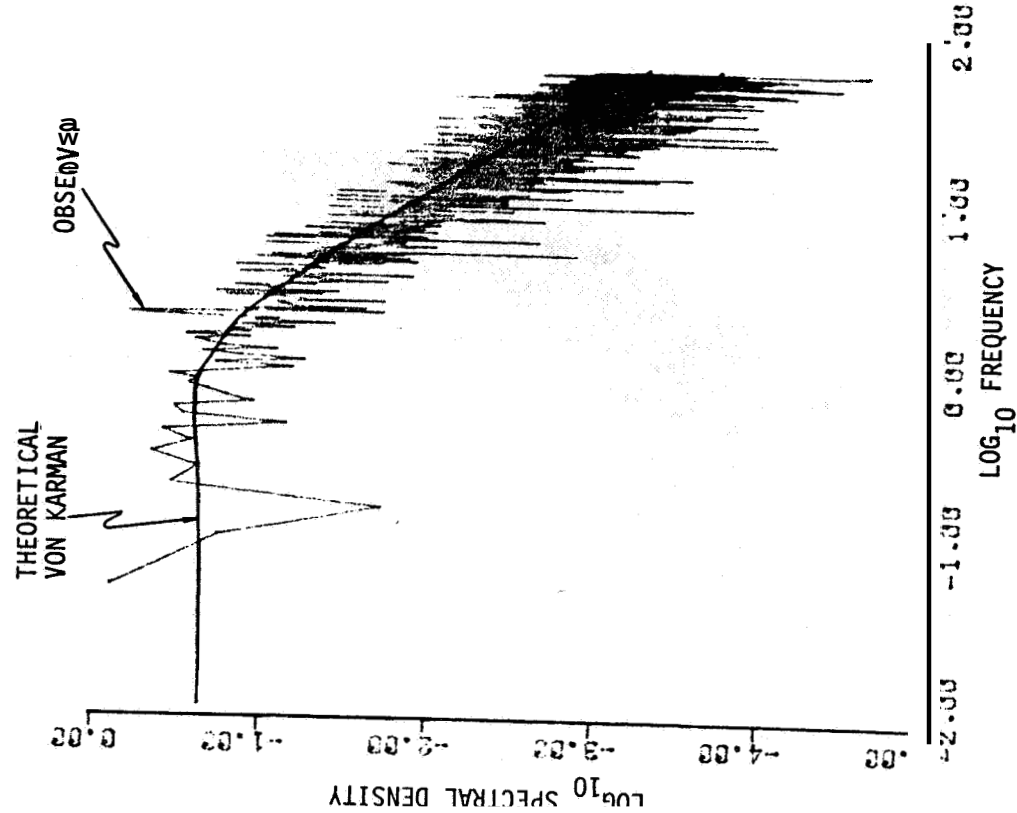


Figure C-9. u_2 - Gust Spectrum, Altitude Band #3

Figure C-10. u_2 - Gust Spectrum, Altitude Band #4

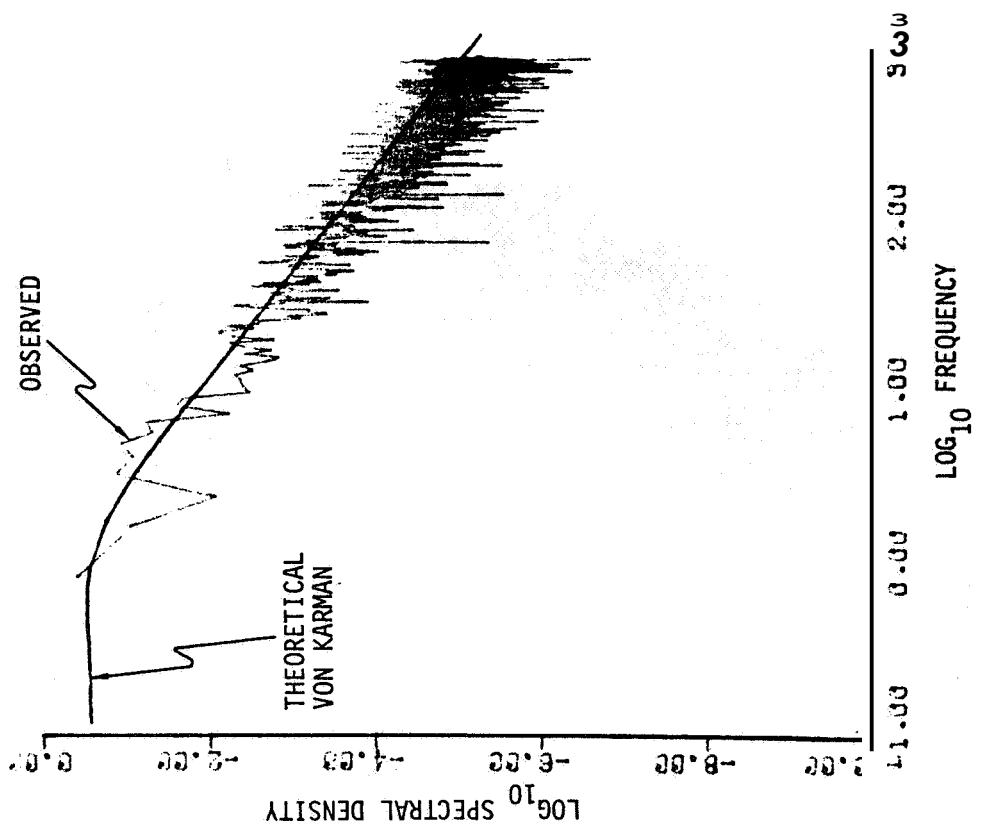


Figure C-12. u_2 - Gust Spectrum, Altitude Band #6

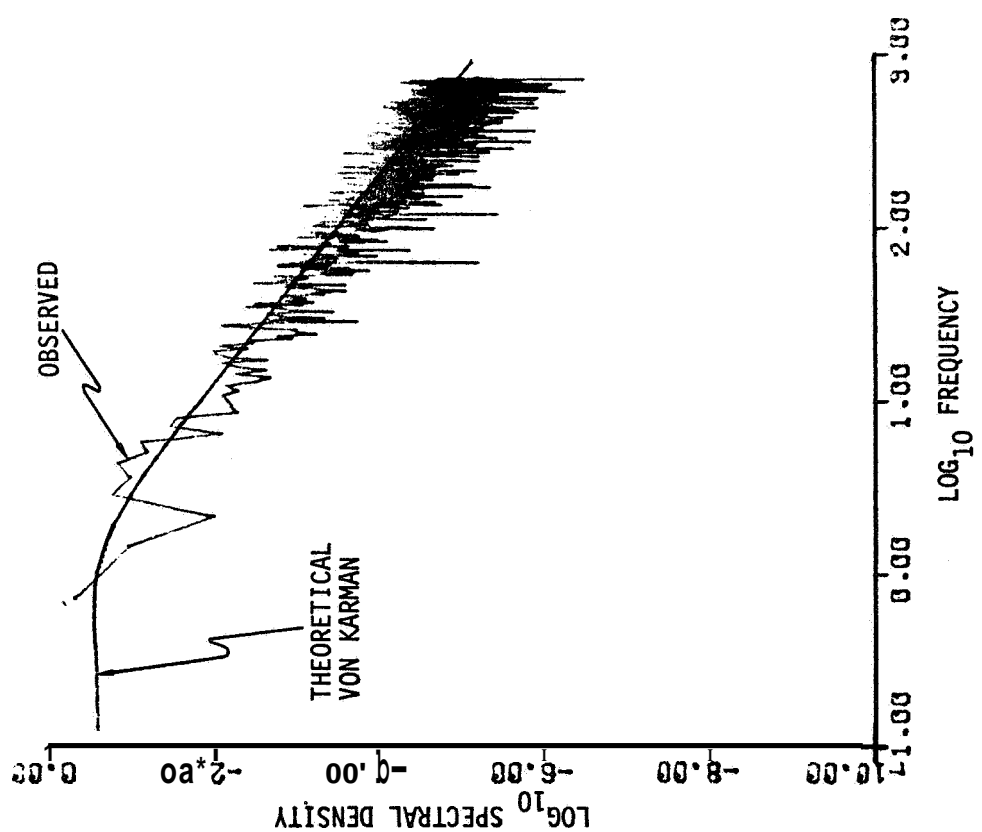


Figure C-11. u_2 - Gust Spectrum, Altitude Band #5

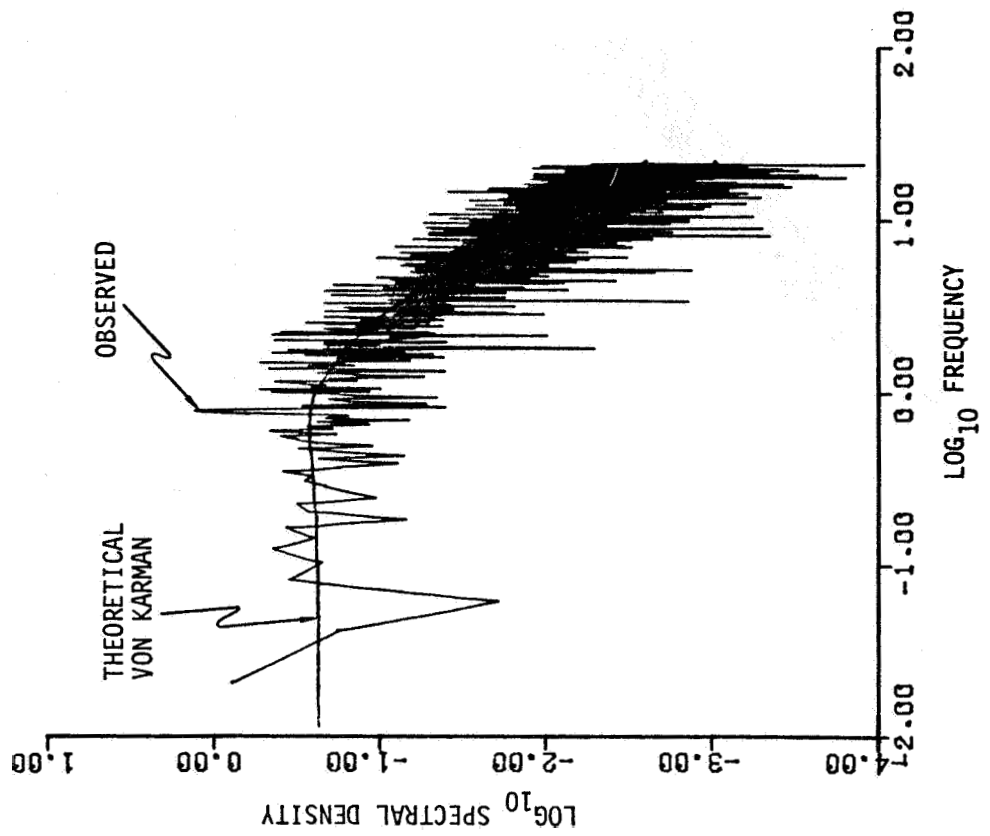


Figure C-14. u_3 - Gust Spectrum, Altitude Band #2

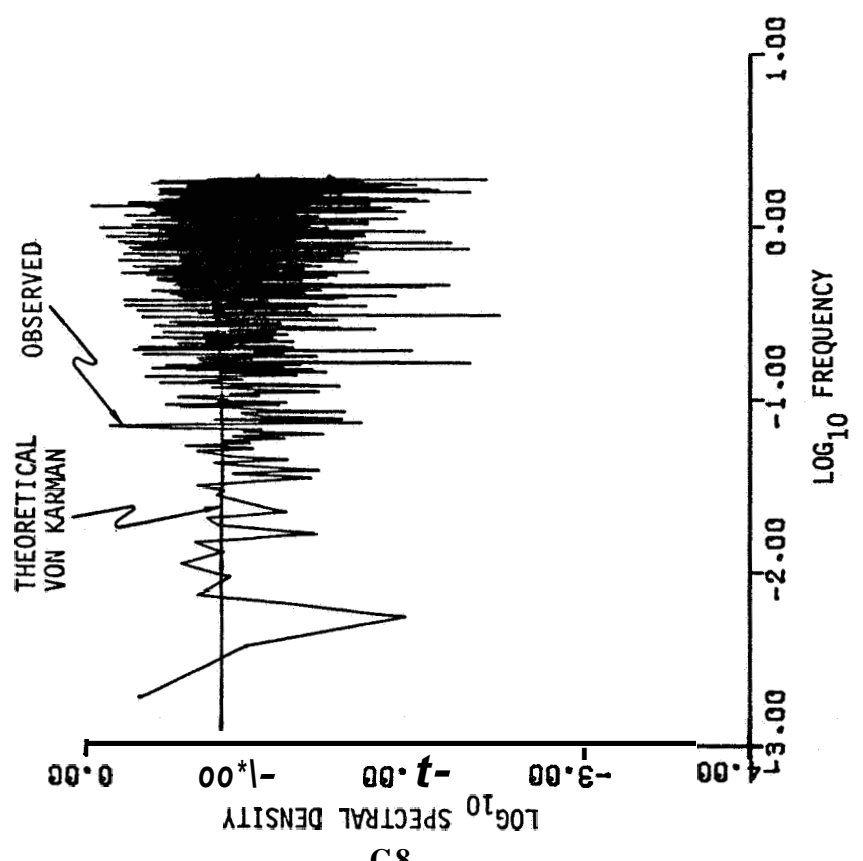
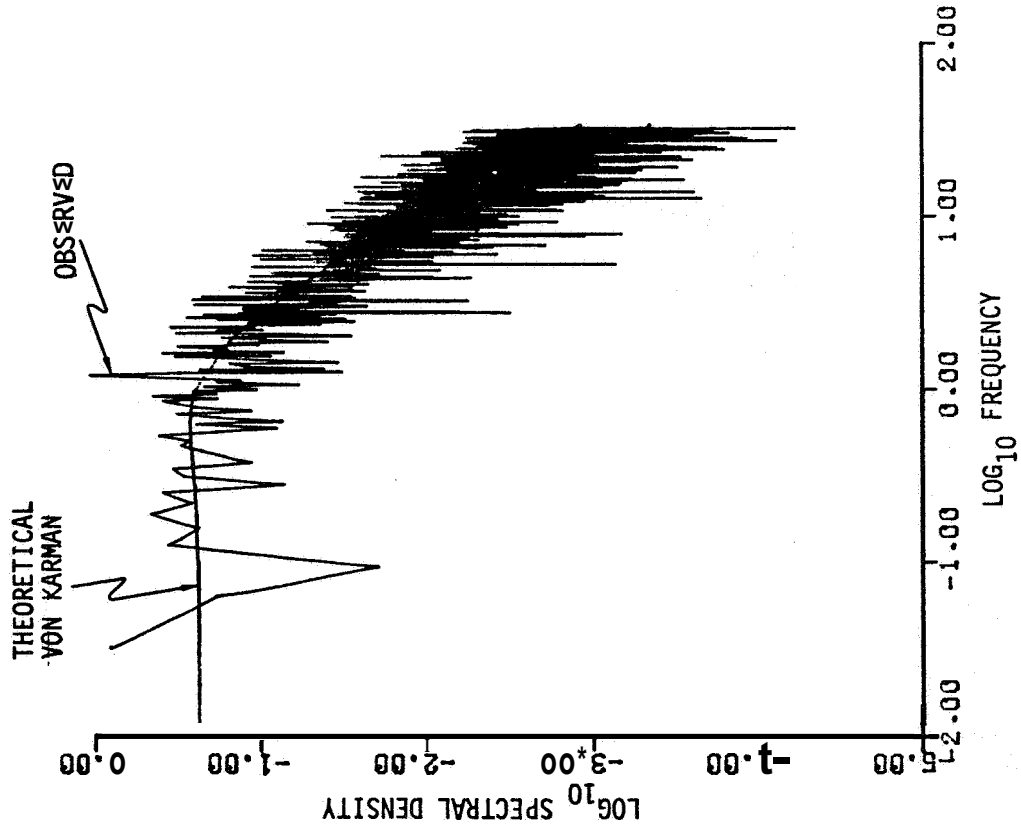


Figure C-13. u_3 - Gust Spectrum, Altitude Band #1



c-9

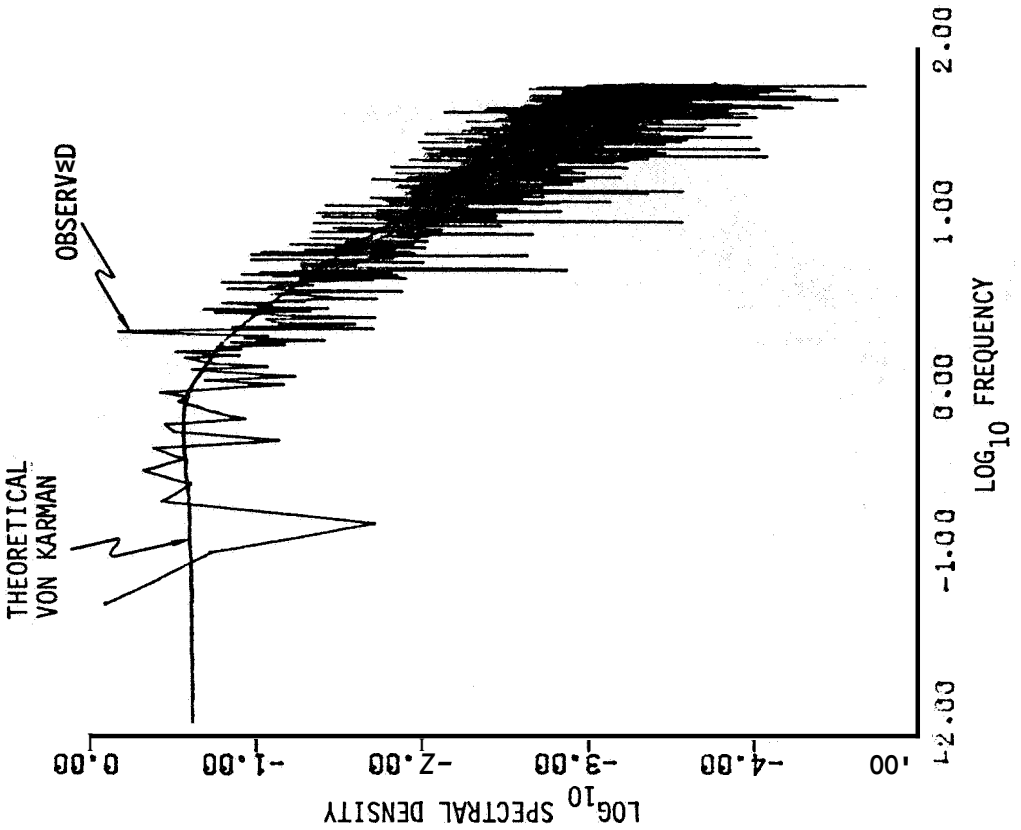


Figure C-15. u_3 - Gust Spectrum, Altitude Band #3

Figure C-16 u_3 - Gust Spectrum, Altitude Band #4

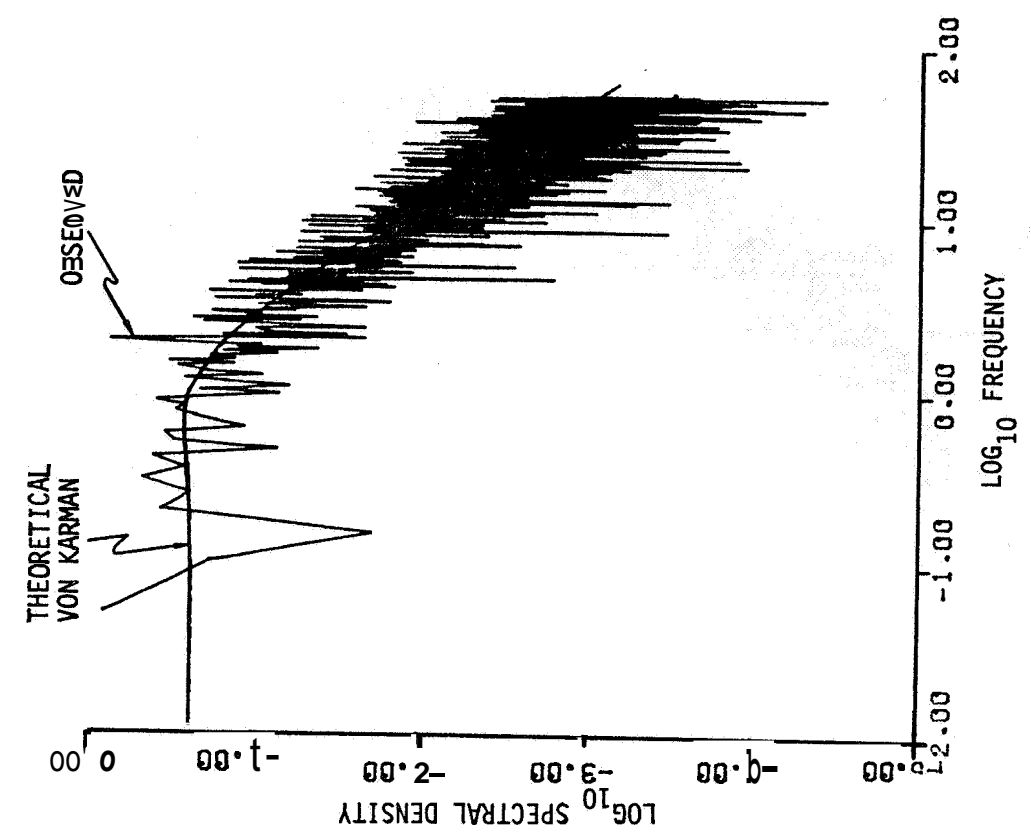


Figure C-18. u_3 - Gust Spectrum, Altitude Band #6

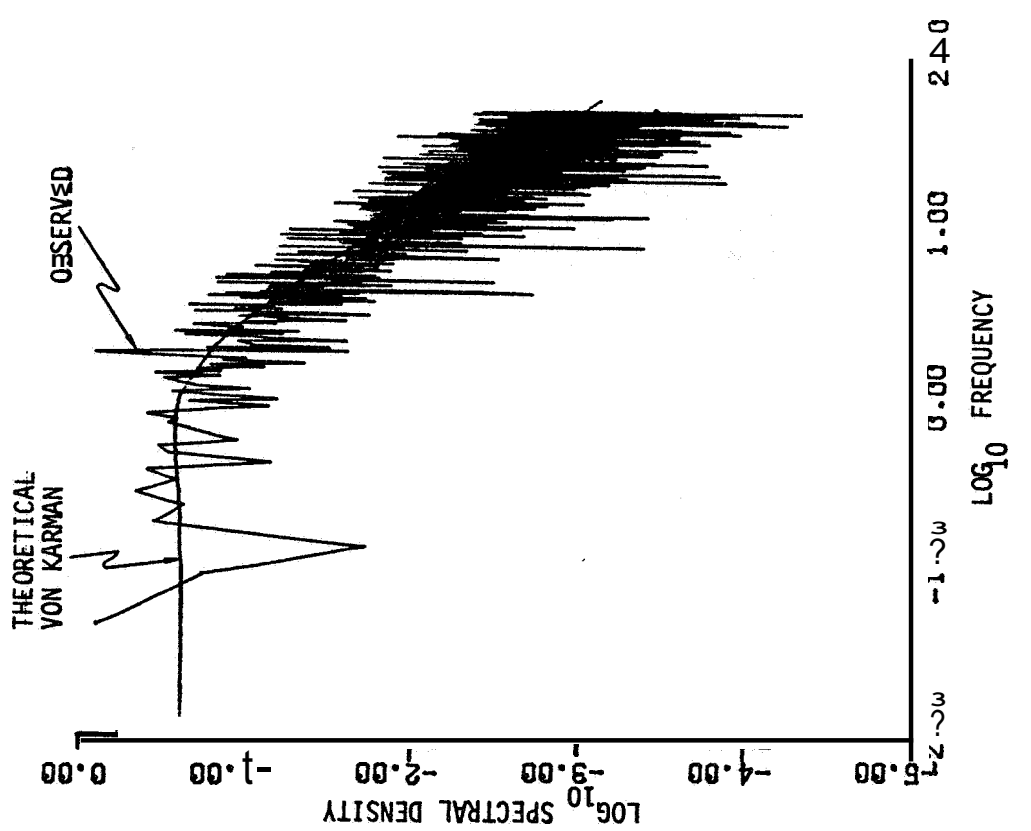


Figure C-17 u_3 - Gust Spectrum, Altitude Band #5

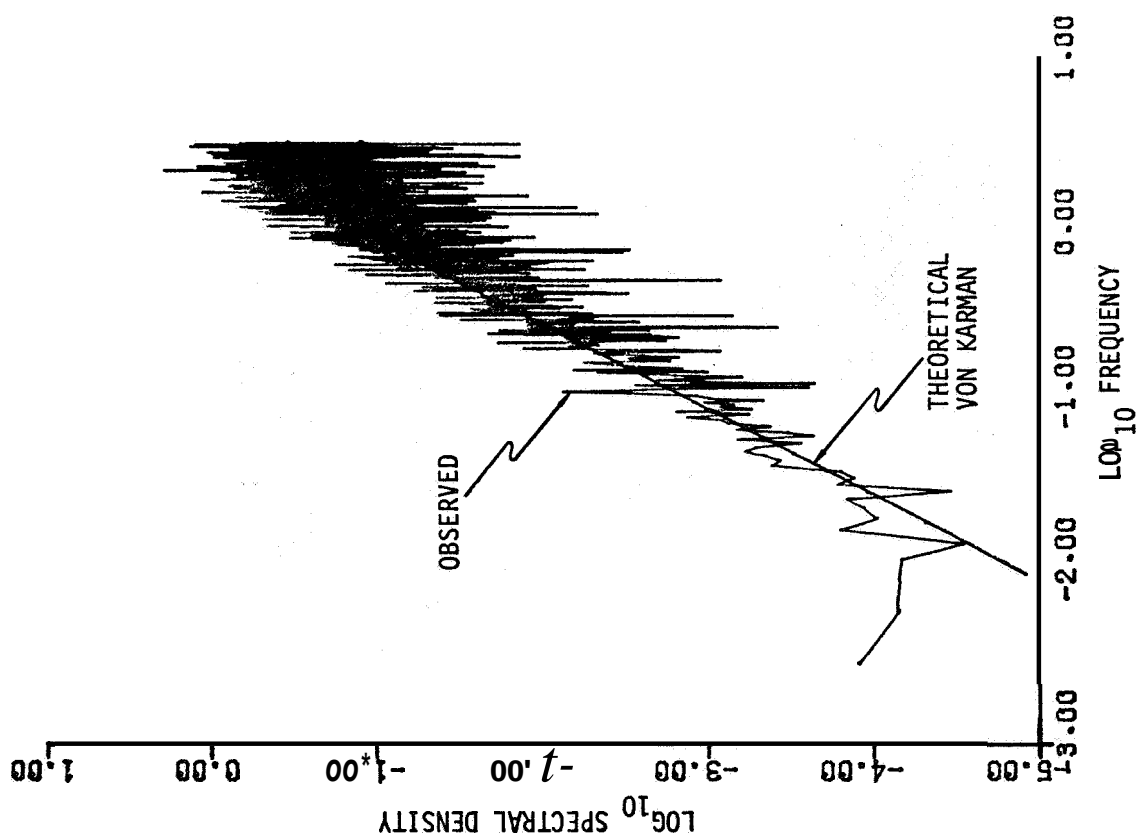


Figure C-19. $\partial u_2 / \partial x_1$ ~ Gust Gradient Spectrum,
Altitude Band #1

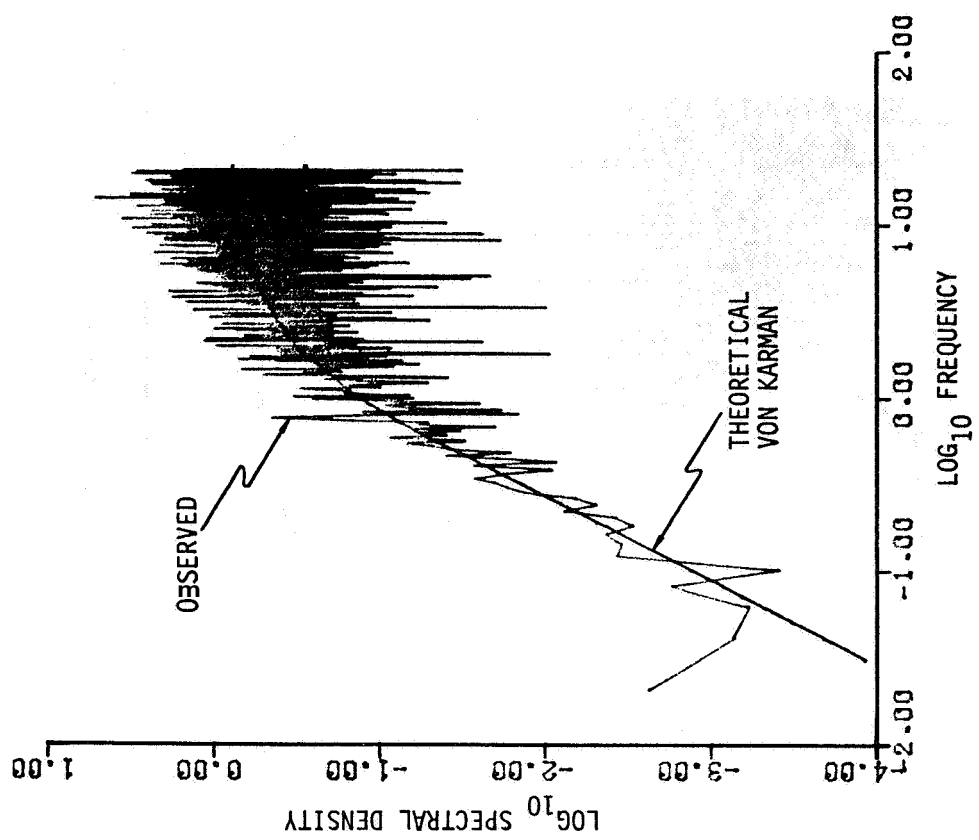


Figure C-20. $\partial u_2 / \partial x_1$ ~ Gust Gradient Spectrum,
Altitude Band #2

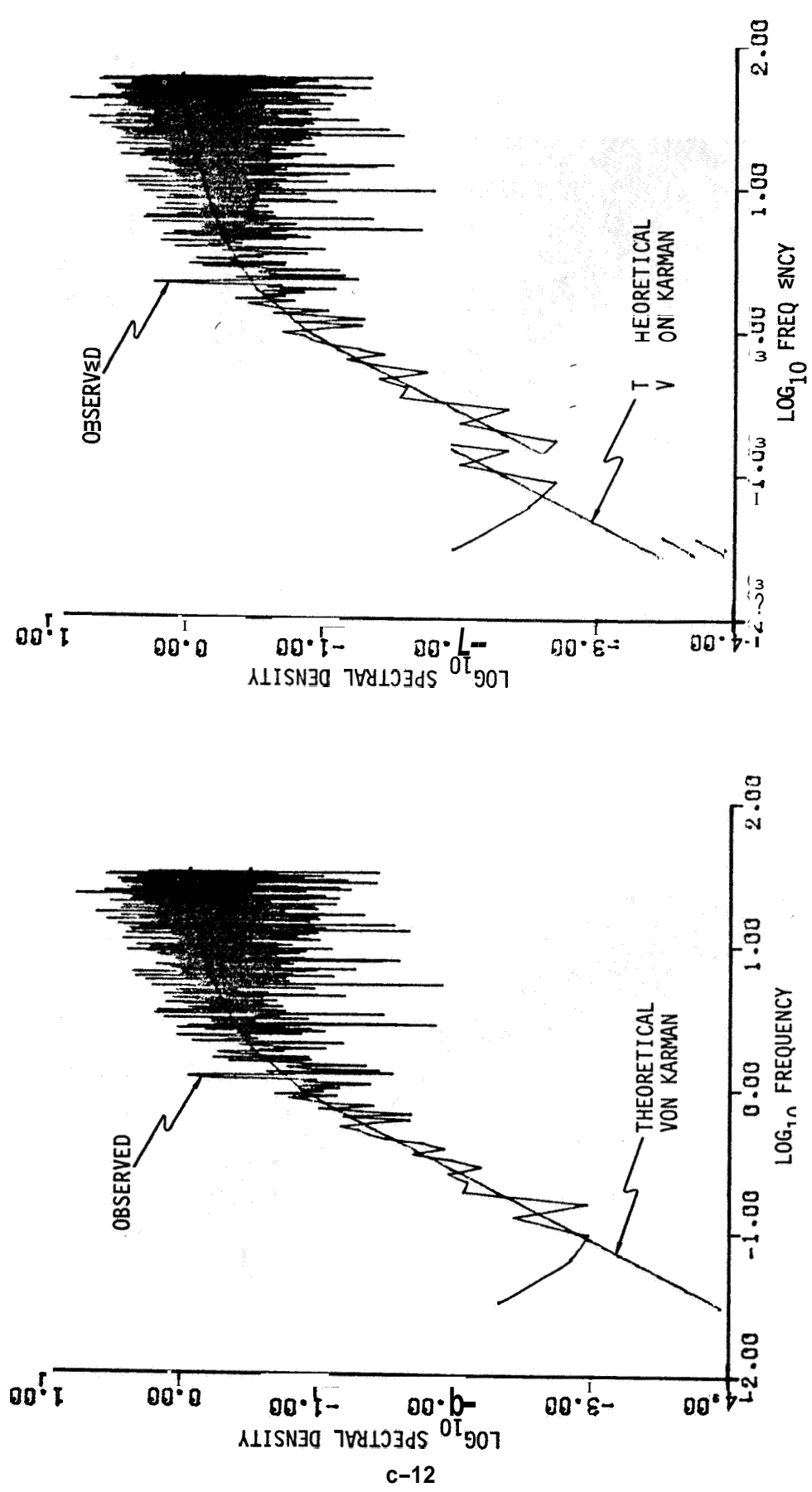


Figure C-21. $\partial u_2 / \partial x_1 \sim$ Gust Gradient Spectrum,
Altitude Band #3

Figure C-22. $\partial u_2 / \partial x_1 \sim$ Gust Gradient Spectrum,
Altitude Band #4

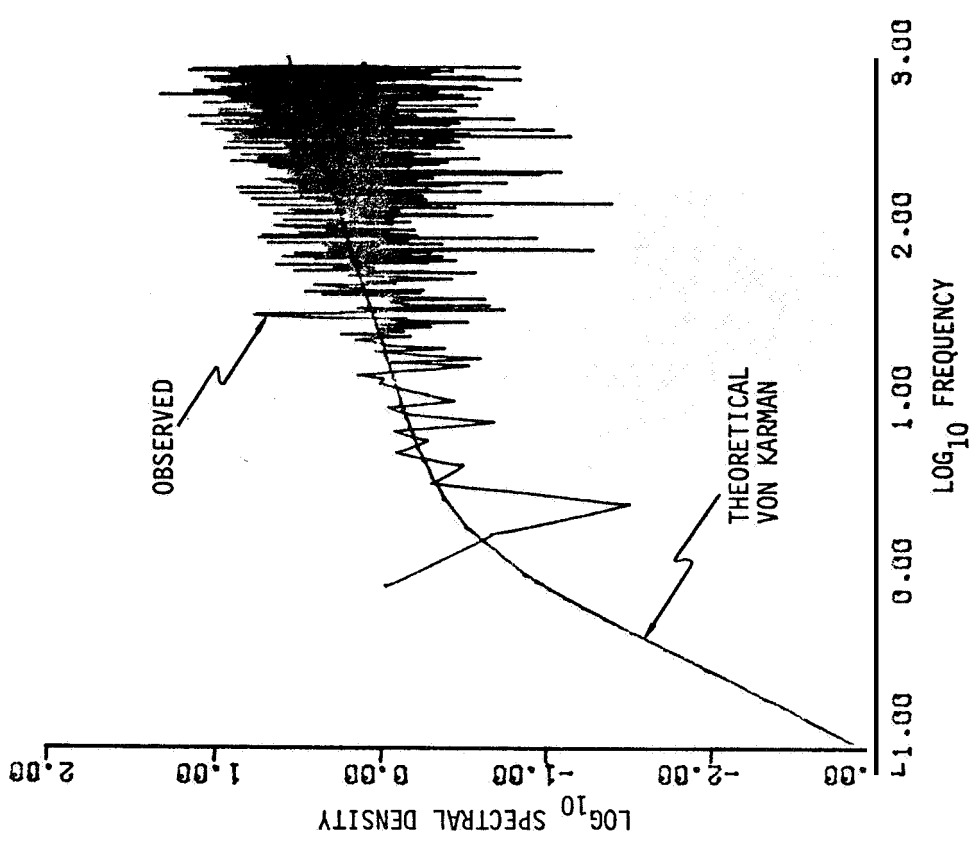


Figure C-23. $\partial u_2 / \partial x_1$ ~ Gust Gradient Spectrum,
Altitude Band #5

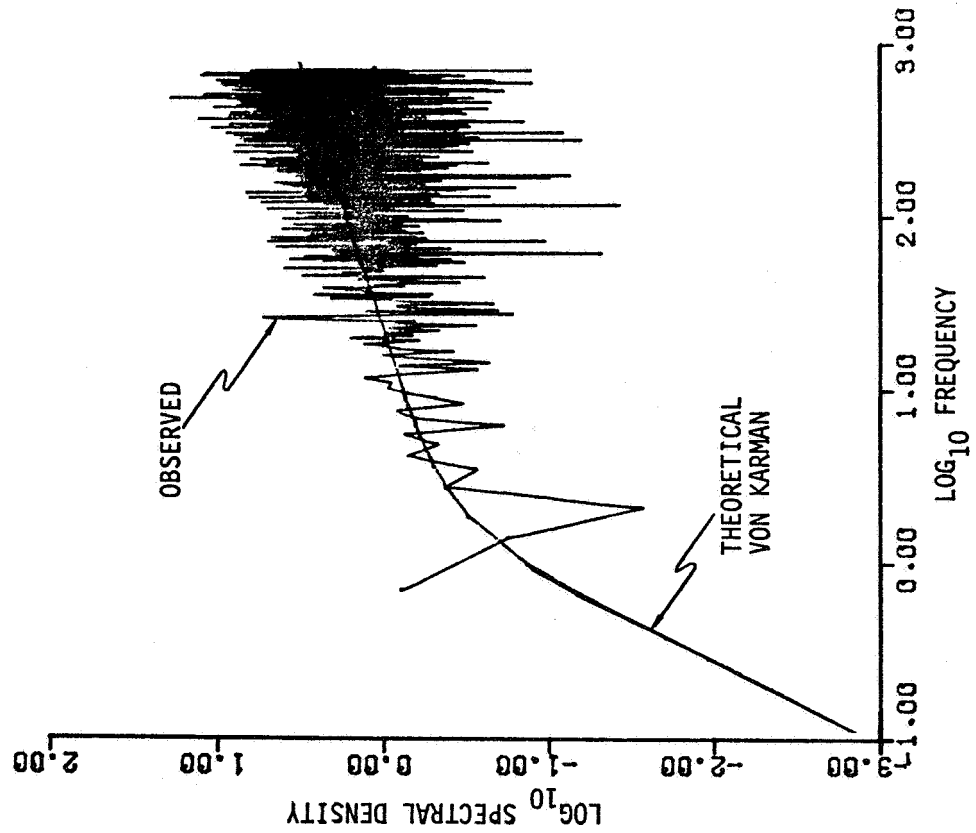


Figure C-24. $\partial u_2 / \partial x_1$ ~ Gust Gradient Spectrum,
Altitude Band #6

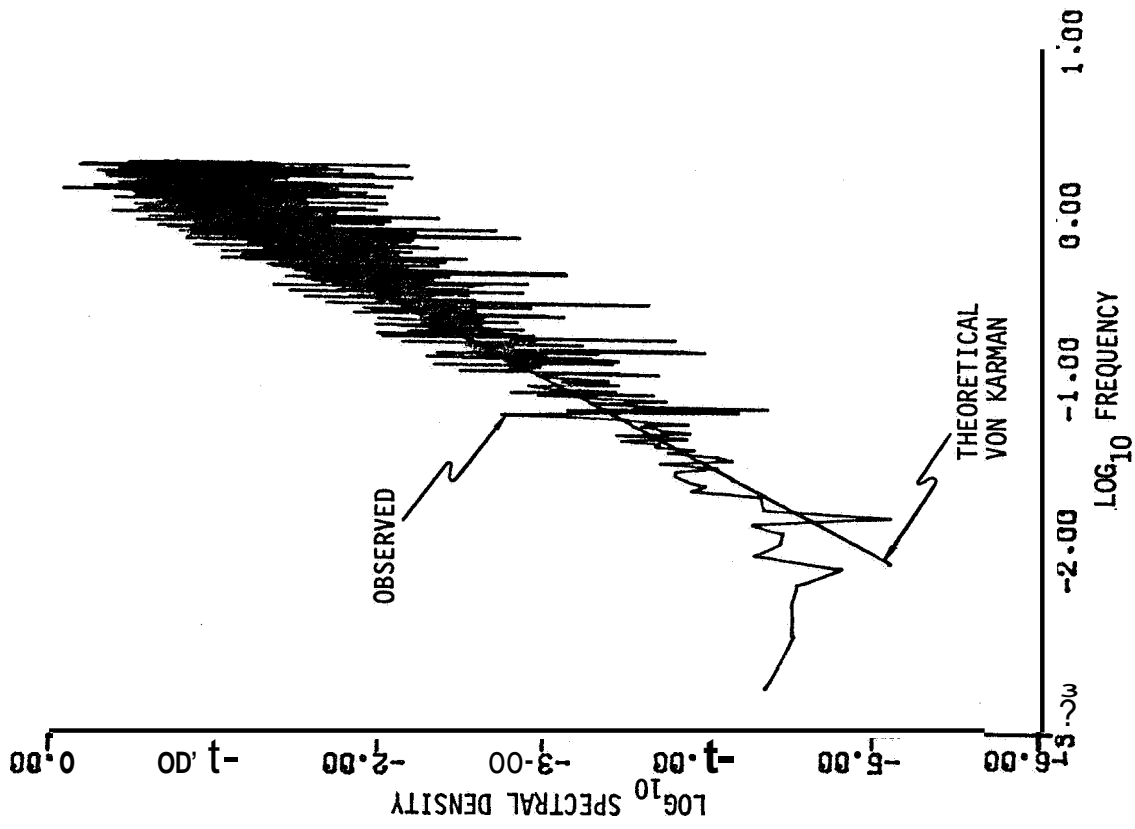


Figure C-25 $\partial u_3 / \partial x_1$ ~ Gust Gradient Spectrum,
Altitude Band #1

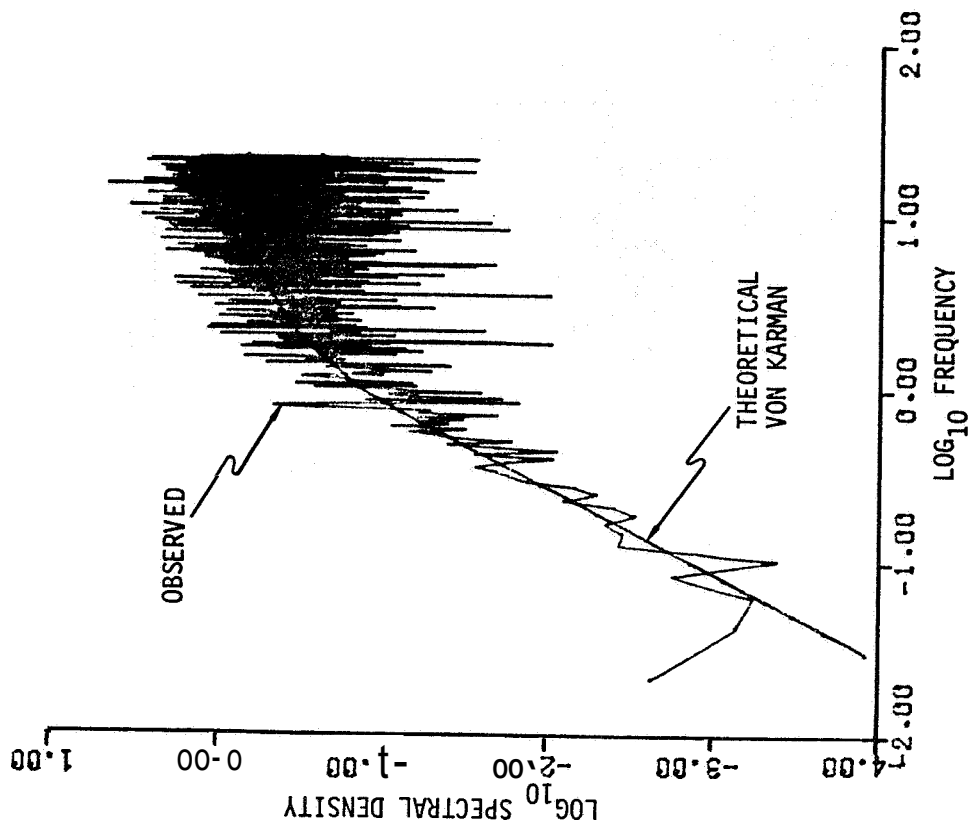


Figure C-26. $\partial u_3 / \partial x_1$ ~ Gust Gradient Spectrum,
Altitude Band #2

Figure C-27. $\partial u_3 / \partial x_1$ - Gust Gradient Spectrum,
Altitude Band #3

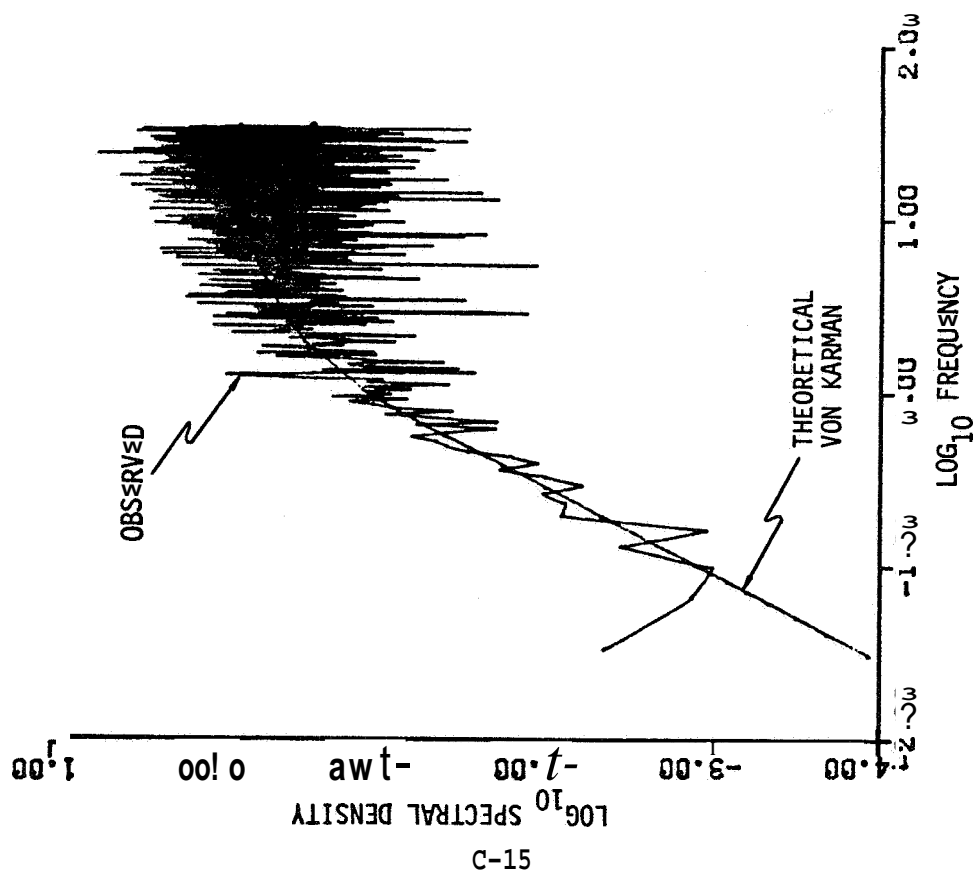
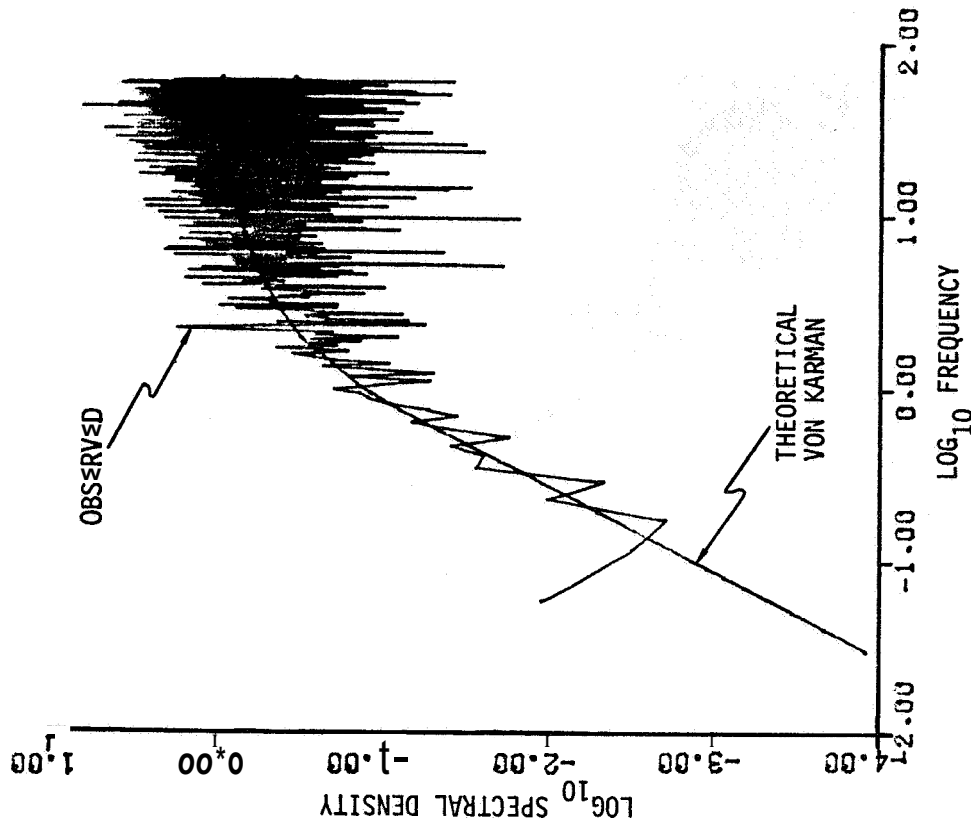


Figure C-28. $\partial u_3 / \partial x_1$ - Gust Gradient Spectrum,
Altitude Band #4



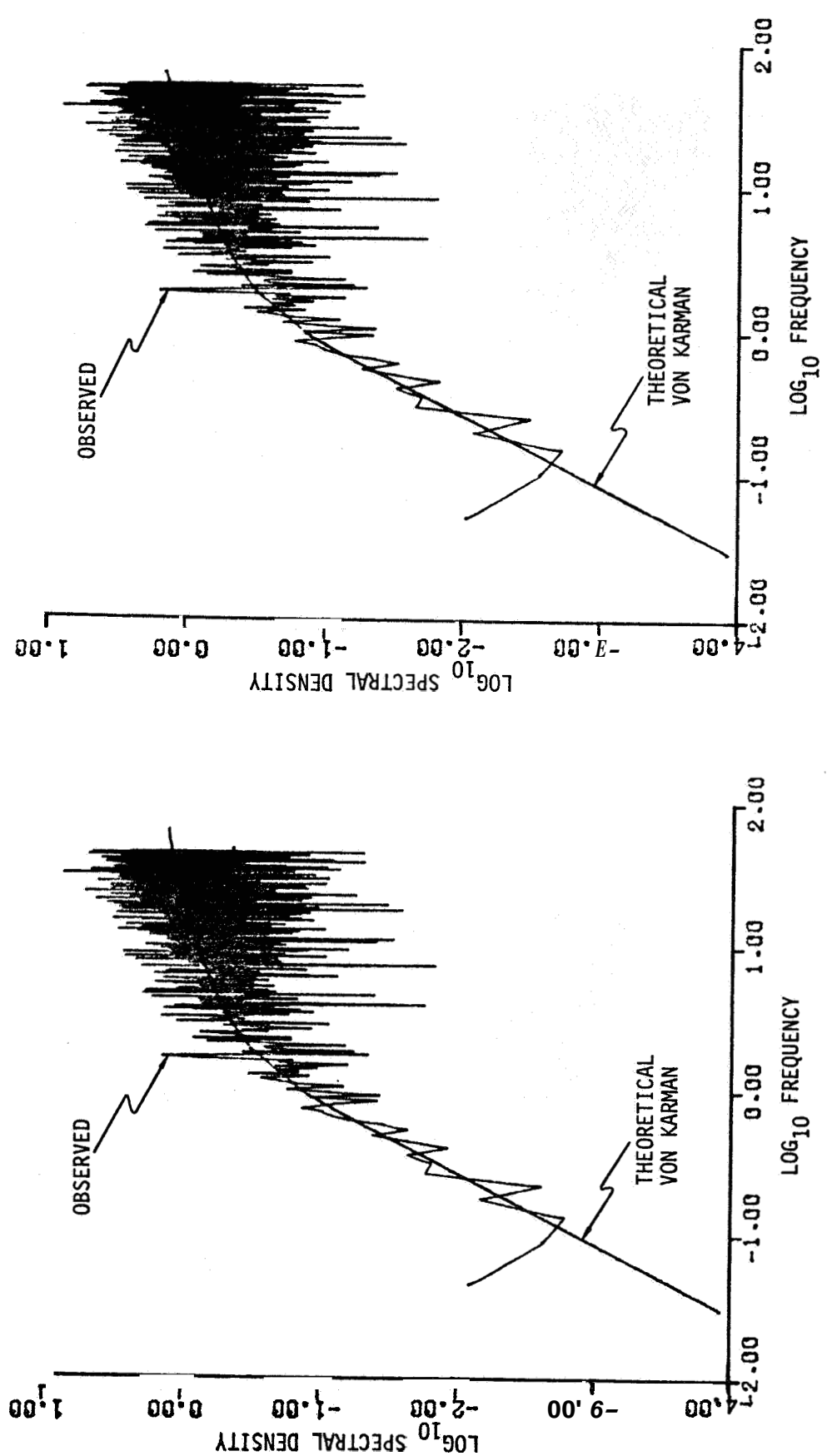


Figure C-29. $\partial u_3 / \partial x_1 \sim$ Gust Gradient Spectrum,
Altitude Band #5

Figure C-30. $\partial u_3 / \partial x_1 \sim$ Gust Gradient Spectrum,
Altitude Band #6

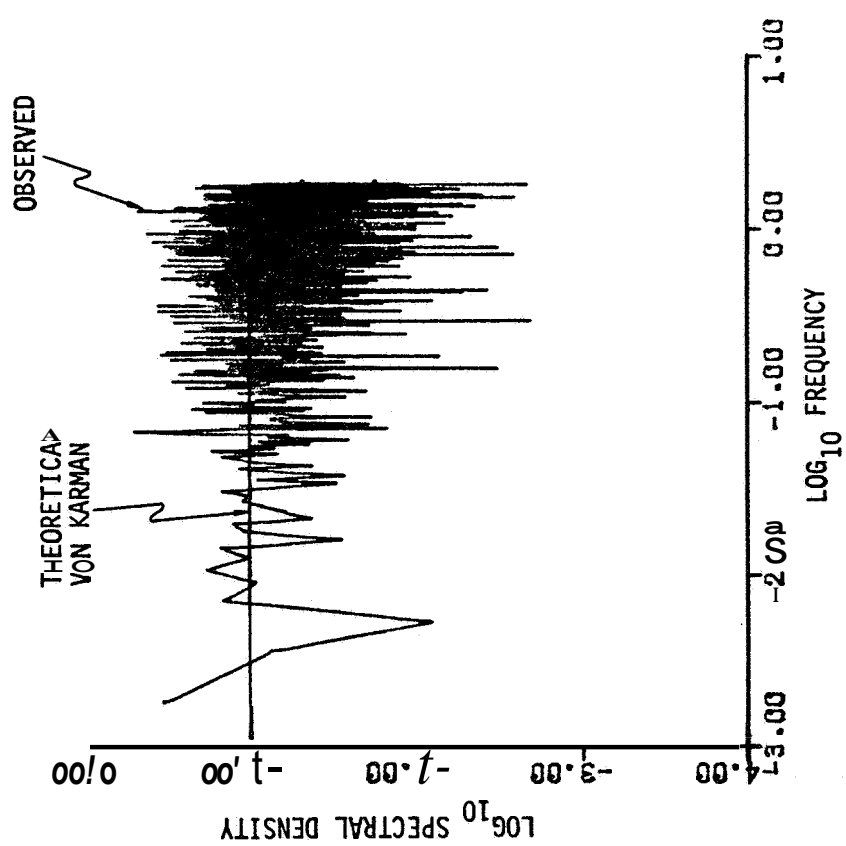
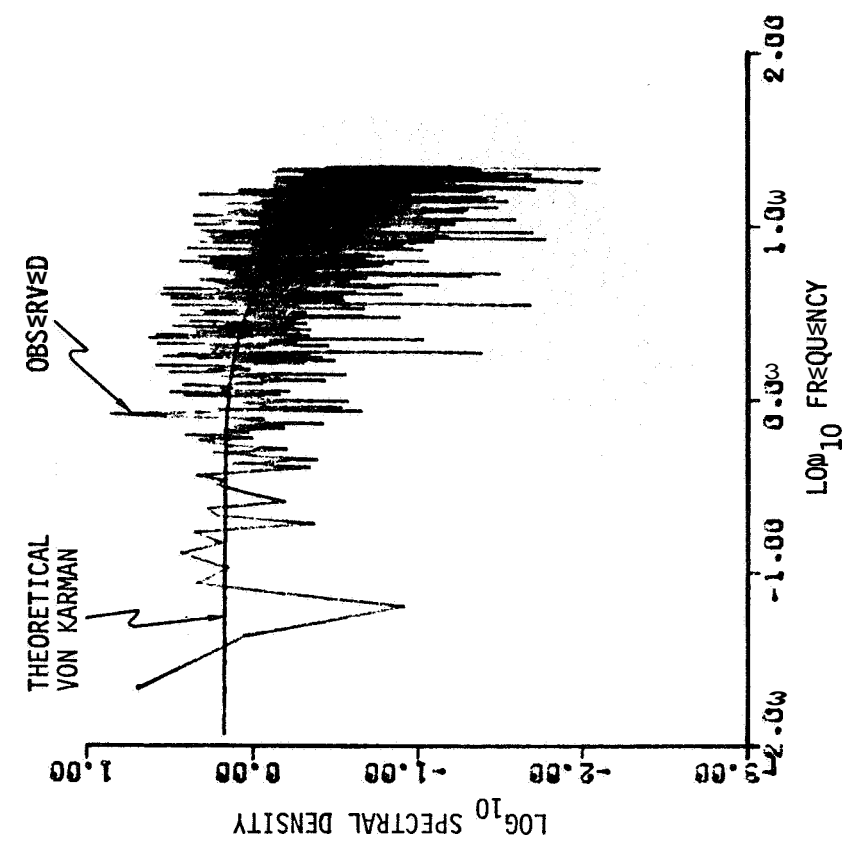


Figure C-31. $\partial u_3 / \partial x_2 \sim$ Gust Gradient Spectrum,
Altitude Band #1

Figure C-32. $\partial u_3 / \partial x_2 \sim$ Gust Gradient Spectrum,
Altitude Band #2

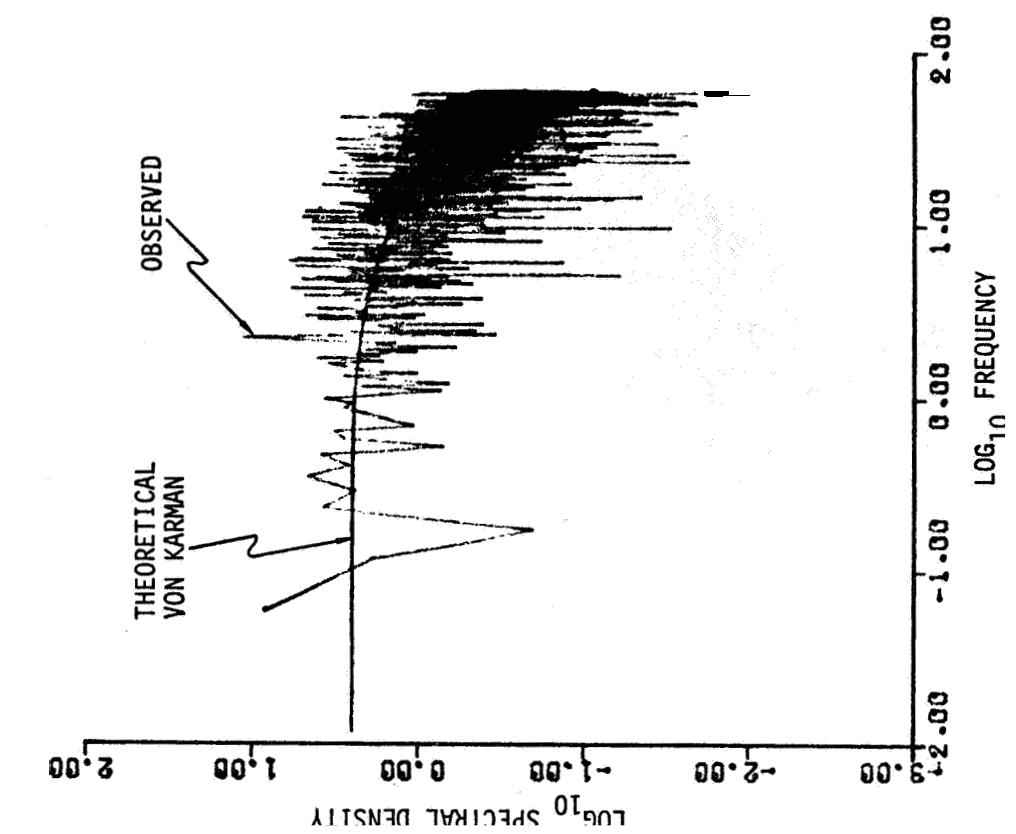


Figure C-33. $\partial u_3 / \partial x_2 \sim$ Gust Gradient Spectrum,
Altitude Band #3

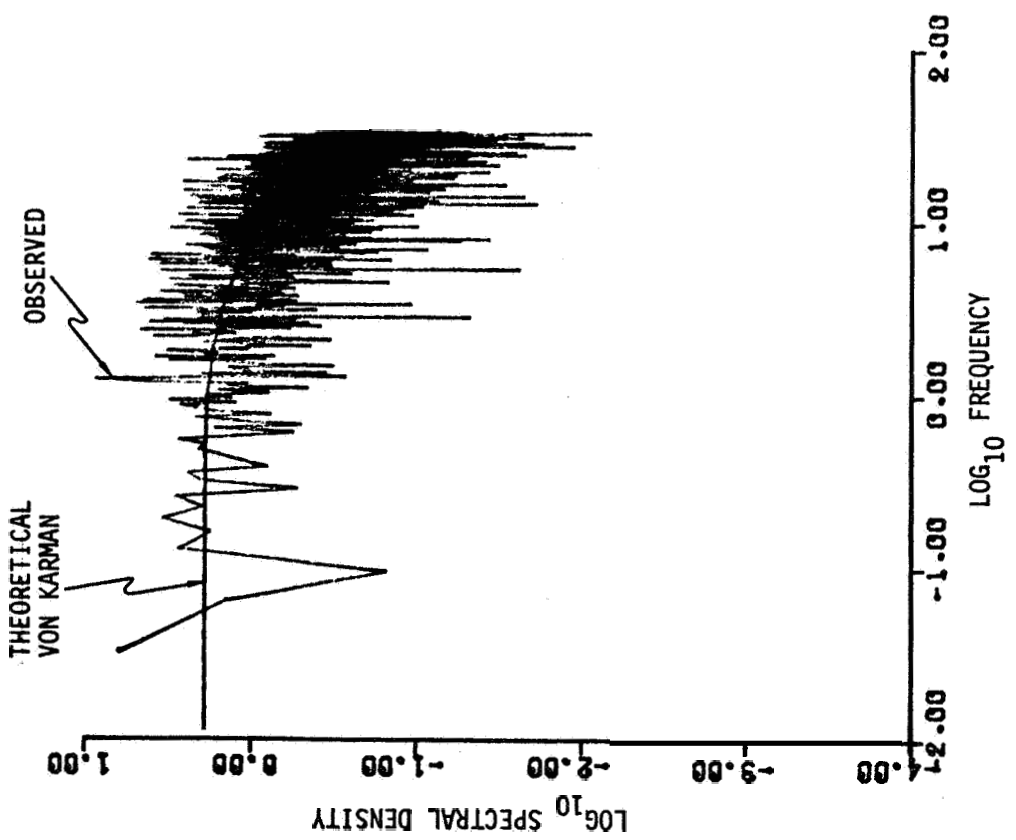


Figure C-34. $\partial u_3 / \partial x_2 \sim$ Gust Gradient Spectrum,
Altitude Band #4

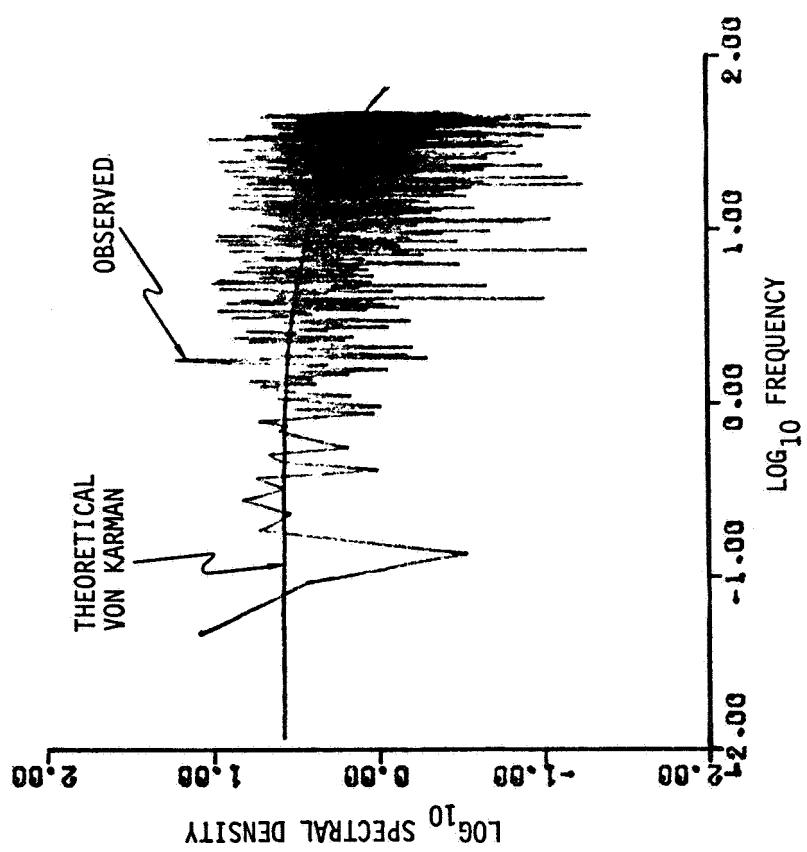
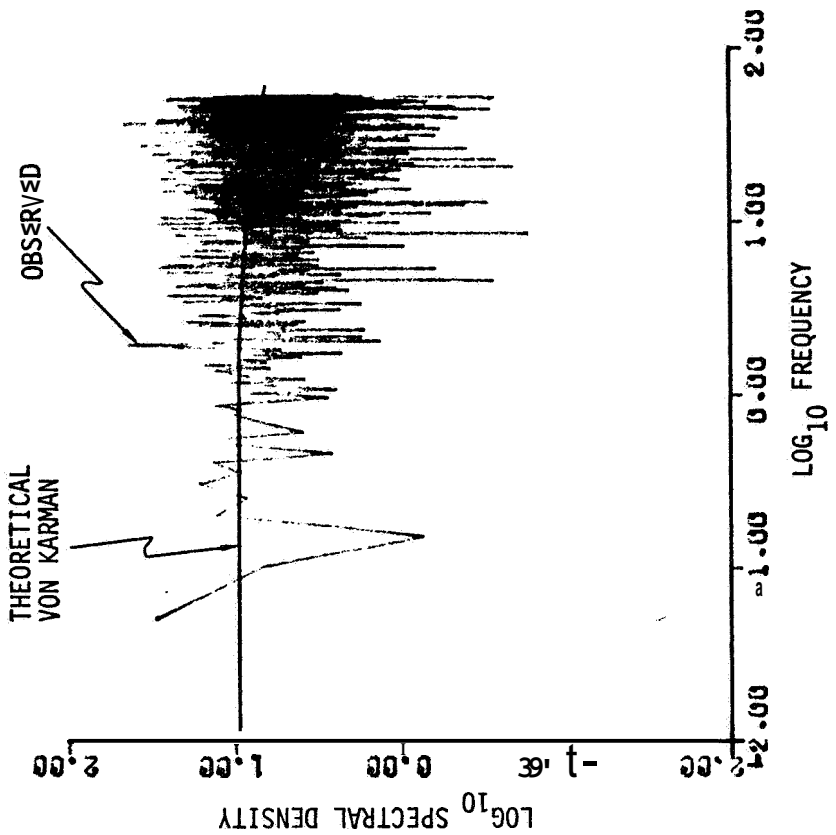


Figure C-35. $\partial u_3 / \partial x_2$ - Gust Gradient Spectrum,
Altitude Band #5

Figure C-36. $\partial u_3 / \partial x_2$ - Gust Gradient Spectrum,
Altitude Band #6

APPENDIX D

STATISTICAL ANALYSIS OF SIMULATED TURBULENCE

By means of standard statistical analysis procedures each of the SSTT has been analyzed to determine its mean value, standard deviation, and probability density distribution. The resulting mean values are presented in Table D-1 while Table D-2 contains the resulting standard deviations. As expected all mean values were near zero. The standard deviations represent the square root of the energy content. The ratio of the theoretical energy content (from Table 2-5) to the square of the corresponding standard deviation (from Table D-2) is presented in Table D-3. The agreement appears quite satisfactory.

The gust and gust gradient probability density distributions are presented in Figures D-1 through D-36 in accordance with Table D-4. In each figure the corresponding theoretical normal distribution is also presented. The results indicate that both the gust and gust gradient time series are very close to normal distributions.

TABLE D-1. MEAN VALUE OF GUST AND GUST GRADIENTS

SERIES TYPE	ALTITUDE BAND					
	1	2	3	4	5	6
u_1	-.019295	-.042050	-.051852	-.088142	-.0455	-.0464
u_2	-.010671	-.029576	-.0371	-.049431	-.0428	-.0441
u_3	-.006806	-.029652	-.037043	-.049370	-.043788	-.046637
$\partial u_2 / \partial x_1$	-.000002	-.001572	-.002794	-.005628	-.172152	-.206385
$\partial u_3 / \partial x_2$	-.000001	-.001591	-.002798	-.005649	-.004293	-.004893
$\partial u_3 / \partial x_1$	-.005760	-.073072	-.103823	-.160303	-.171448	-.288178

*

The statistical analysis involved the first 4096 terms of each time series except for bands 5 and 6 for the u_1 and u_2 gusts. For these cases 8192 terms were used.

TABLE D-2. STANDARD DEVIATION OF GUST AND GUST GRADIENTS

SERIES TYPE	ALTITUDE BAND					
	1	2	3	4	5	6
u_1	.788959	.927098	.946351	.964271	.99888	.99996
u_2	.707845	.925201	.94619	.964152	.99764	.99863
u_3	.524571	.915606	.938552	.958985	.961845	.967651
$\partial u_2 / \partial x_1$.766627	3.625937	4.976618	7.356808	41.717292	48.052734
$\partial u_3 / \partial x_2$.390512	3.488677	4.758426	7.037516	6.458092	7.216648
$\partial u_3 / \partial x_1$.394539	3.508280	4.784378	7.075349	9.778736	19.790119

TABLE D-3. RATIO OF THE THEORETICAL ENERGY CONTENT*
TO THE SQUARE OF THE OBSERVED STANDARD DEVIATION†

SERIES TYPE	ALTITUDE BAND					
	1	2	3	4	5	6
u_1	1.0001	1.0000	1.0000	1.0000	.9999	1.0001
u_2	.9999	1.0000	.9999	1.0000	1.0000	1.0000
u_3	1.0001	1.0000	1.0000	1.0001	1.0000	.9999
$\partial u_2 / \partial x_1$	1.0000	1.0000	1.0000	1.0000	.9998	1.0000
$\partial u_3 / \partial x_2$	1.0000	1.0000	1.0000	1.0000	1.0001	1.0000
$\partial u_3 / \partial x_1$	1.0002	1.0000	1.0000	1.0000	1.0000	.9999

*

Theoretical energy content taken from Table 2-3.

*Observed standard deviation taken from Table D-2.

TABLE D-4. MATRIX OF STATISTICAL ANALYSIS FIGURES

SERIES TYPE	ALTITUDE BAND					
	1	2	3	4	5	6
u_1	D-1	D-2	D-3	D-4	D-5	D-6
u_2	D-7	D-8	D-9	D-10	D-11	D-12
u_3	D-13	D-14	D-15	D-16	D-17	D-18
$\partial u_2 / \partial x_1$	D-19	D-20	D-21	D-22	D-23	D-24
$\partial u_3 / \partial x_1$	D-25	D-26	D-27	D-28	D-29	D-30
$\partial u_3 / \partial x_2$	D-31	D-32	D-33	D-34	D-35	D-36

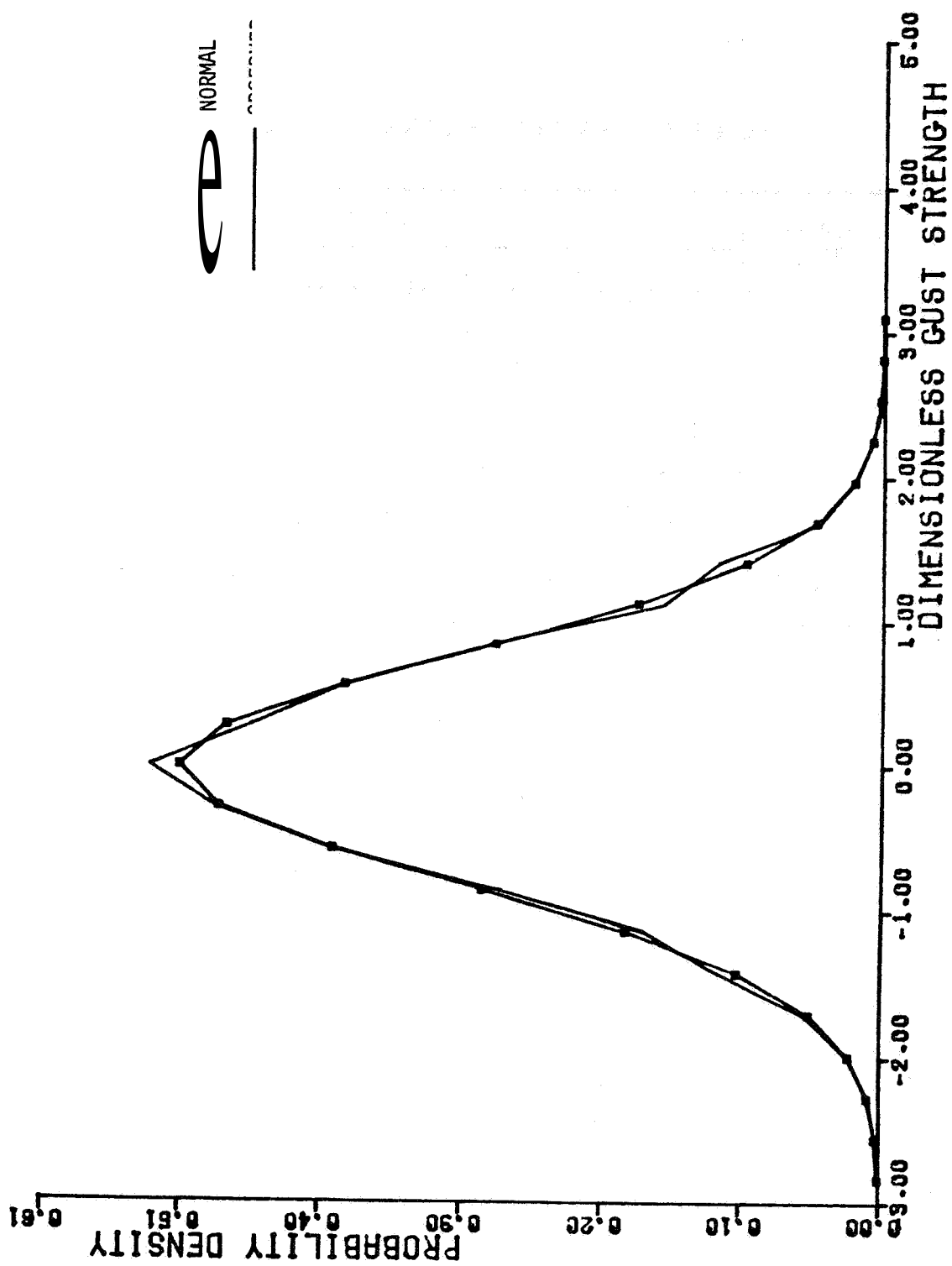


Figure D-1. u_1 - Gust Probability Density Distribution, Altitude Band #1

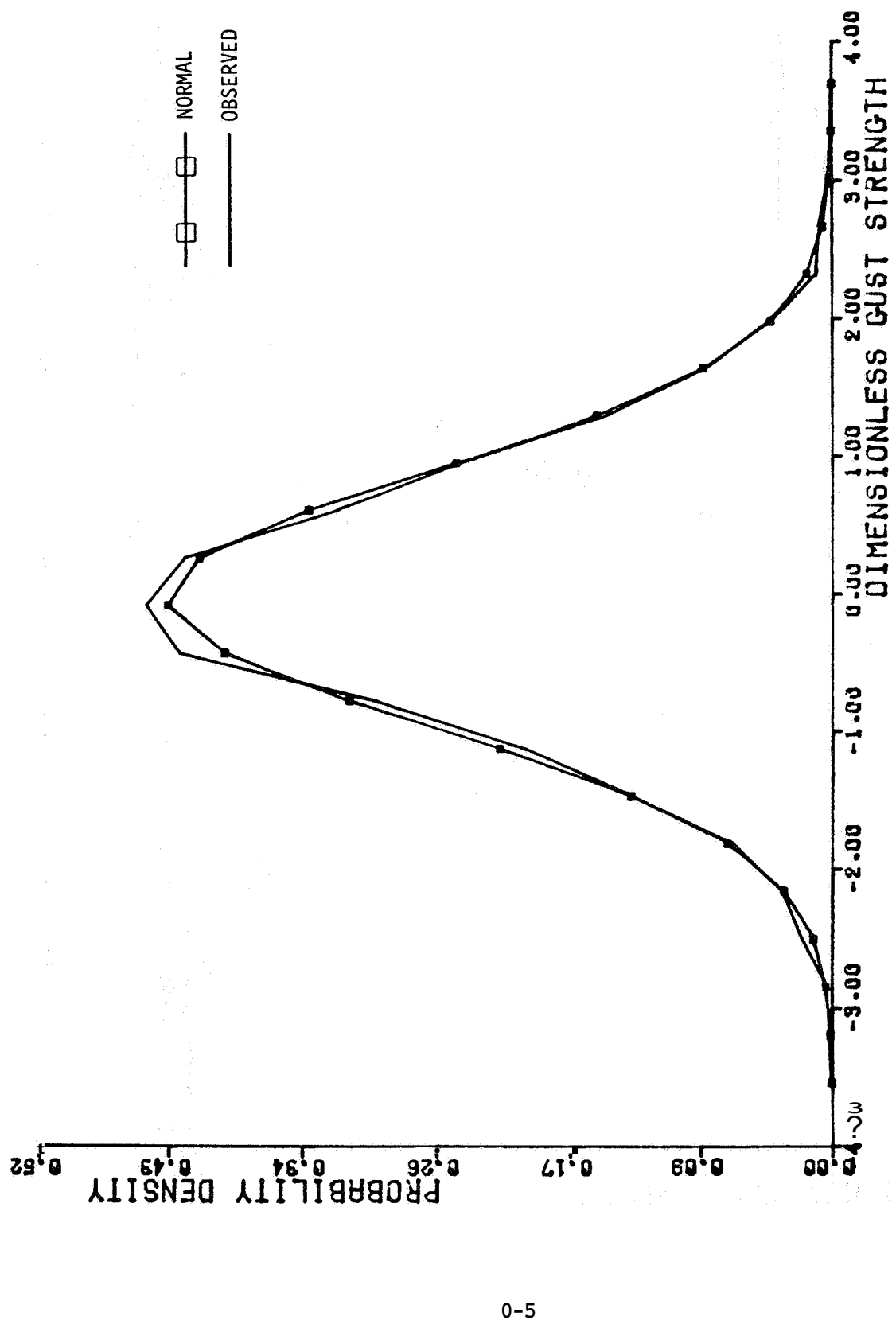


Figure D-2 u_1 - Gust Probability Density Distribution, Altitude Band #2

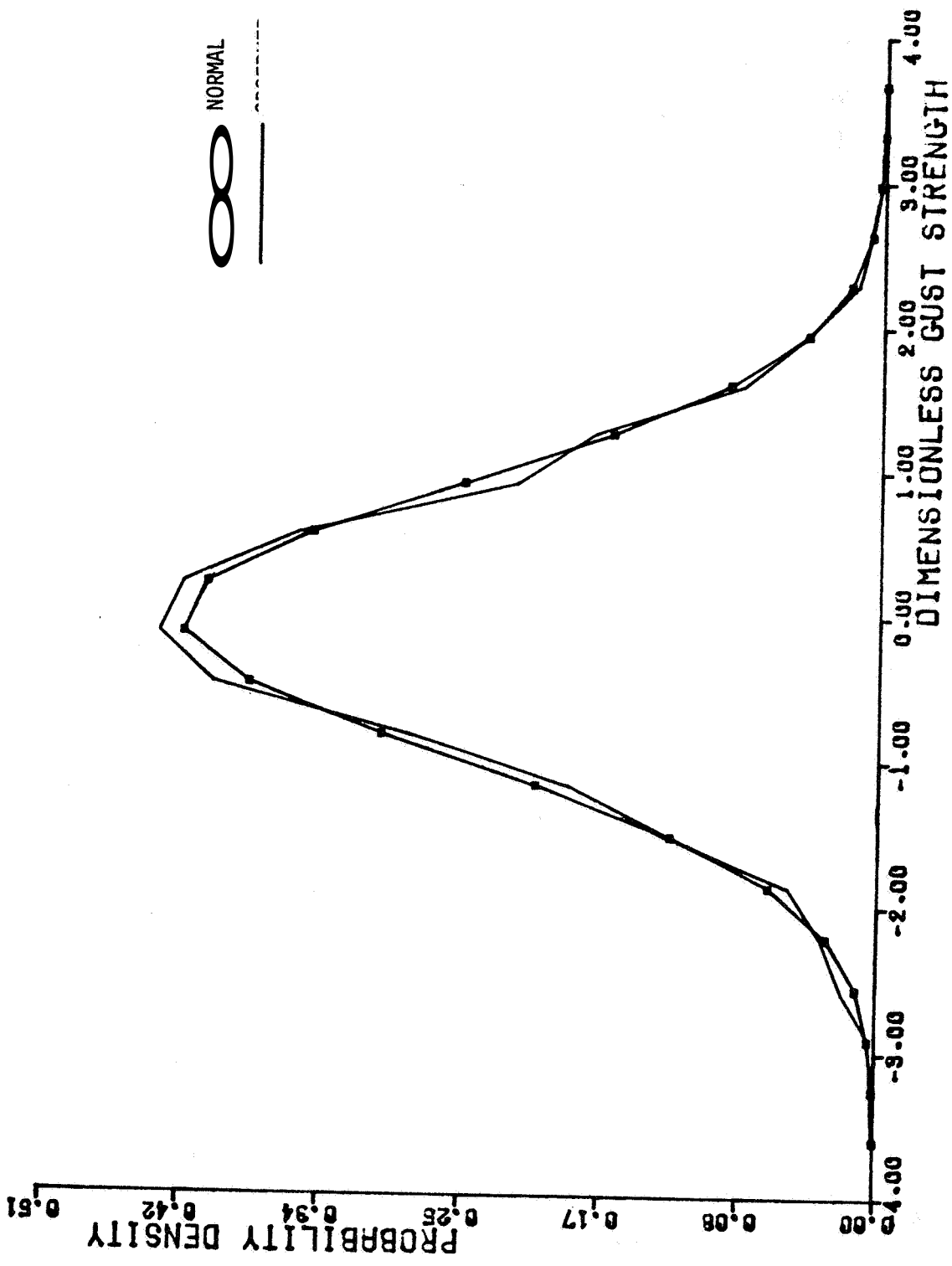


Figure D-3. u_1 - Gust Probability Density Distribution, Altitude Band #3

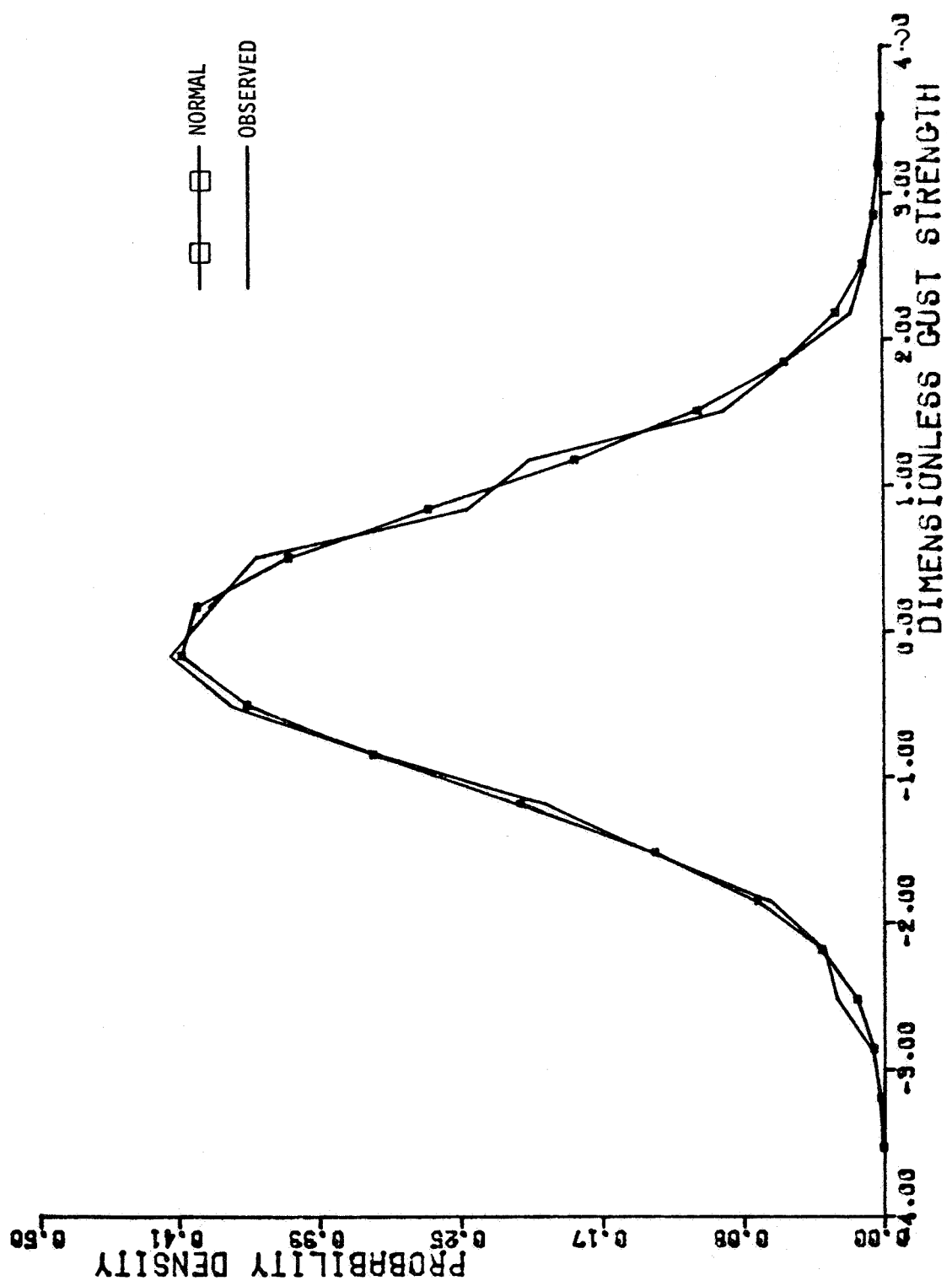


Figure D-4. u_1 - Gust Probability Density Distribution, Altitude Band #4

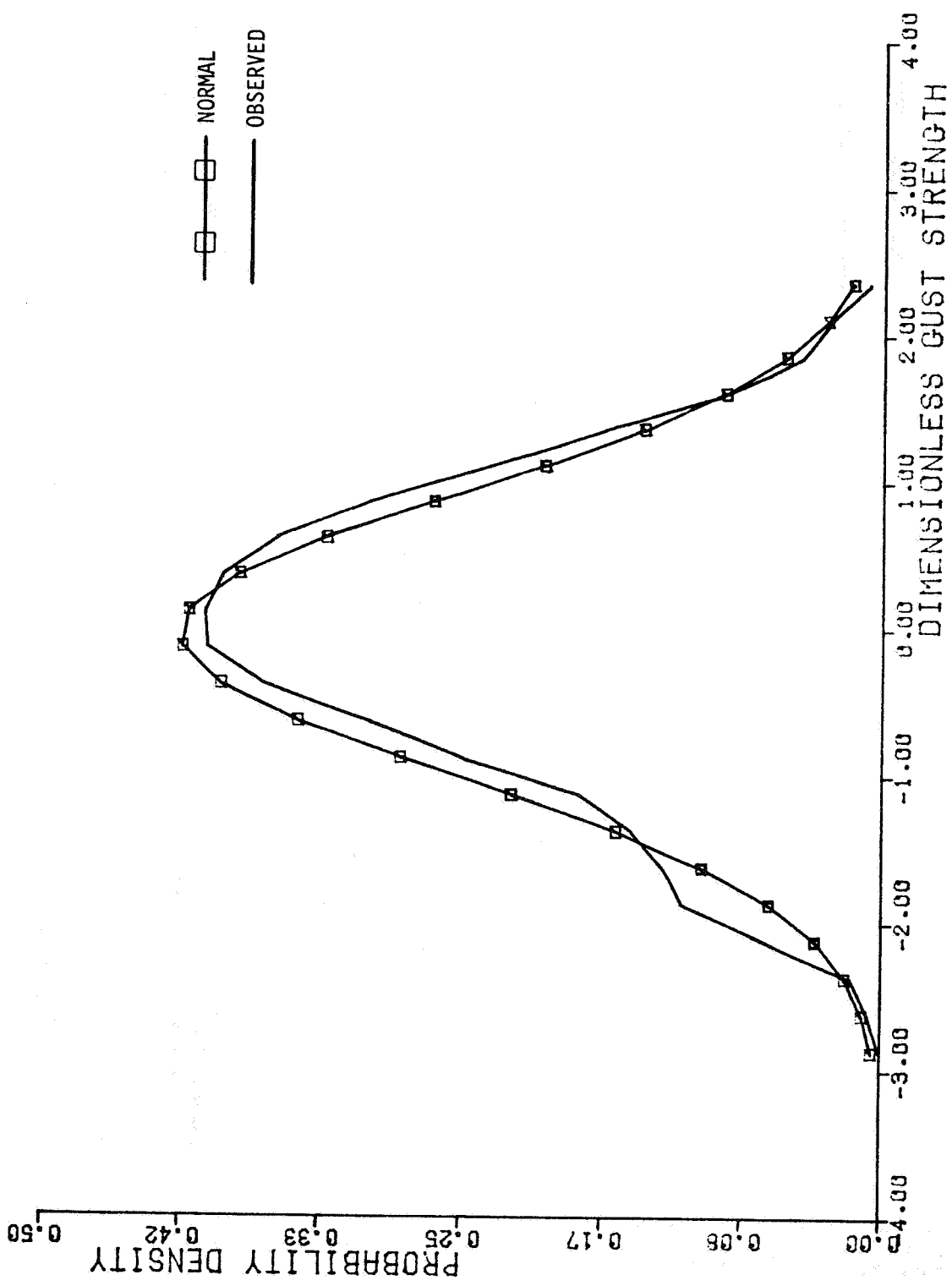


Figure D-5. u_1 - Gust Probability Density Distribution, Altitude Band #5

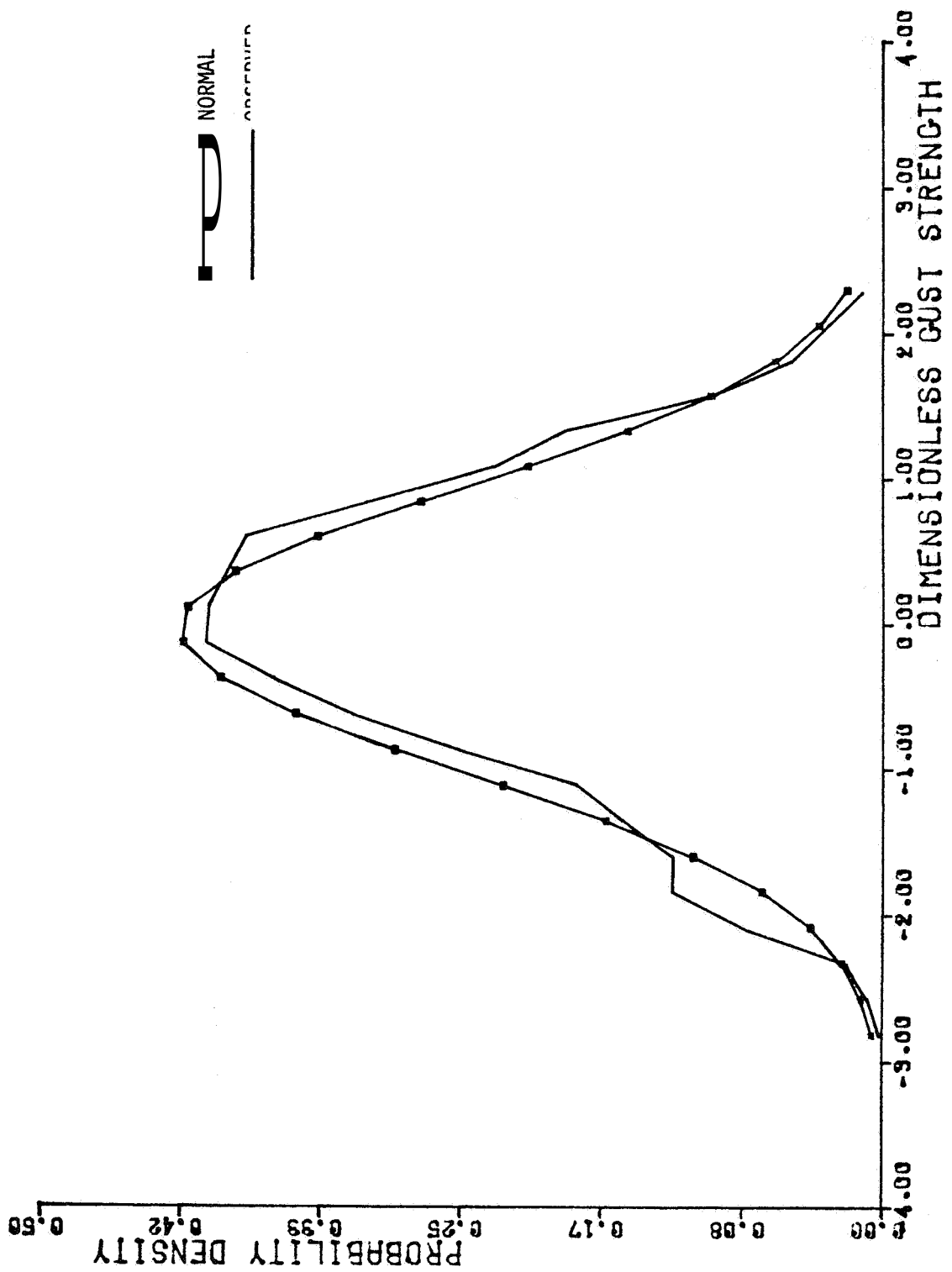


Figure D-6. u_1 - Gust Probability Density Distribution, Altitude Band #6

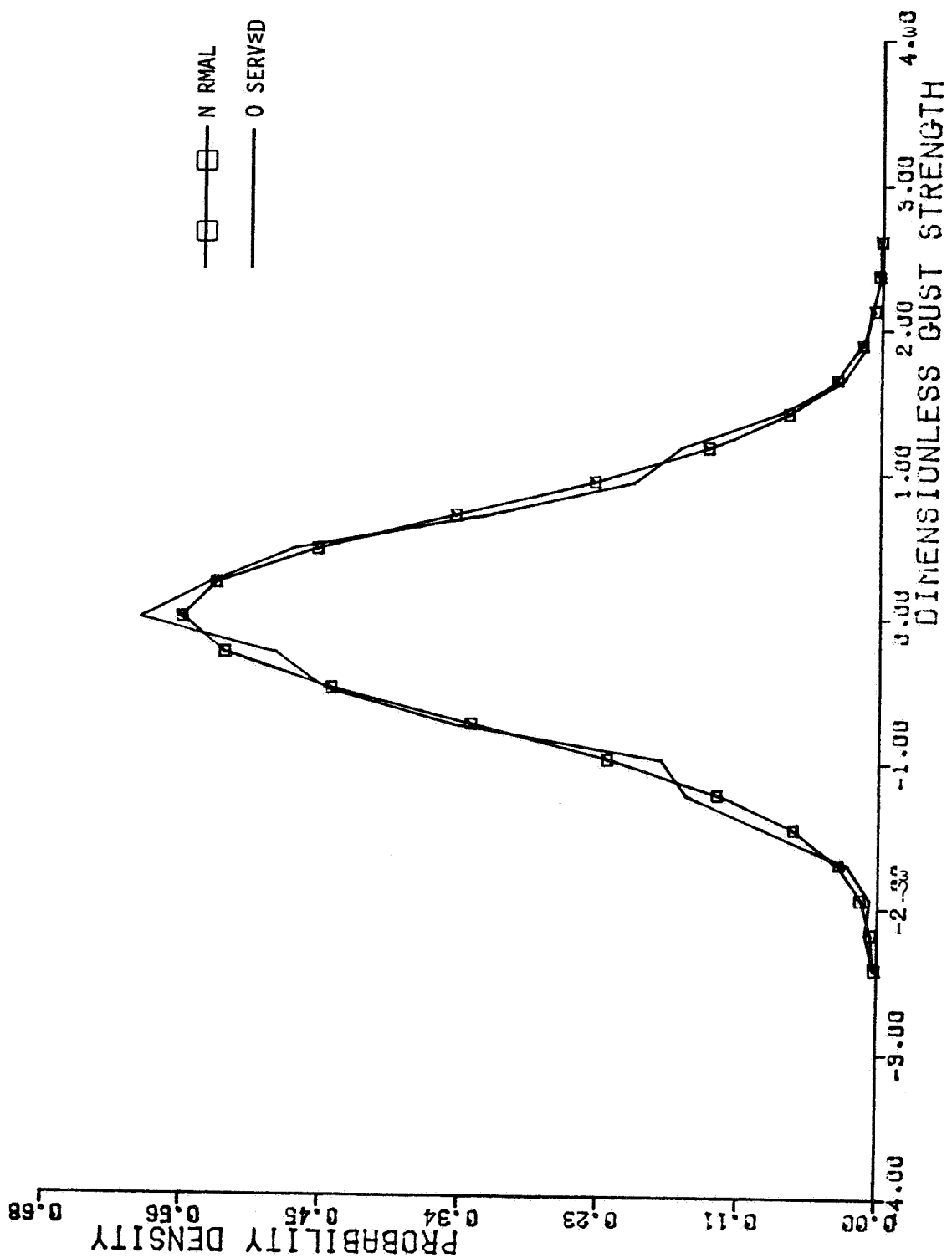


Figure D-7 u_2 - Gust Probability Density Distribution, Altitude Band #1

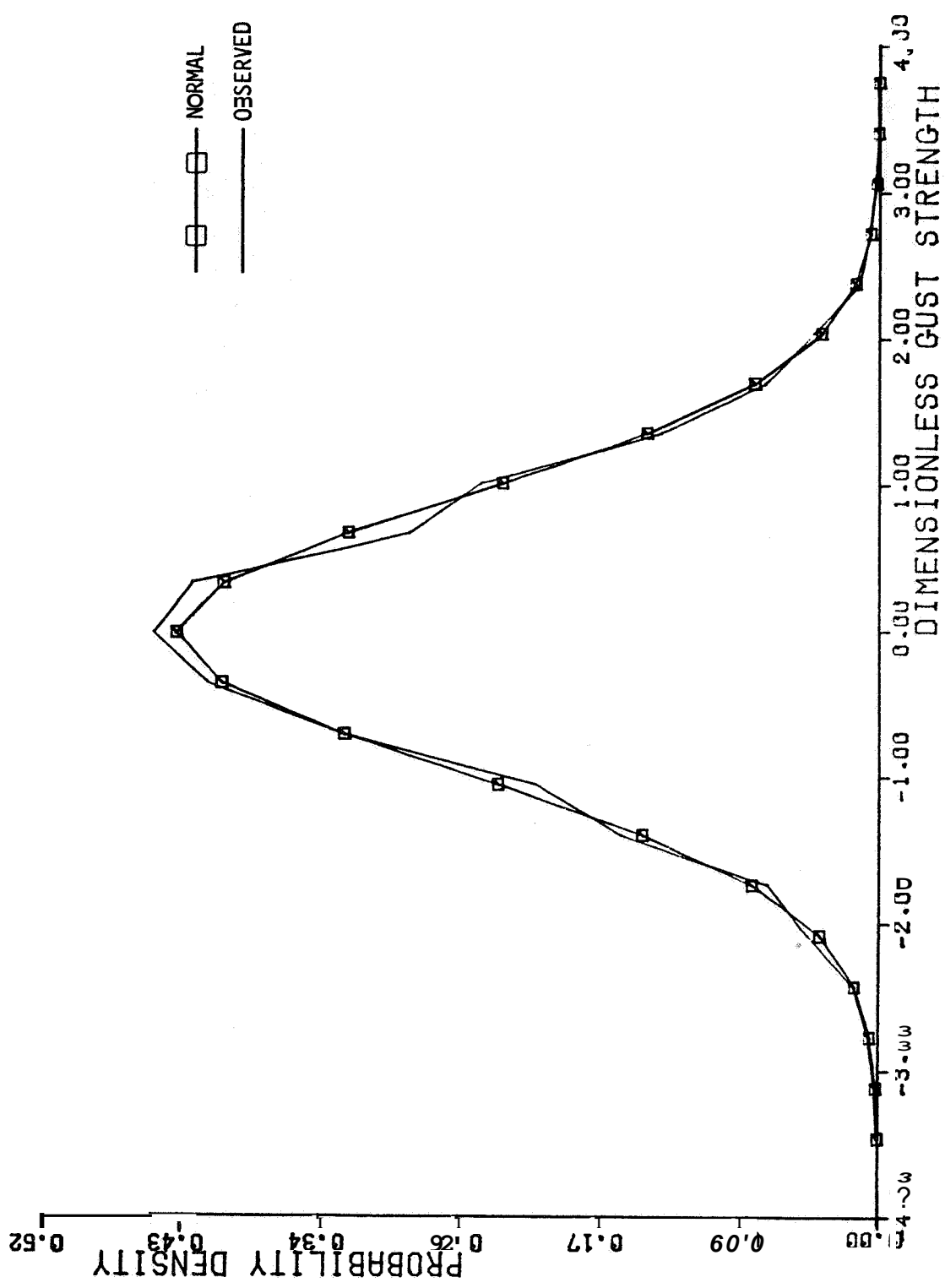


Figure D-8. u_2 - Gust Probability Density Distribution, Altitude Band #2

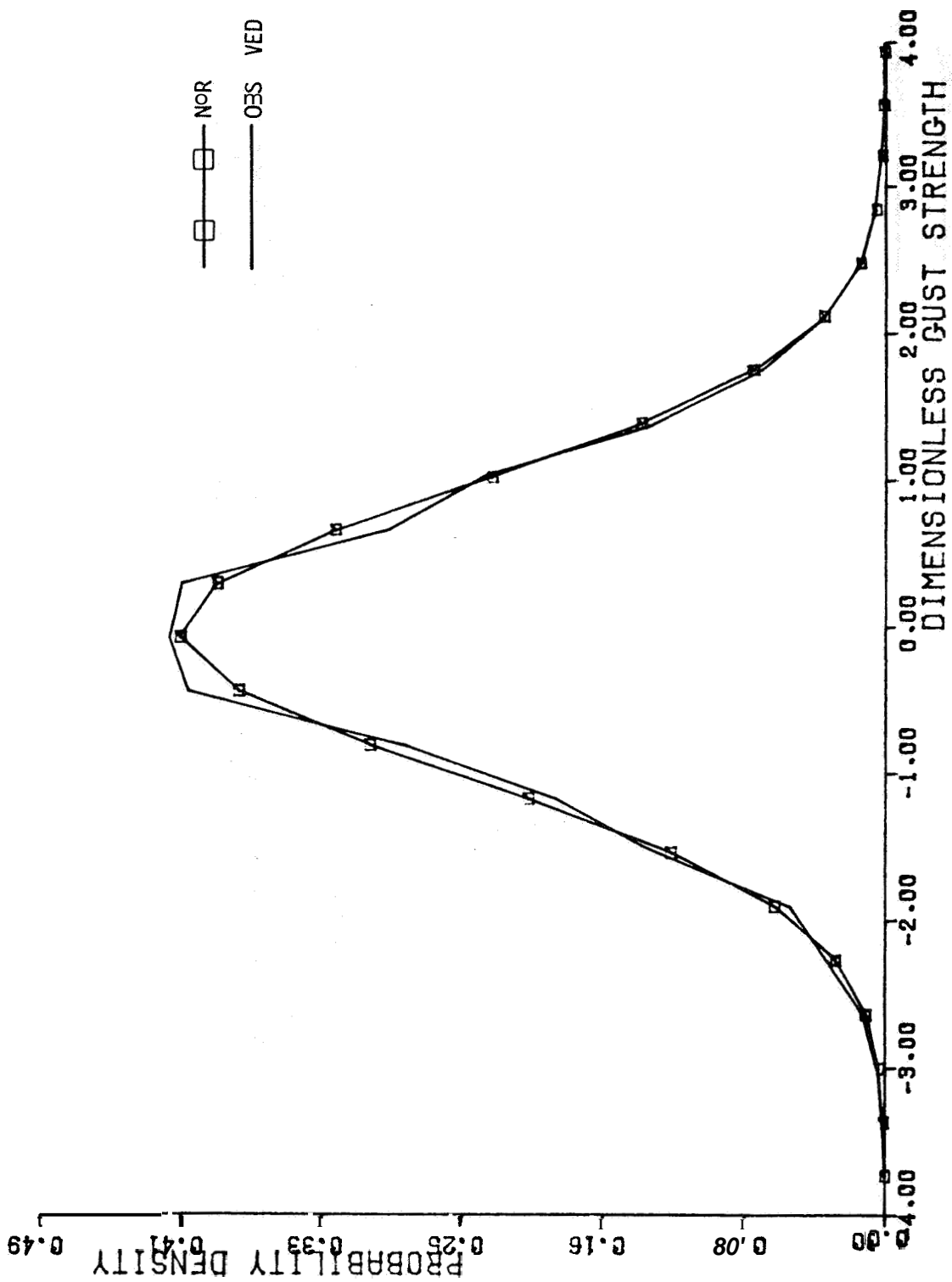


Figure D-9. w_2 - Gust Probability Density Distribution, Altitude Band #3

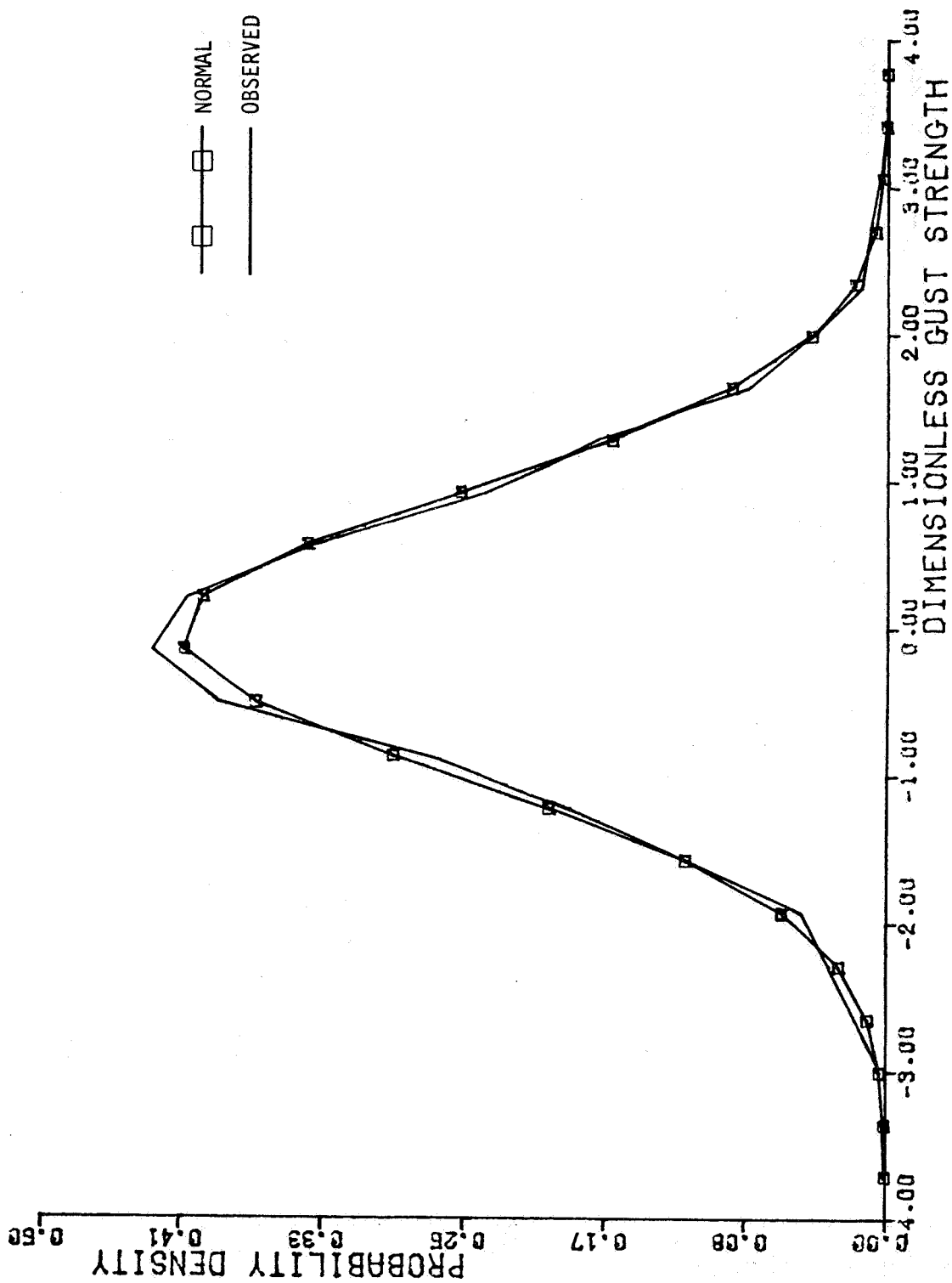


Figure D-10. u_2 - Gust Probability Density Distribution, Altitude Band #4

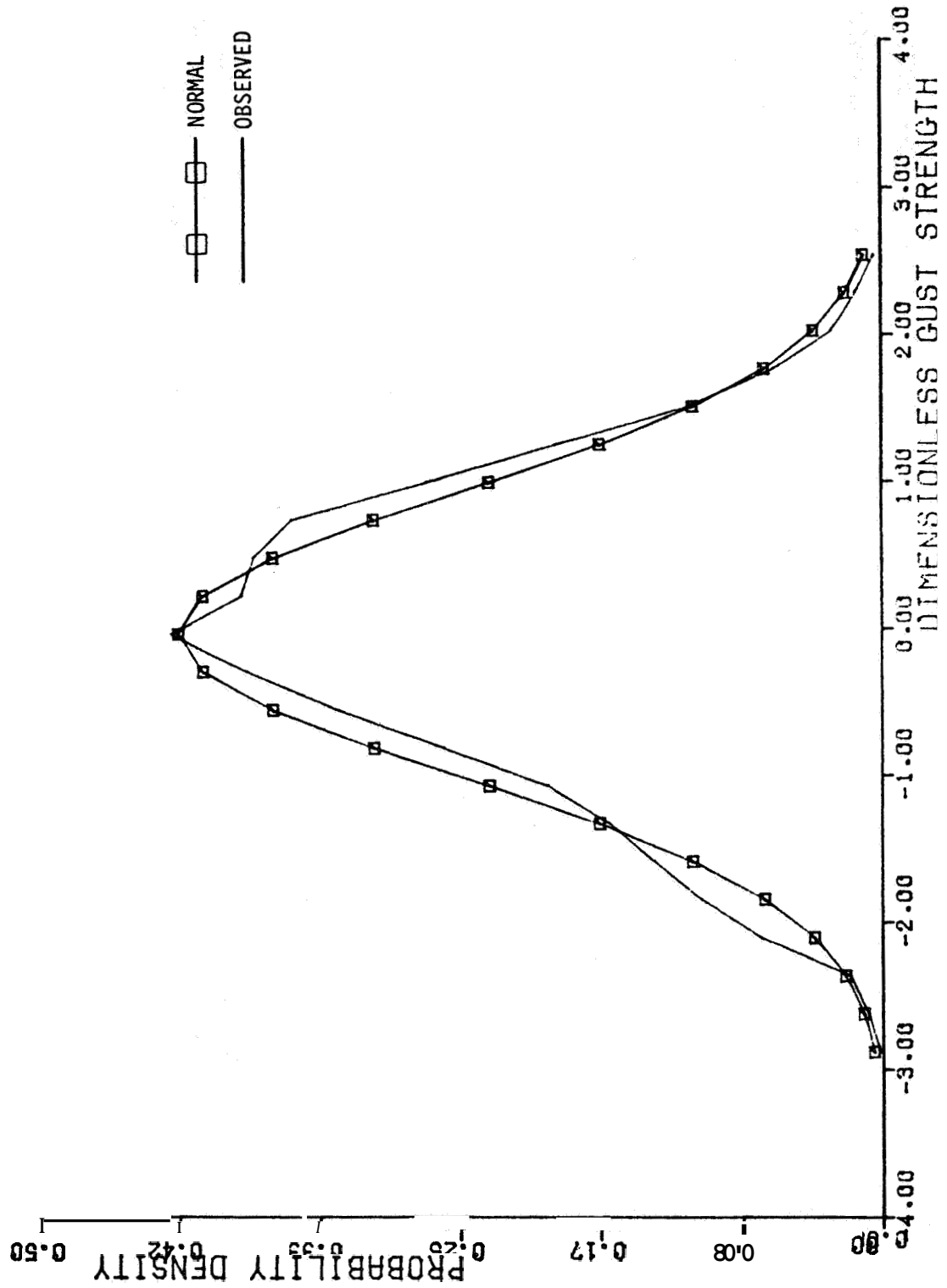


Figure D-11. u_2 - Gust Probability Density Distribution, Altitude Band #5

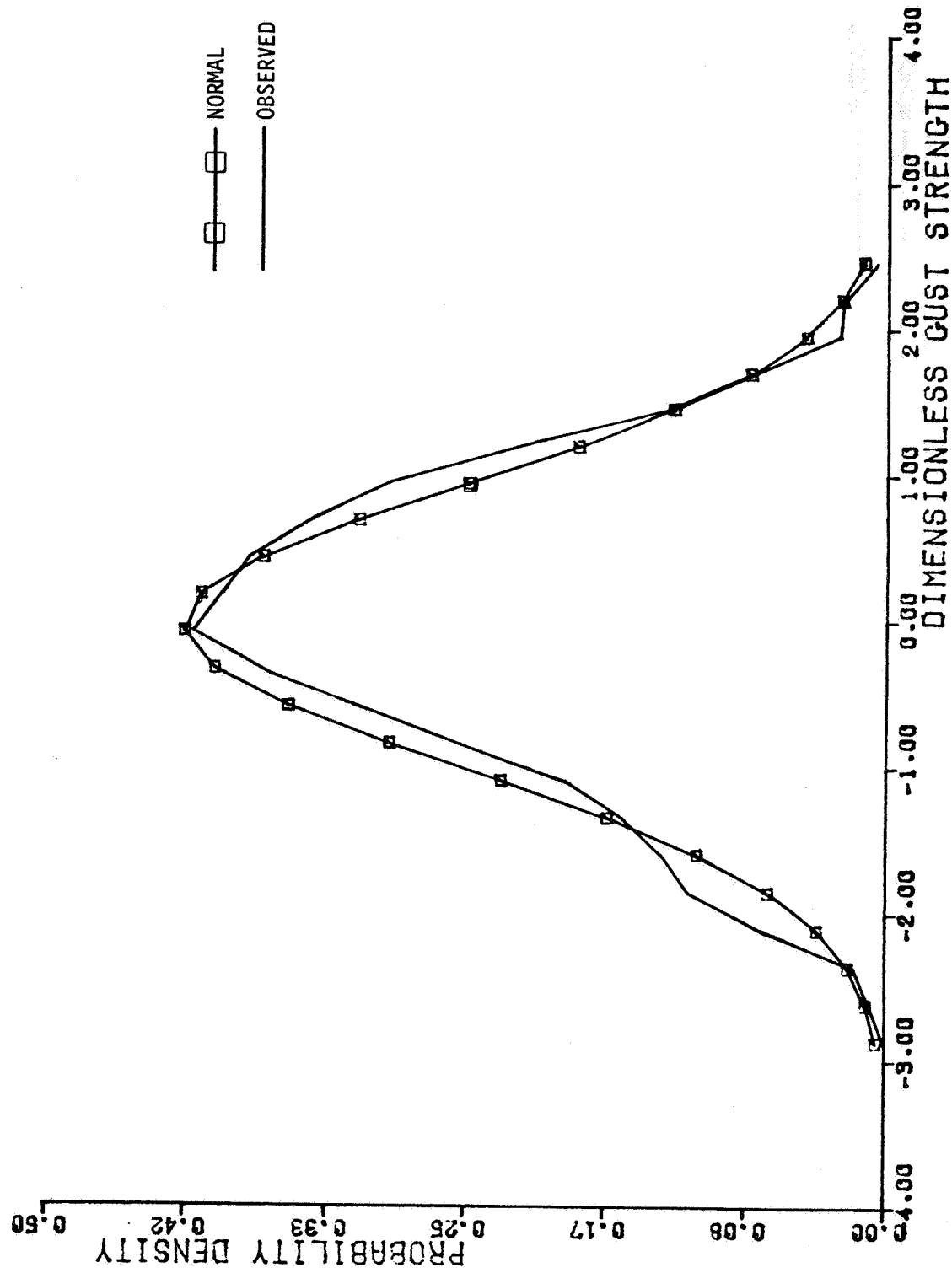


Figure D-12 u_2 - Gust Probability Density Distribution, Altitude Band #6

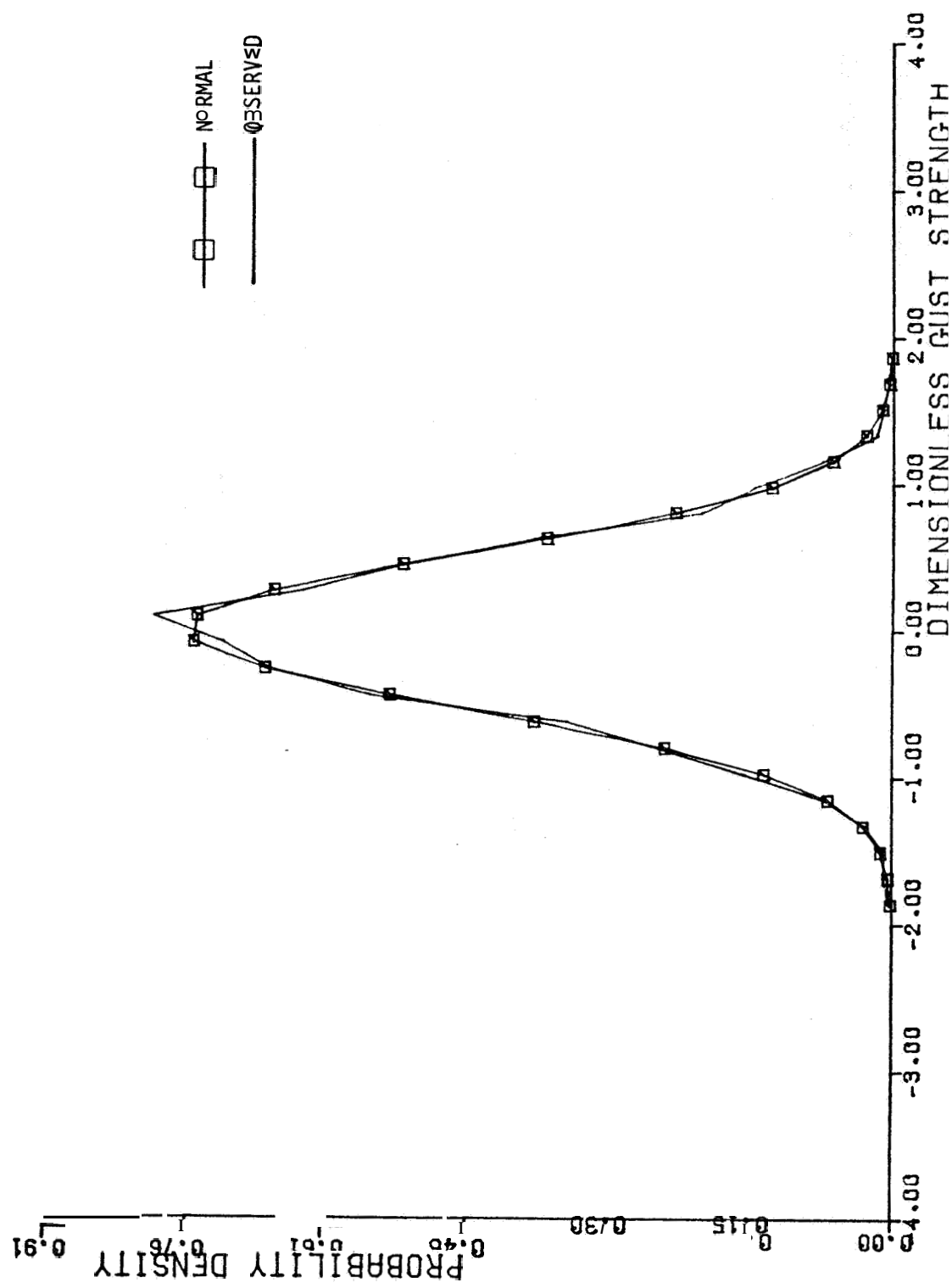


Figure D-13 u_3 - Gust Probability Density Distribution, Altitude Band #1

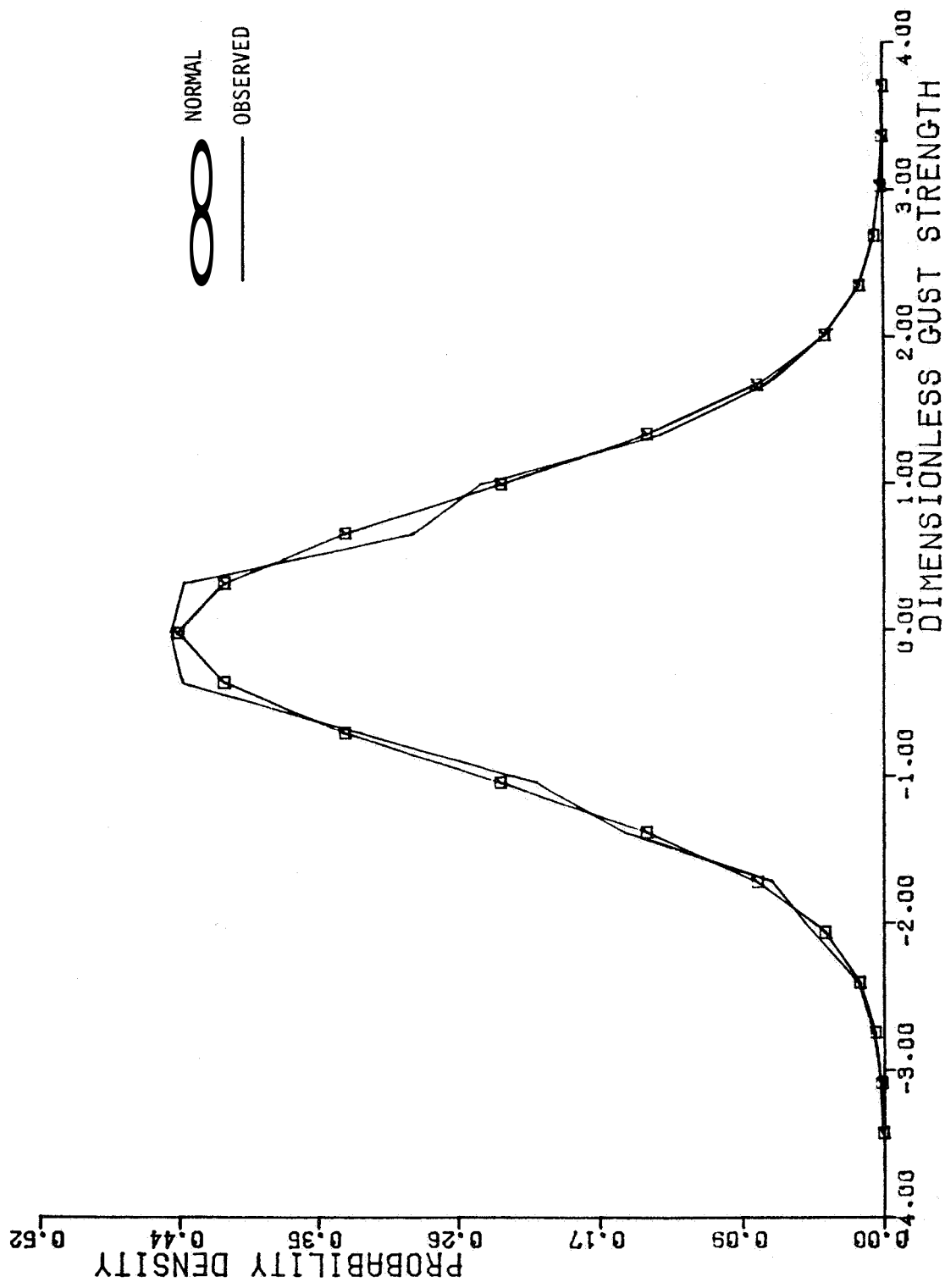


Figure D-14. u_3 - Gust Probability Density Distribution, Altitude Band #2

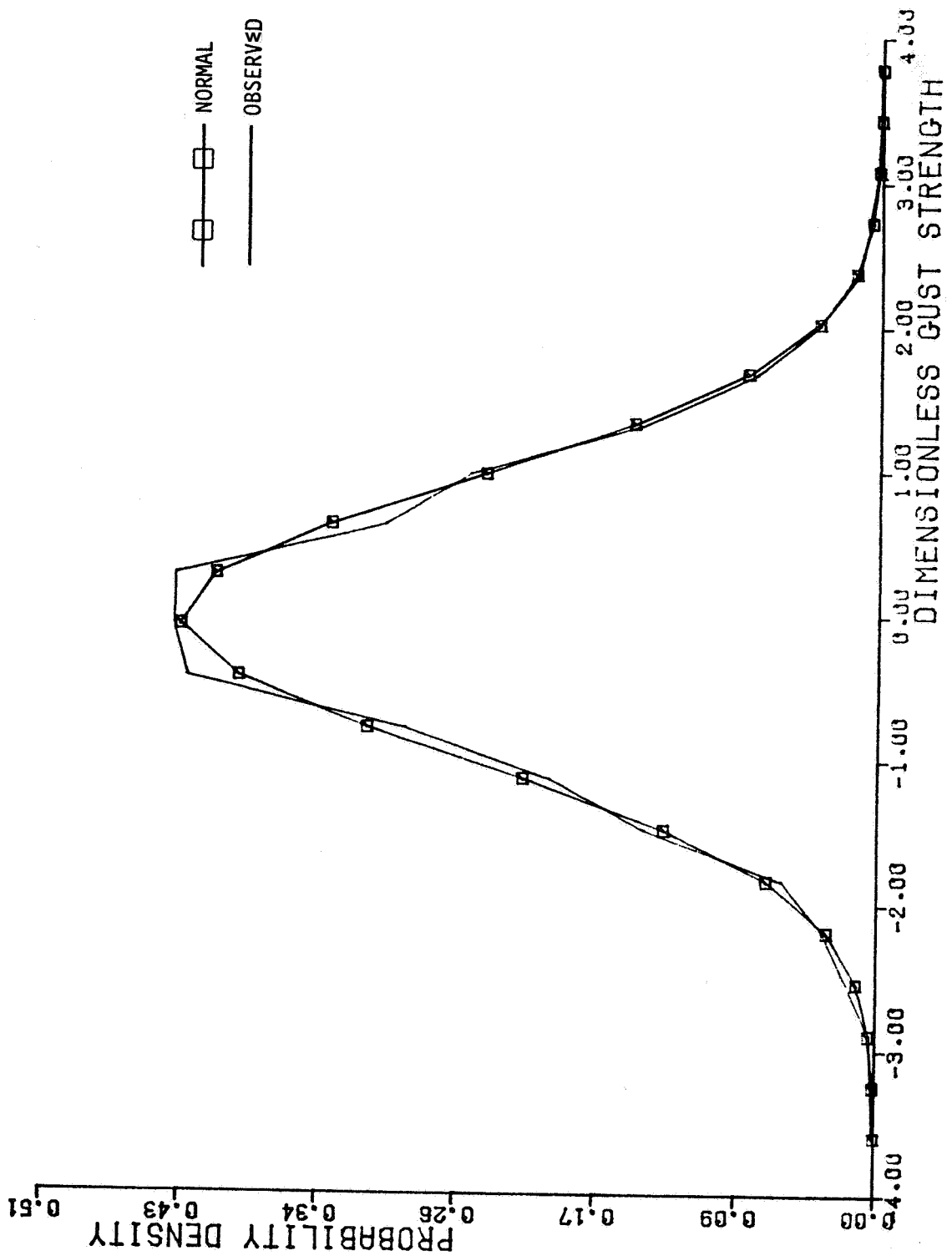


Figure D-15 u_3 - Gust Probability Density Distribution, Altitude Band #3

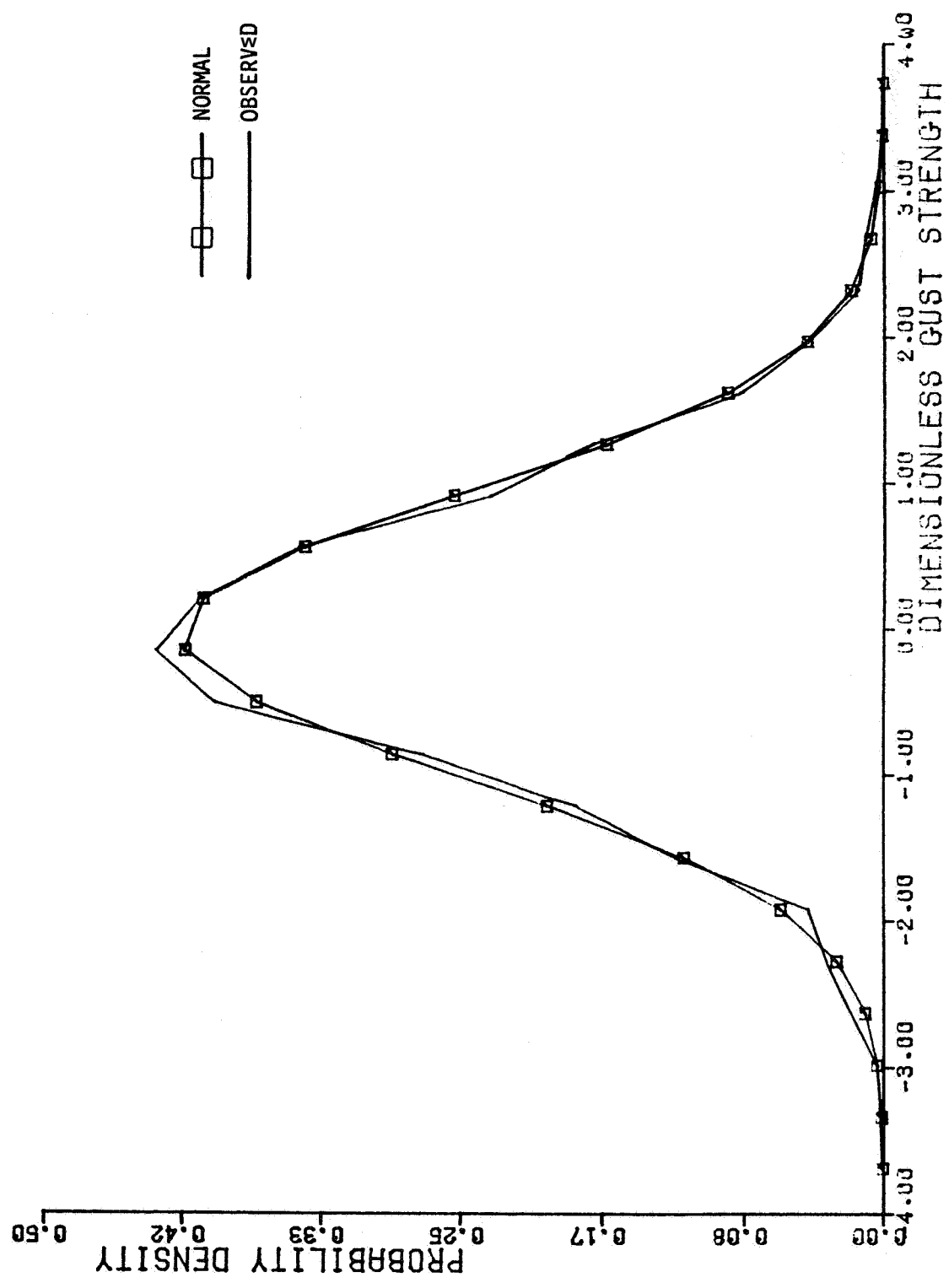


Figure D-16. u_3 - Gust Probability Density Distribution, Altitude Band #4

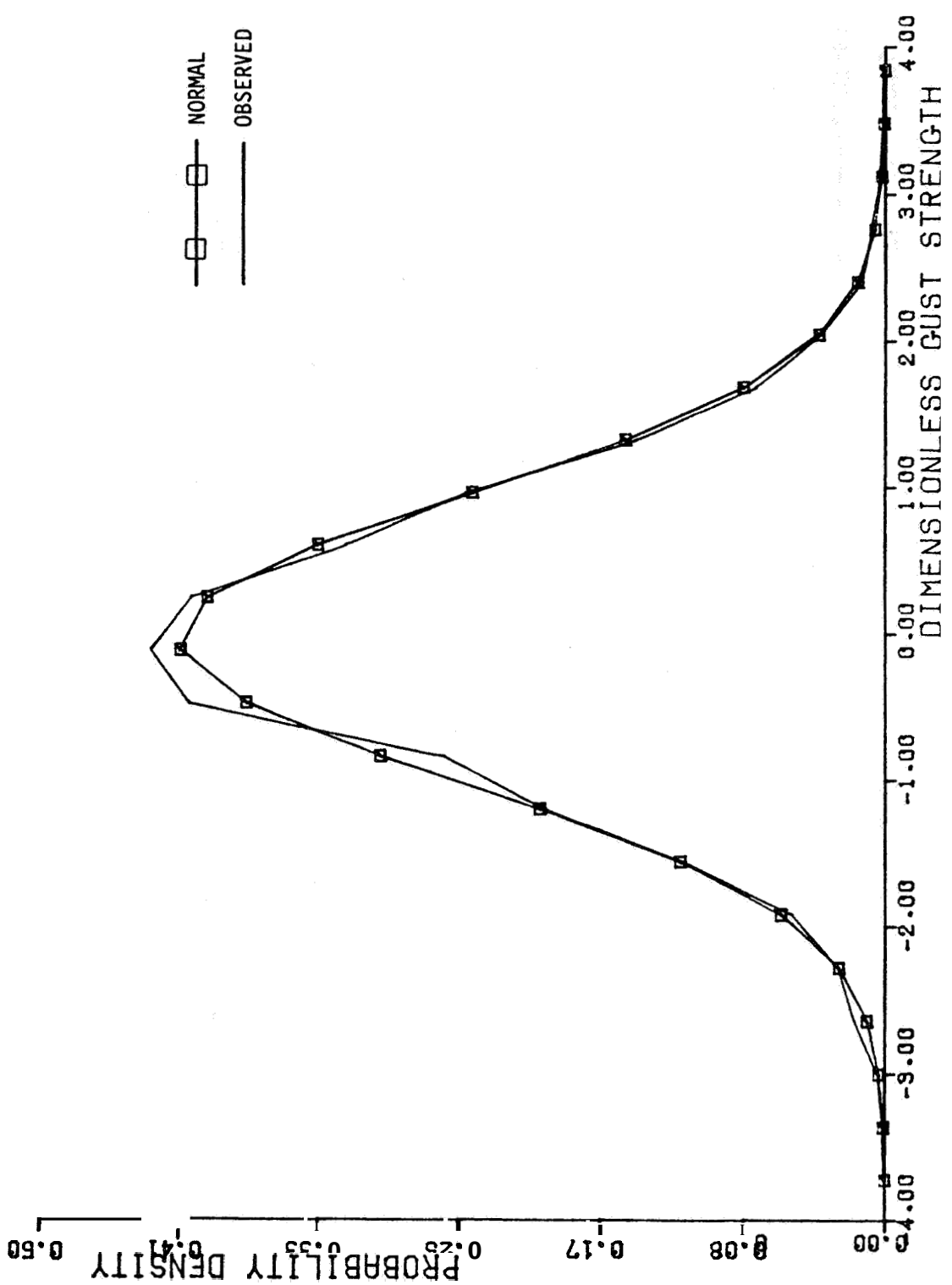


Figure D-17. u_3 - Gust Probability Density Distribution, Altitude Band #5

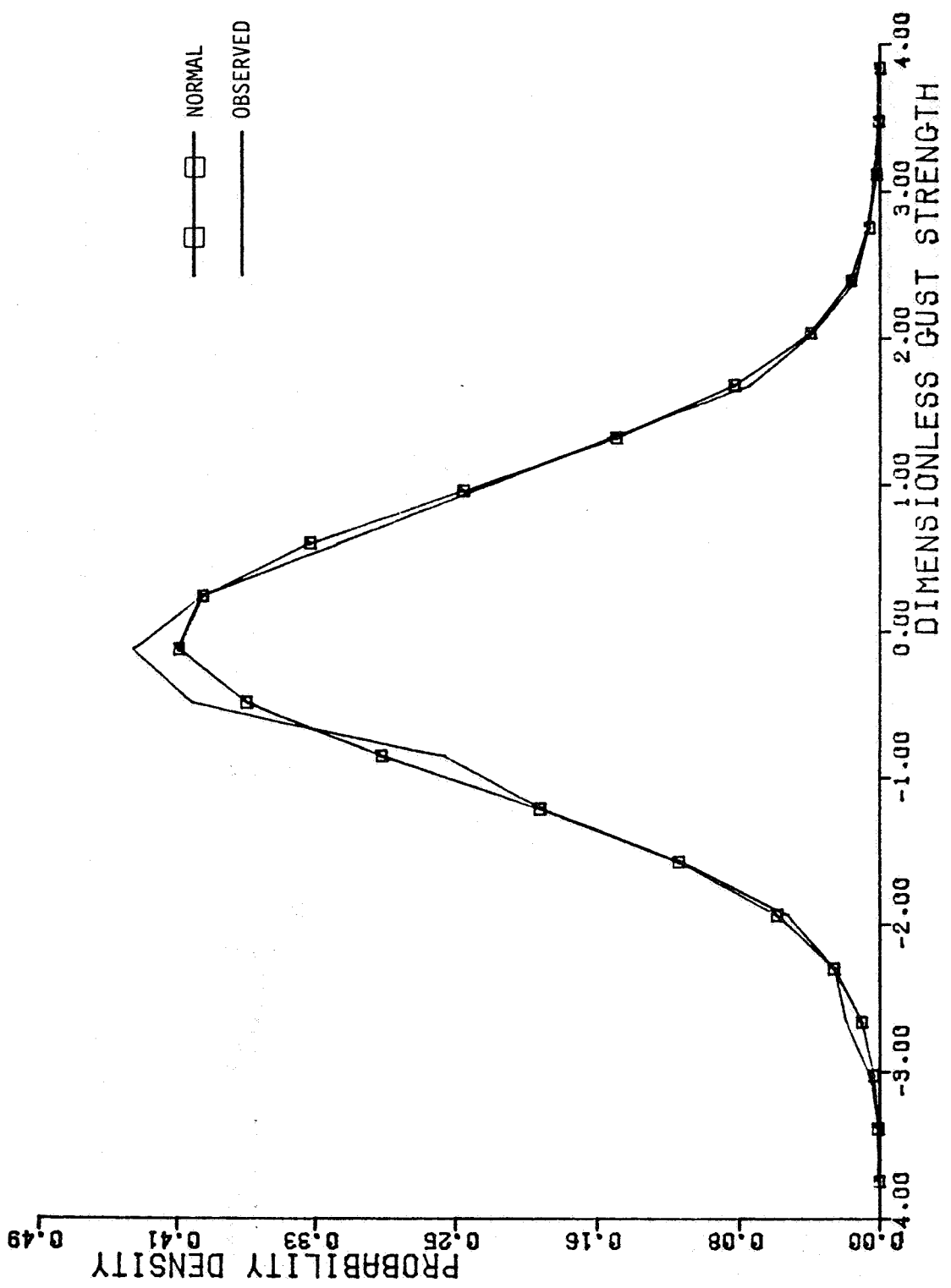


Figure D-18 w_3 - Gust Probability Density Distribution, Altitude Band #6

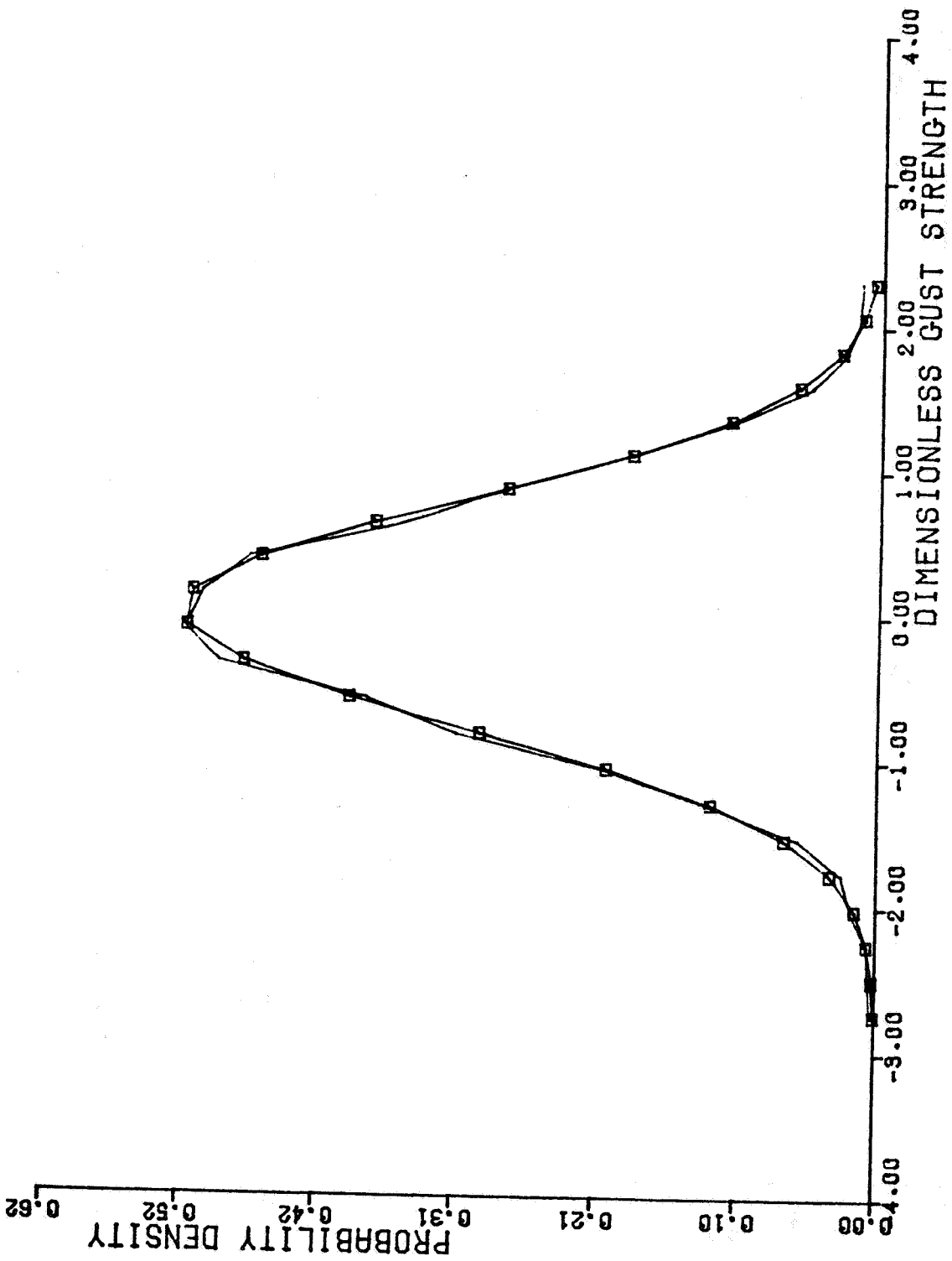


Figure D-19. $\partial u_2 / \partial x_1$ - Gust Gradient Probability Density Distribution, Altitude Band #1

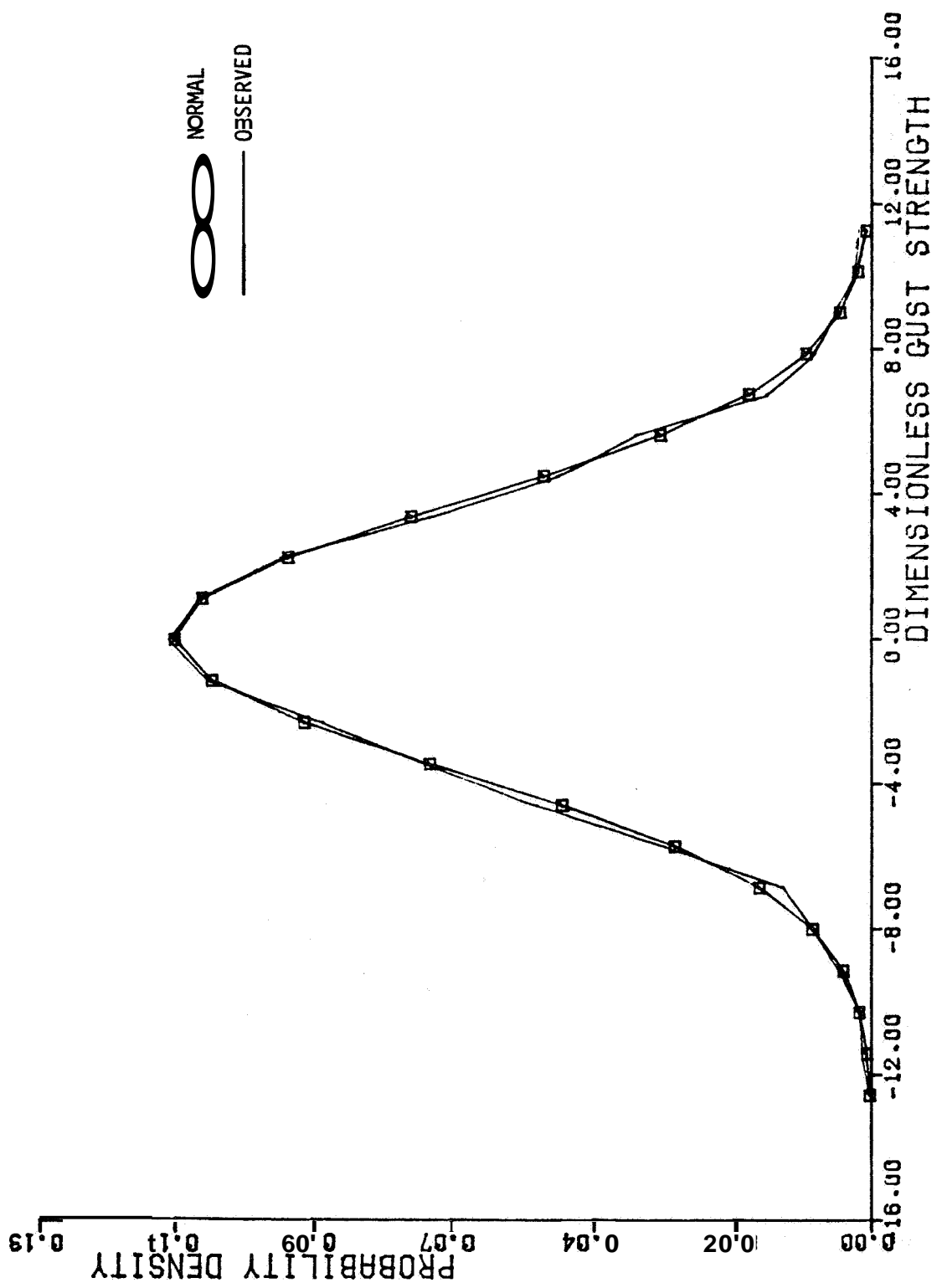


Figure D-20. $\partial u_2 / \partial x_1$ - Gust Gradient Probability Density Distribution, Altitude Band #2

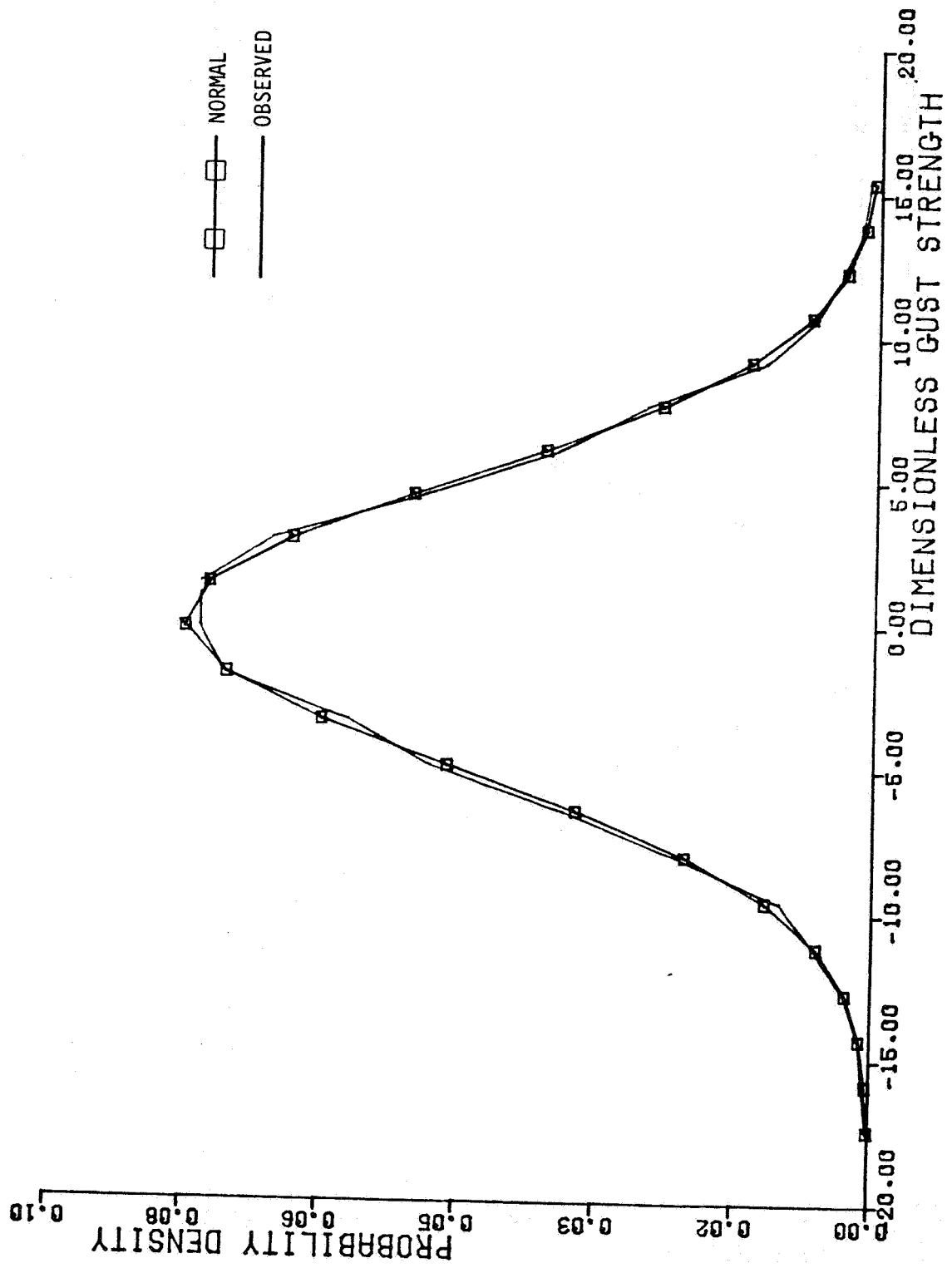


Figure D-21. $\partial u_2 / \partial x_1$ - Gust Gradient Probability Density Distribution, Altitude Band #3

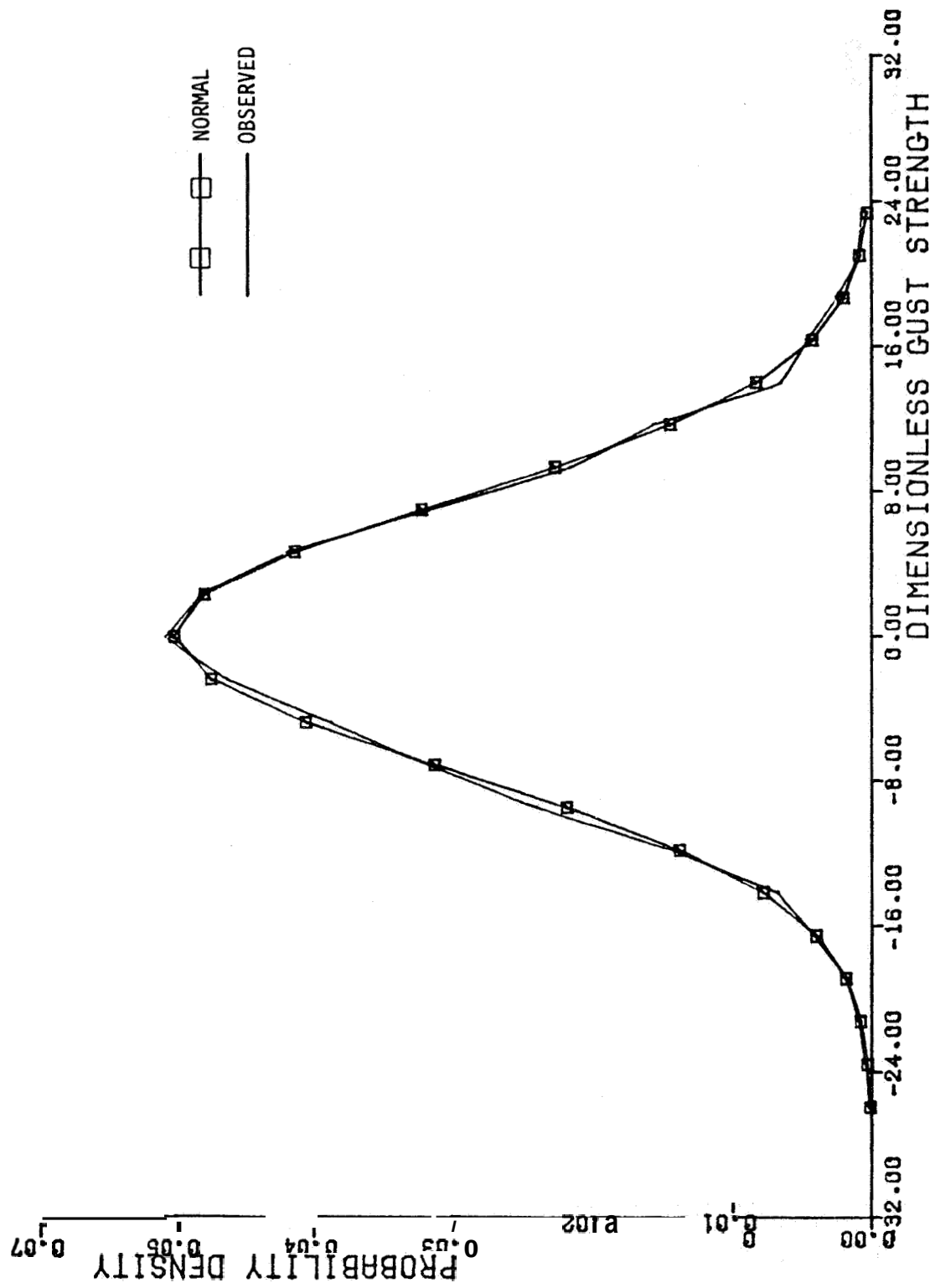


Figure D-22. $\partial u_2 / \partial x_1$ - Gust Gradient Probability Density Distribution, Altitude Band #4

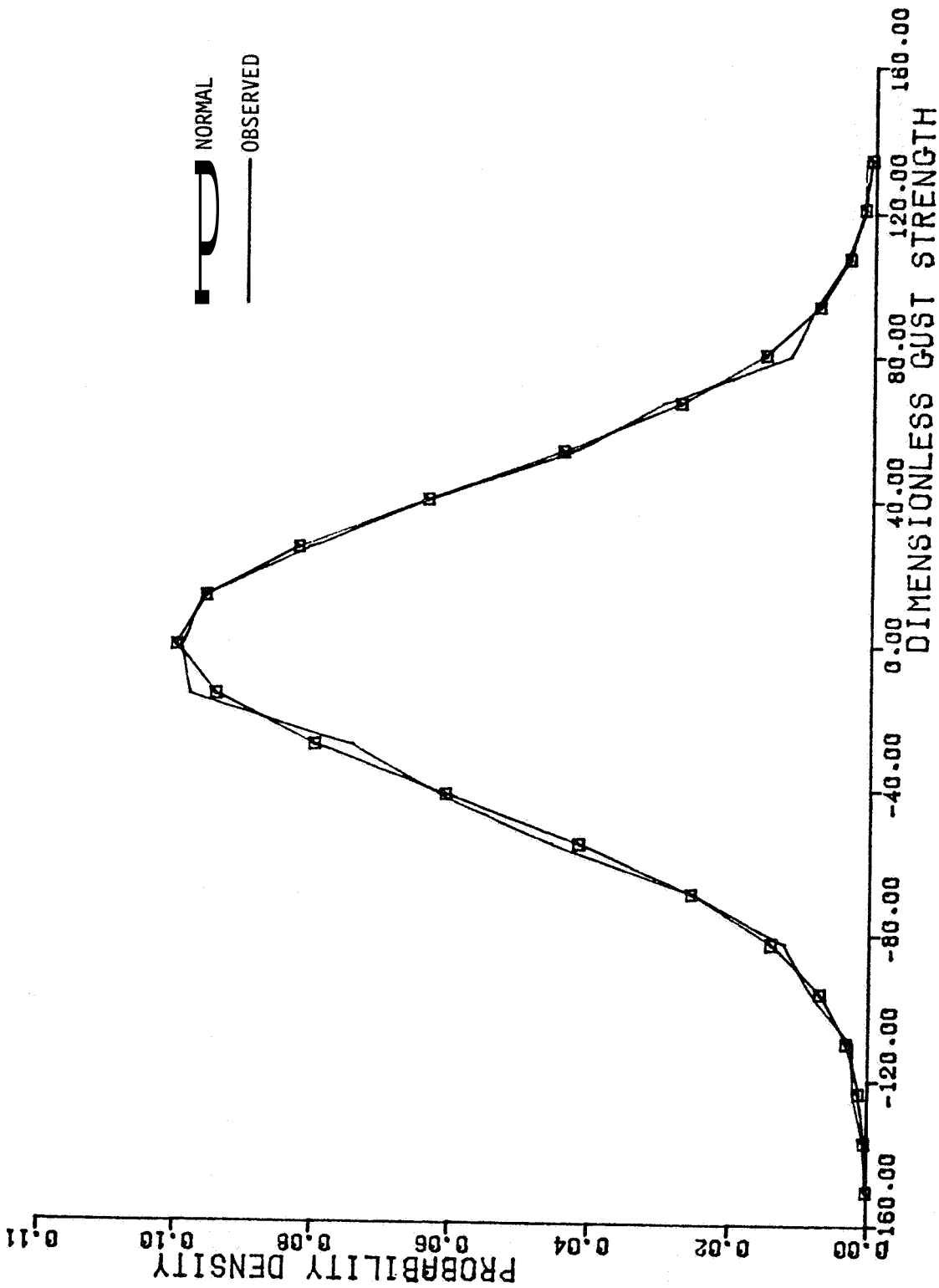


Figure D-23 $\partial u_2 / \partial x_1$ - Gust Gradient Probability Density Distribution, Altitude Band #5

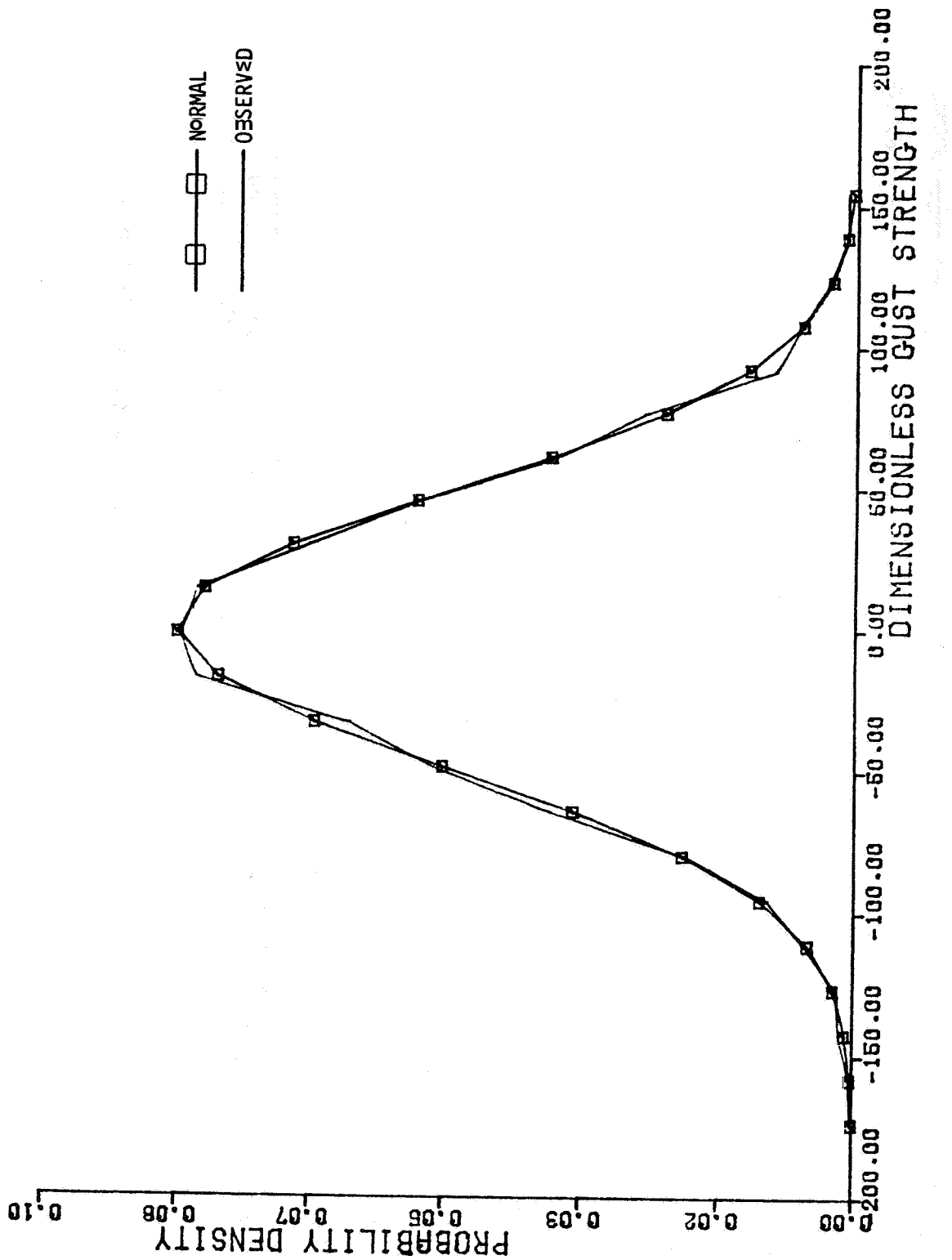


Figure D-24. $\partial u_2 / \partial x_1$ - Gust Gradient Probability Density Distribution, Altitude Band #6

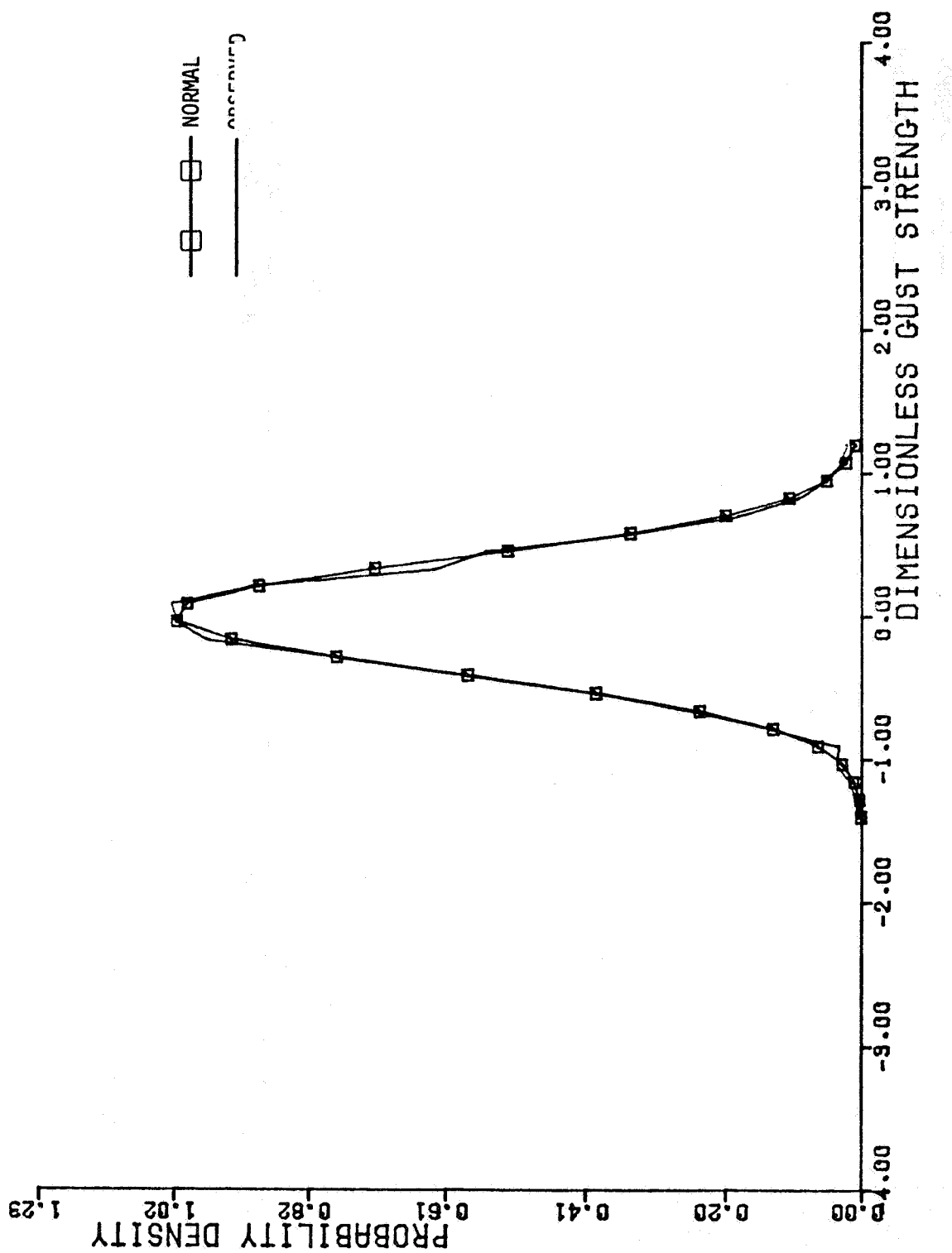


Figure D-25. $\partial u_3 / \partial x_1$ - Gust Gradient Probability Density Distribution, Altitude Band #1

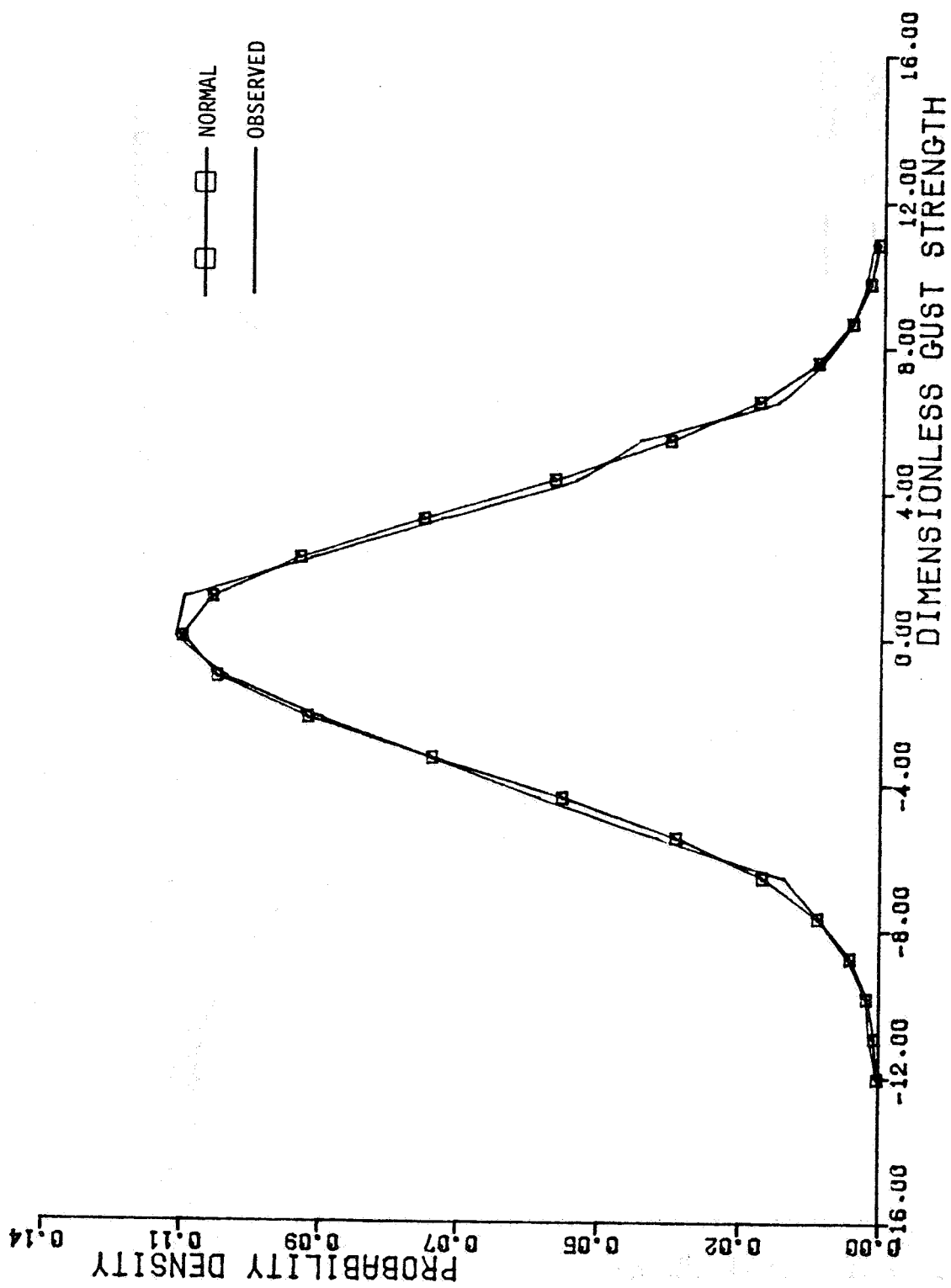


Figure D-26. $\frac{\partial u_3}{\partial x_1}$ - Gust Gradient Probability Density Distribution, Altitude Band #2

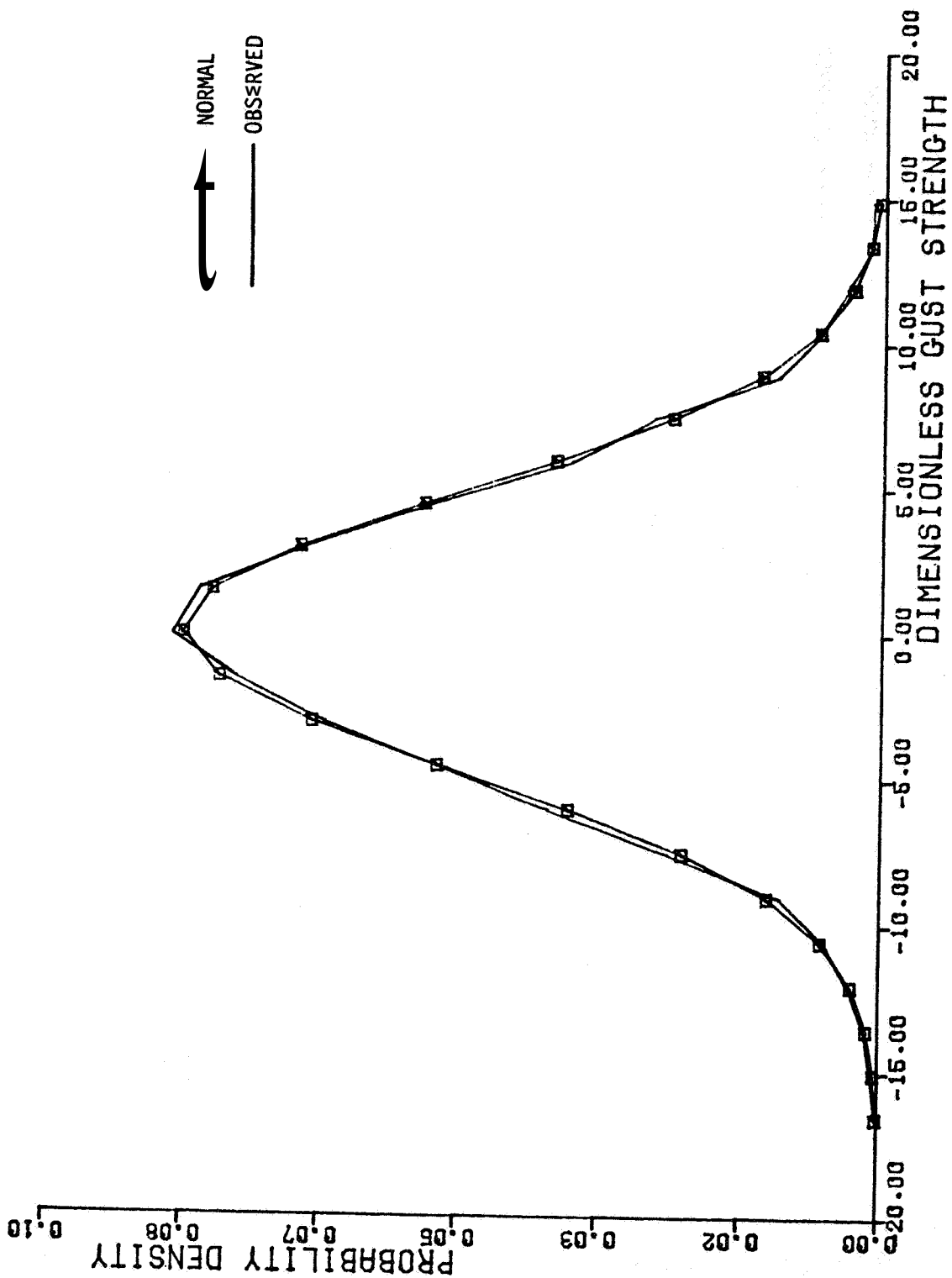


Figure D-27 $\partial u_3 / \partial x_1$ = Gust Gradient Probability Density Distribution, Altitude Band #3

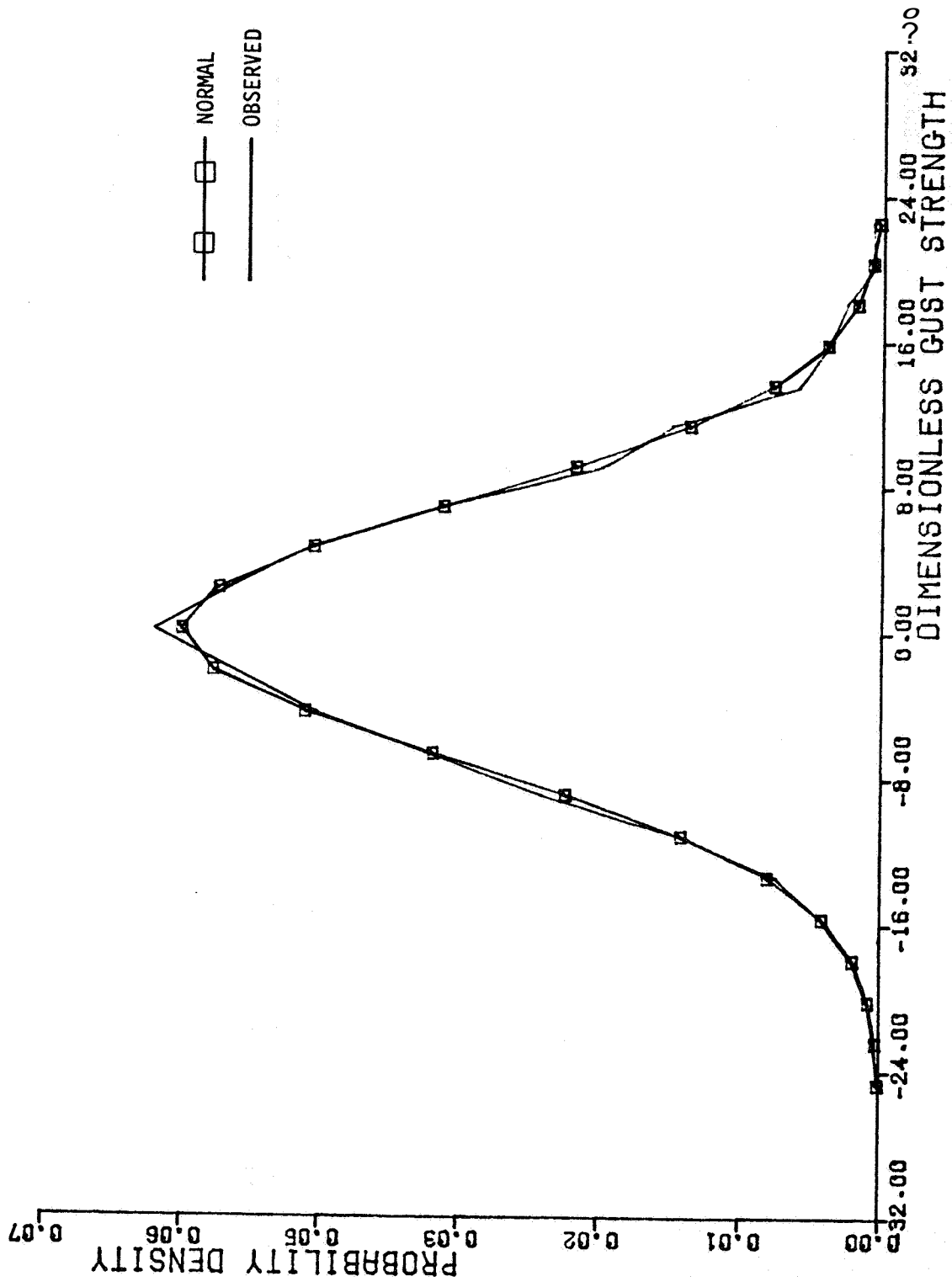


Figure D-28. $\partial u_3 / \partial x_1$ - Gust Gradient Probability Density Distribution, Altitude Band #4

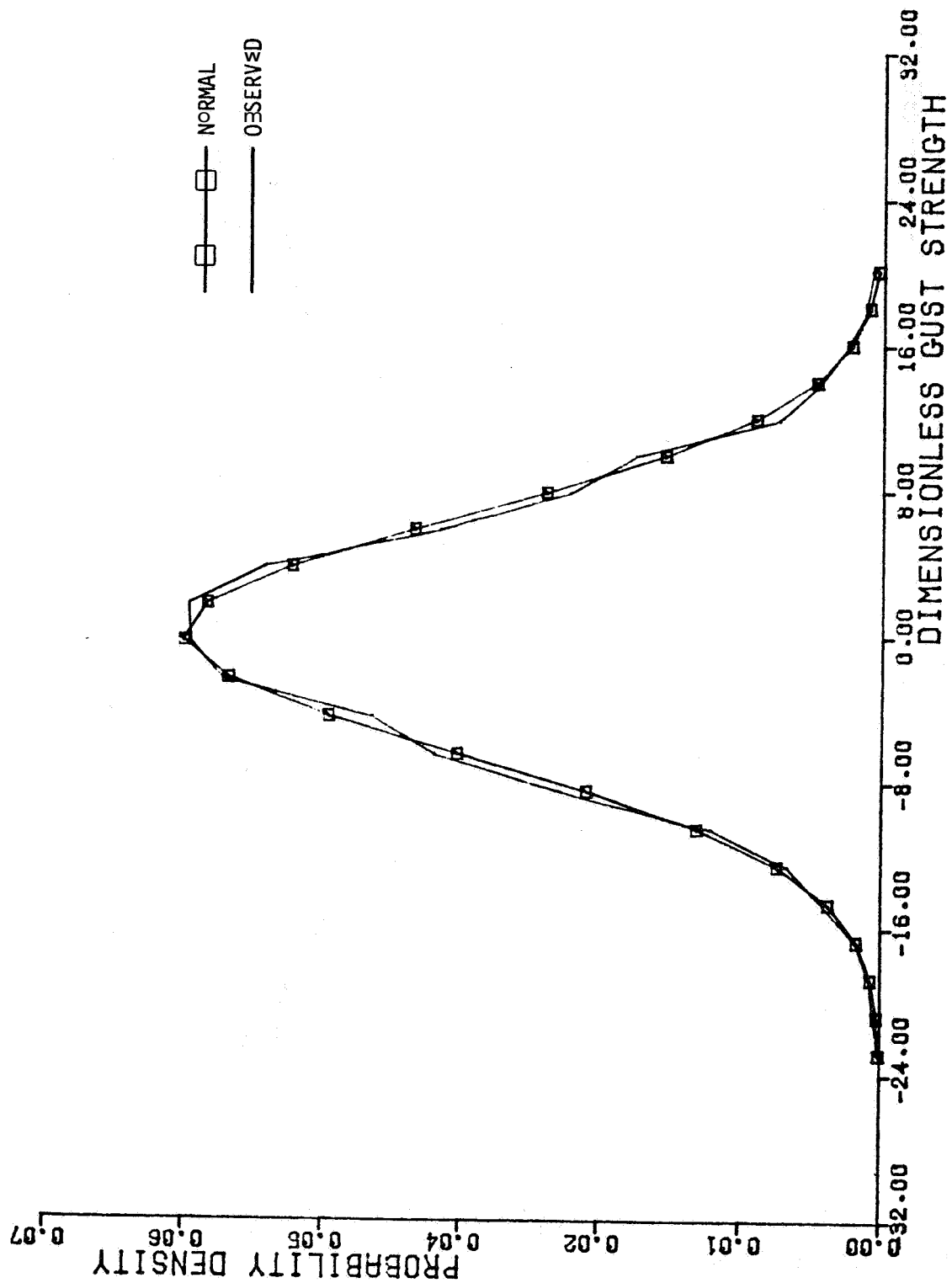


Figure D-29 $\partial u_3 / \partial x_1$ - Gust Gradient Probability Density Distribution, Altitude Band #5

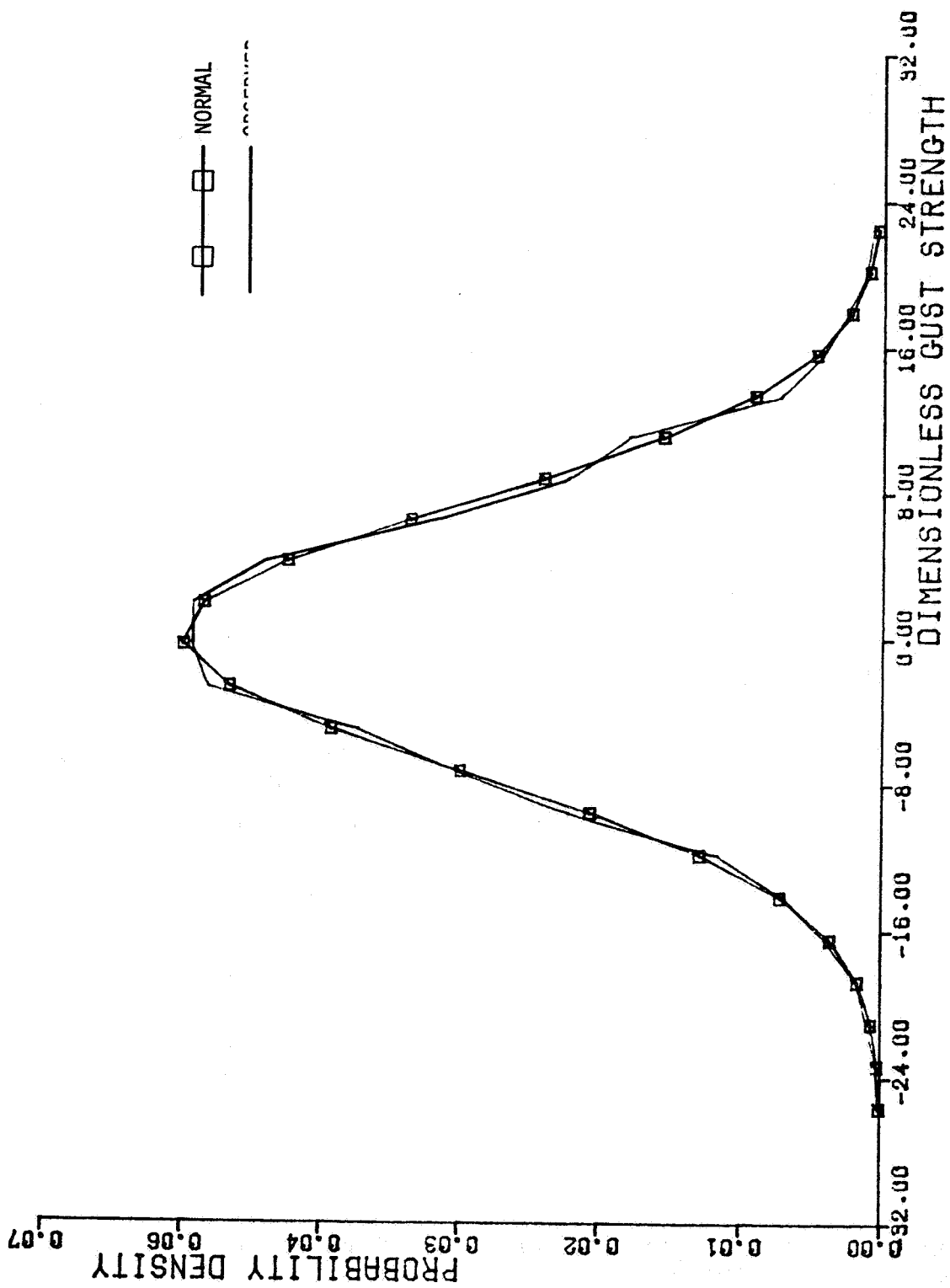


Figure D-30 $\frac{\partial \omega_3}{\partial x_1}$ - Gust gradient probability density distribution Altitude Zonal #6

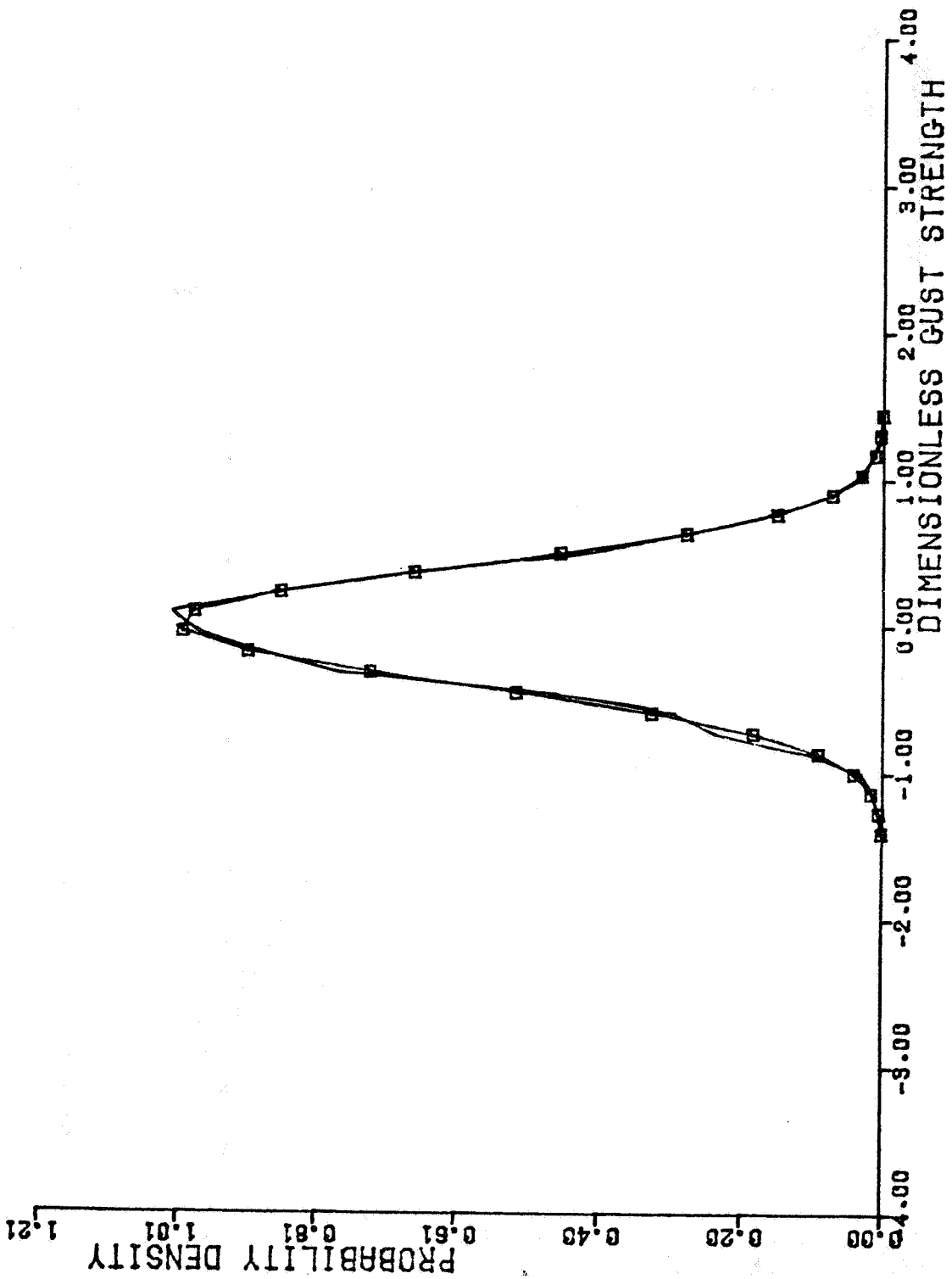


Figure D-31. $\partial u_3 / \partial x_2$ - Gust Gradient Probability Density Distribution, Altitude Band #1

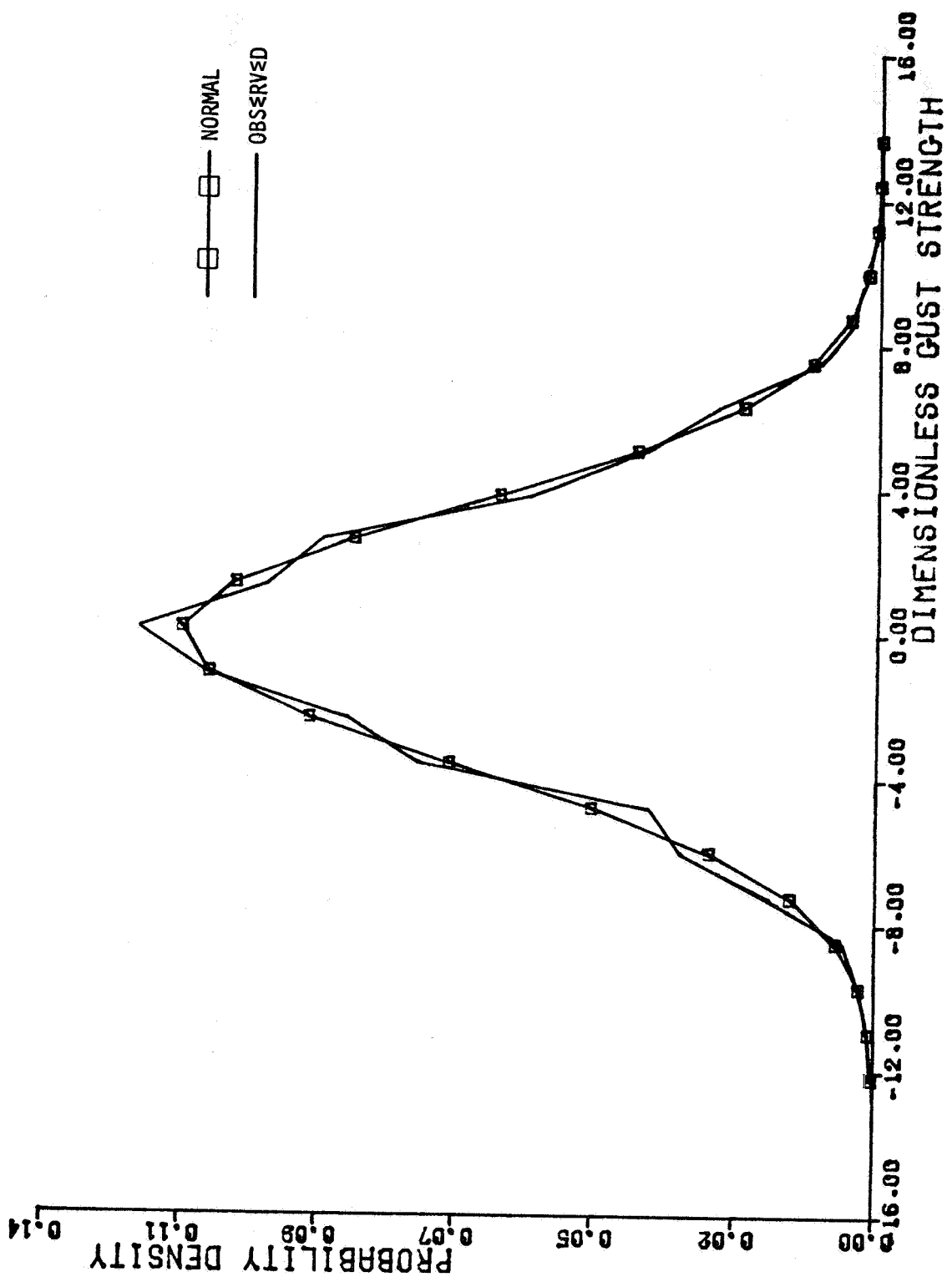


Figure D-32. $\partial u_3 / \partial x_2$ - Gust Gradient Probability Density Distribution, Altitude Band #2

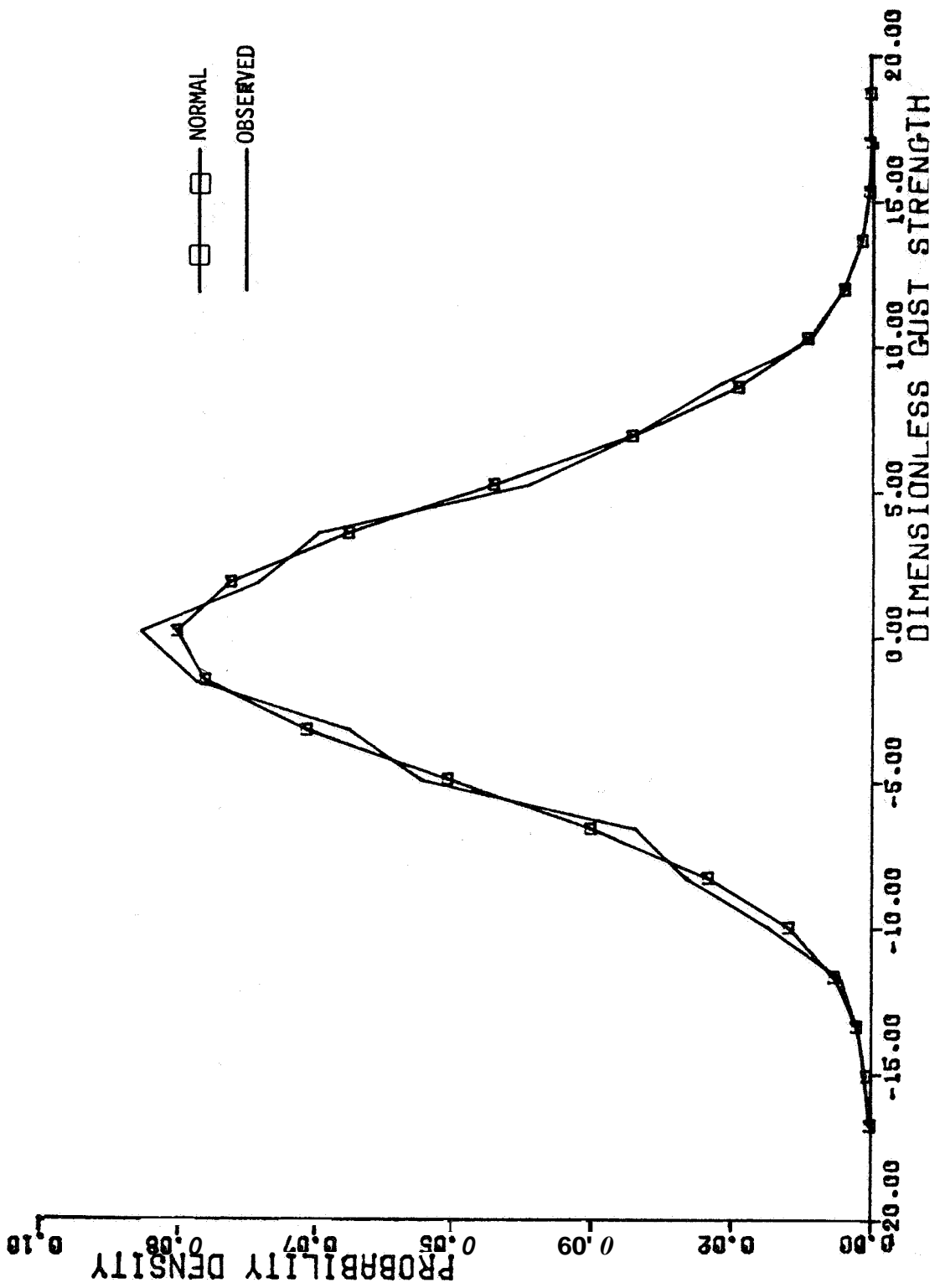


Figure D-33 $\frac{\partial u_g}{\partial x_2}$ - Gust Gradient Probability Density Distribution Altitude Band #3

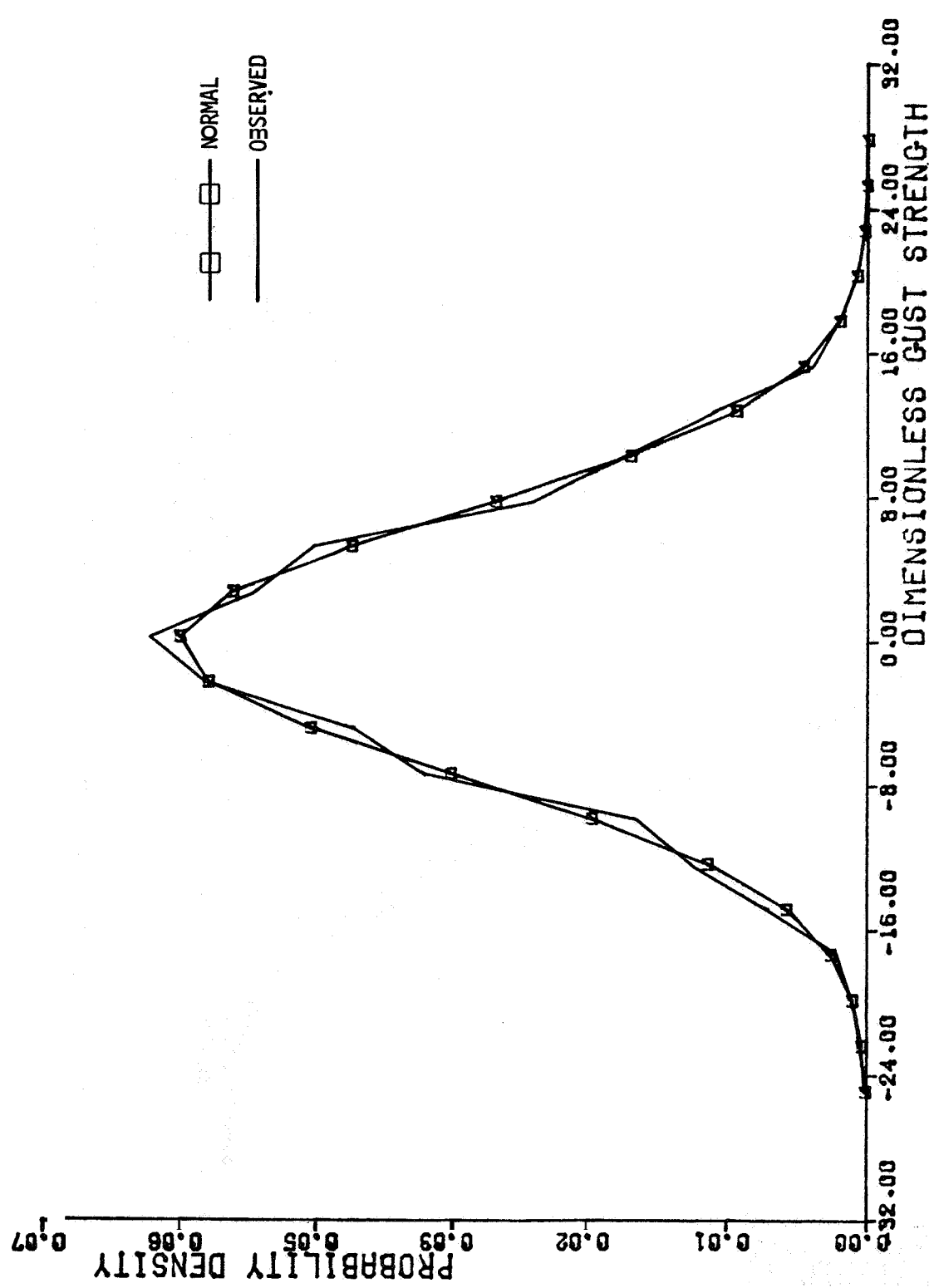


Figure D-34. $\partial u_3 / \partial x_2$ - Gust Gradient Probability Density Distribution, Altitude Band #4

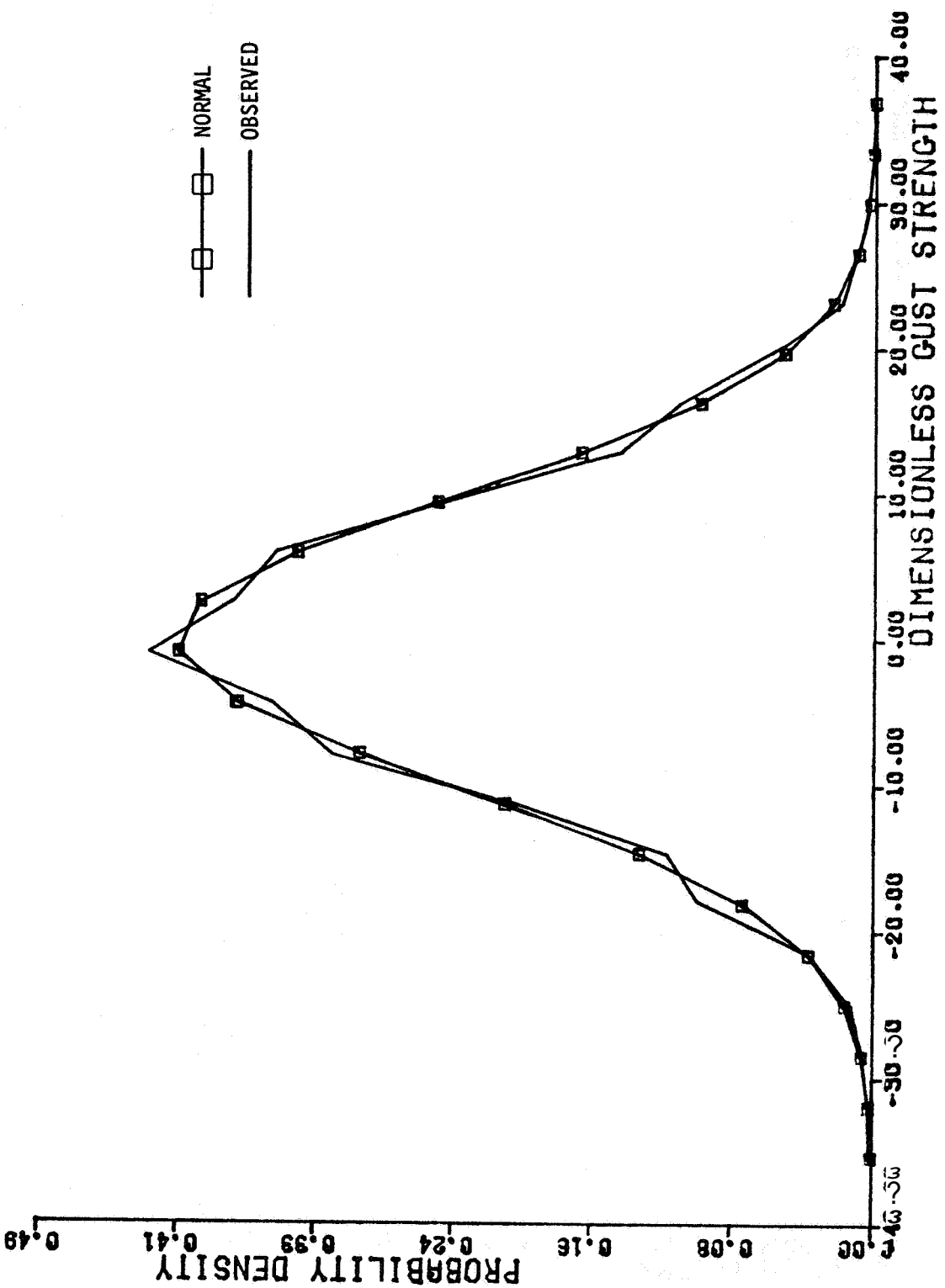


Figure D-35 $\frac{\partial u_g}{\partial x_2}$ - Gust Gradient Probability Density Distribution, Altitude Band #5

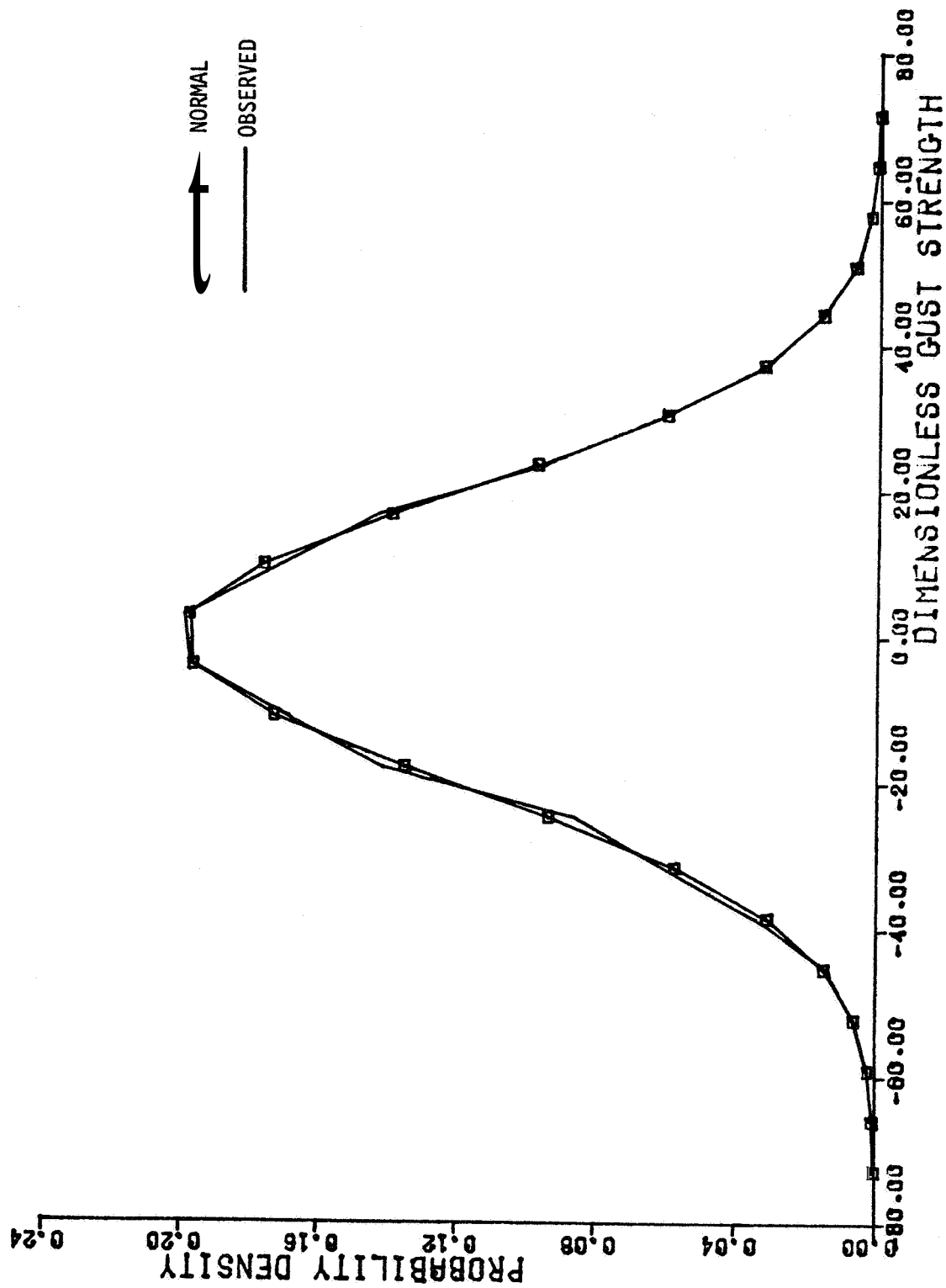


Figure D-36. $\partial u_3 / \partial x_2$ - Gust Gradient Probability Density Distribution, Altitude Band #6

1. REPORT NO. NASA CR-3541	2. GOVERNMENT ACCESSION NO.	3. RECIPIENT'S CATALOG NO.	
4. TITLE AND SUBTITLE Advanced Space Shuttle Simulation Model		5. REPORT DATE April 1982	
7. AUTHOR(S) Frank B. Tatom and S. Ray Smith		6. PERFORMING ORGANIZATION CODE	
9. PERFORMING ORGANIZATION NAME AND ADDRESS Engineering Analysis, Inc. 2109 Clinton Avenue W., Suite 432 Huntsville, Alabama 35805		8. PERFORMING ORGANIZATION REPORT #	
12. SPONSORING AGENCY NAME AND ADDRESS National Aeronautics and Space Administration Washington, D.C. 20546		10. WORK UNIT NO. M-377	
		11. CONTRACT OR GRANT NO. NAS8-33818	
		13. TYPE OF REPORT & PERIOD COVERED Contractor Report	
14. SPONSORING AGENCY CODE			
15. SUPPLEMENTARY NOTES Marshall Technical Monitor: Warren Campbell Interim Report			
16. ABSTRACT The effects of atmospheric turbulence in horizontal and near-horizontal flight during the return of the Space Shuttle are important for determining design, control, and pilot-in-the-loop effects. A nonrecursive model (based on von Karman spectra) for atmospheric turbulence along the flight path of the Shuttle Orbiter has been developed which provides for simulation of instantaneous vertical and horizontal gusts at the vehicle center-of-gravity and also for simulation of instantaneous gust gradients. Based on this model the time series for gusts and gust gradients have been generated and stored on a series of magnetic tapes which are entitled Shuttle Simulation Turbulence Tapes (SSTT). The time series are designed to represent atmospheric turbulence from ground level to an altitude of 120,000 meters.			
A description of the turbulence generation procedure is provided, the results of validating the simulated turbulence are described, and conclusions and recommendations are presented. Appendices provide tabulated one-dimensional von Karman spectra, a discussion of the minimum frequency simulated, and the results of spectral and statistical analyses of the SSTT.			
17. KEY WORDS Fluid Dynamics Turbulence Simulation Flight Mechanics		18. DISTRIBUTION STATEMENT Unclassified - Unlimited	
Subject Category 16			
19. SECURITY CLASSIF. (of this report)	20. SECURITY CLASSIF. (of this page)	21. NO. OF PAGES	22. PRICE
Unclassified	Unclassified	100	A05

For sale by National Technical Information Service, Springfield, Virginia 22161

NASA-Langley, 1982